LBL-5366
c.2

FLUORESCENCE STUDIES ON CHLOROPLAST COUPLING FACTOR

Paul Richard Hartig
(Ph. D. thesis)

September 1976

Prepared for the U. S. Energy Research and
Development Administration under Contract W-7405-ENG-48

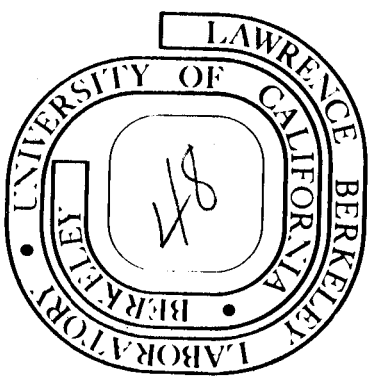

LBL-5366
c.2

DISCLAIMER

FLUORESCENCE STUDIES ON CHLOROPLAST COUPLING FACTOR

Contents

II. (continued)

FLUORESCENCE STUDIES ON CHLOROPLAST COUPLING FACTOR

Paul Richard Hartig

A.B. (St. Louis University) 1971

Laboratory of Chemical Biodynamics
Lawrence Berkeley Laboratory
University of California
Berkeley, California

August 1976

ABSTRACT

A protein known as coupling factor (CF) located on the thylakoid membrane surface produces ATP from ADP and P_i when chloroplasts are illuminated. This process represents the final stage in energy transduction in higher plants whereby absorbed light is converted into the high energy phosphate bond of ATP. It is generally accepted that the major stages in this process include the absorption of light, a primary charge separation leading to a series of electron transport reactions in the membrane, the production of a transmembrane proton electrochemical gradient and the coupling of this gradient to the synthesis of ATP in the active site of CF. To gain insight into the molecular details of this coupling process, we have investigated the structure and dynamics of CF using fluorescence labeling techniques. In addition, we have constructed a novel fluorescence lifetime

system with improved short lifetime capabilities for use in these studies.

The new single photon counting fluorescence lifetime system utilizes optimized light pulser and photomultiplier operating conditions, and an improved constant fraction discriminator to measure lifetimes as short as 90 psec. The discriminator has upper and lower level adjustments and a time walk of no more than $\pm$ 35 psec over a 50 mV to 5 V input pulse amplitude variation. We have introduced a number of experimental procedures which enable us to minimize artifacts in the measurement of short lifetimes. We investigated the origin of the early and late secondary pulses observed in all photon counting systems. Various schemes in use for pulse pileup rejection are discussed and the existence of certain "blind spots" which can lead to substantial experimental errors is revealed. We have determined fluorescence lifetimes of 4.94 $\pm$ 0.07 nsec for anthracene in cyclohexane, 640 $\pm$ 30 psec for diphenylbutadiene in cyclohexane, and 90 $\pm$ 30 psec for erythrosin in water. These values agree well with available published data. Sources of measurement error are discussed. Single component lifetimes of 90 psec or longer can be accurately measured on the system.

We have isolated the spinach chloroplast coupling factor to greater than 95% purity using an improved method. Purified CF has been labeled with a new sulfhydryl specific fluorescent label, 5-iodoacetamidofluorescein (5-IAF). The physical and spectroscopic properties of 5-IAF are described. 5-IAF labels the chloroplast

phosphorylation coupling factor at a single site on the β subunit. Over 85% of the ATPase activity and over 60% of the photophosphorylation reconstitution activity of CF is retained after labeling. Trypsin activation of the ATPase activity of 5-IAF labeled CF dramatically alters the fluorescence properties at the labeling site, indicating an involvement of this site in ATPase activation. Studies of the fluorescence emission spectra, fluorescence polarization and postassium iodide quenching of 5-IAF and 5-IAF labeled CF demonstrate that the labeling site is in a partially buried hydrophobic region which is partially accessible to potassium iodide quenching from the solvent phase and which restricts the motion of the fluorescent label. The fluorescence shows little change upon substrate binding. We conclude that the label is located in a cleft region remote from the enzyme active site.

The degree of attachment of the fluorescent label 5-iodoacetamidofluorescein (5-IAF) to the chloroplast phosphorylation coupling factor (CF) undergoes significant changes as the pH is varied from 6.4 to 8.5. Addition of ATP to the labeling mixture decreases the extent of labeling over the entire pH range studied. We examine several alternative explanations for these effects and conclude that substrate and pH induced conformational changes occur in CF. The subunit localization of these conformational changes is examined by SDS gel electrophoresis of the labeled protein. At pH 6.6, addition of ATP to the labeling mixture causes a strong decrease in the extent of labeling of the γ subunit. Literature reports indicate that ATP does not bind to the γ subunit. We conclude that conformational changes induced by ATP binding on

remote subunits are transmitted to the γ subunit by intersubunit forces. Our results show that the pH and ATP effects are not independent. The existence of interdependent pH and substrate induced conformational changes suggests a model of conformational coupling in which the transmembrane electrochemical gradient directly induces conformational changes in CF leading to net ATP synthesis. We propose a special role for the γ subunit as an allosteric mediator which transmits pH induced conformational forces to the active site for net ATP synthesis. The elements of this new model of conformational coupling of phosphorylation are discussed. Evidence in the literature supporting this model is reviewed.

ACKNOWLEDGMENTS

I am greatly indebted to Professor Kenneth Sauer for instructing me in the art of science. His insightful questioning and analyses helped to transform my experimental wanderings into a directed random walk.

I thank Branko Leskovar, C. C. Lo, and Nancy Bertrand for collaborating on complementary studies to the work described in chapters three and four.

My thanks also to the members of Professor Sauer's research group and the people of the Biodynamics Laboratory for providing the support and expertise that I often needed, both in and out of the laboratory.

To the friends and more who shared these five up and down years belong my favorite memories of Berkeley and my lasting gratitude.

This research was supported in part by a National Science Foundation Predoctoral Fellowship (1971-1974) and in part by the Energy Research and Development Agency.

To the experience of Berkeley:

Raffiniert ist der Herr Gott, aber Boshaft ist er nicht.

(God is subtle, but He is not malicious)

A. Einstein

Training is everything. The peach was once a bitter almond; cauliflower is nothing but a cabbage with a college education.

Mark Twain

Love without reserve

Enjoy without restraint

Live without dead time

Scrawled on a wall
Telegraph Avenue
Berkeley, 1974

I. INTRODUCTION

I. INTRODUCTION

Energy Flow

Every minute, over 100 million tons of matter disappears from the sun. This vanishing mass is converted into electromagnetic radiation which forms the primary energy flux of the solar system. The energy radiates outward from the sun and is captured by photosynthetic systems on our planet to provide the primary energy flow utilized by all life forms. The origin of this solar energy flux is the fusion reaction in which four hydrogens become one helium in the thermonuclear solar reactor. For every four grams of helium produced, 0.029 g of mass that was present before the transformation is lost and an equivalent amount of energy is released, following the Einstein relation $E = m\,c^2$. This energy radiates outward in all directions and a small fraction of it strikes the earth at the rate of approximately 1.7×10^{17} joules/sec (watts). A portion of this electromagnetic energy falls within the wavelength range classified as visible light and approximately 4×10^{13} watts of visible light energy is captured by photosynthetic organisms (0.02% of the incident flux) in the process of carbon fixation. In addition to providing the ultimate energy source for all plant and animal life, the vast majority of man's current energy needs are supplied by fossil fuels which release an ancient store of biologically captured solar energy.

It has been estimated that the total annual biological energy flux exceeds the energy expenditure of all man-made machines by a factor

of 100. Photosynthetic energy transductions are of fundamental scientific importance and their potential as a societal energy source provides further interest. A fundamental understanding of the biology of photosynthesis is relevant for both goals. (Pseusner, 74; Lehninger,65)

Photophosphorylation

Photosynthetic organisms produce ATP by a process known as photophosphorylation. Light energy is captured by the absorption of a photon in an array of chlorophyll molecules. The disappearance of the photon coincides with the production of an excited state in the chlorophyll molecule which migrates to a special reaction center chlorophyll via exciton and excitation transfer mechanisms within the array. The excited reaction center donates an electron to an acceptor molecule producing a reduced acceptor and an oxidized reaction center (Clayton,65). The reduced acceptor passes the electron to another species in the photosynthetic membrane and the process continues until ultimately a molecule of reduced NADPH is produced. The sequence of molecules involved in these one electron oxidation and reduction processes is known as the electron transport chain. At certain sites along this chain, the oxidation-reduction energy is coupled by an unknown mechanism to the production of ATP from ADP, which is a dehydration reaction (or, depending on the pH, a dehydroxylation reaction). The production of ATP during photosynthetic electron transport is termed photophosphorylation (Arnon, 56; Jagendorf and Uribe, 66; Avron and Neumann,68).

Three different types of photophosphorylation have been identified. In non-cyclic photophosphorylation, an electron acceptor is reduced

(NADP in native chloroplasts) oxygen is evolved from the oxidation of water and ATP is formed simultaneously (Avron and Neumann, 68). This is the process responsible for the bulk of the ATP formed in vivo in plants under normal circumstances. Cyclic photophosphorylation is a process requiring the addition of an exogenous electron carrier for a light induced ATP formation which is not accompanied by any net oxidation or reduction. Thus, ATP formation is coupled to a cyclic flow of electrons (Avron and Neumann, 68). It is widely accepted that there are two sequential light reactions, termed photosystems I and II, in chloroplasts (see Figure 1.1; Clayton, 65). Non-cylic photophosphorylation involves electron transport through both photosystems in the production of ATP while cyclic photophosphorylation involves only photosystem I. Further details on the exact sites of coupling of electron transport to ATP production will be discussed later. Controversy exists over the role of cyclic photophosphorylation in vivo (Avron, 71). It is known that the dark reactions of photosynthesis require 1.5 molecules of ATP for every molecule of NADPH utilized (Clayton, 65). Since non-cyclic photophosphorylation is thought to produce only one ATP per NADPH, many investigators believe that cyclic photophosphorylation takes up the slack and produces the extra ATP required. The issue is complex however, and the question is far from resolved.

Pseudocyclic photophosphorylation occurs when molecular oxygen serves as the terminal electron acceptor in a non-cyclic electron transport. Oxygen and electron acceptors must be present for this process to occur (Arnon, 68; Epel and Neumann, 73). It was recently observed that

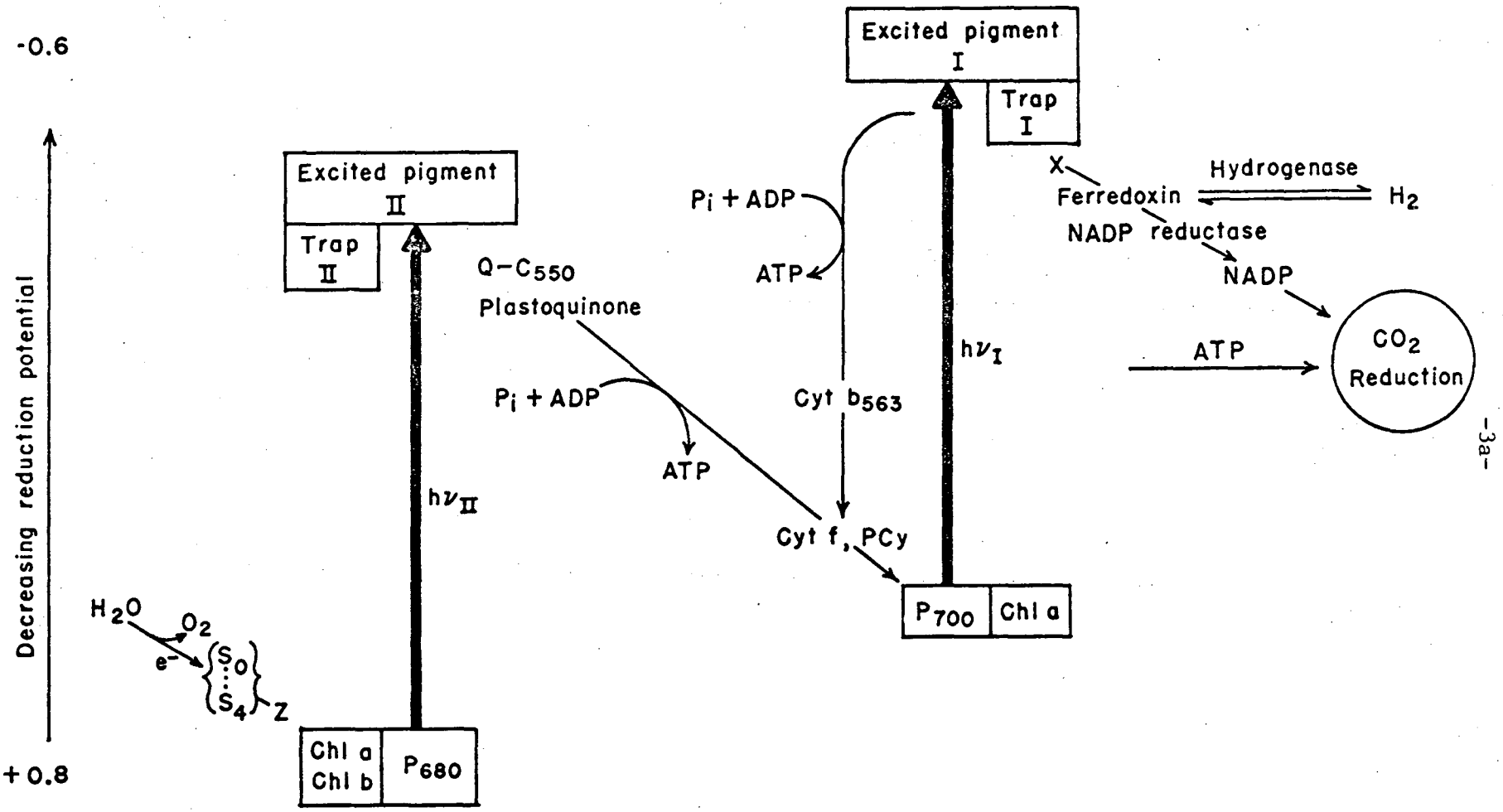

XBL7410-5395 A

Fig. 1.1. The "Z" scheme for the light reactions of photosynthesis.

oxygen reduction occurs at photosystem I in a univalent reduction of oxygen to superoxide (Asada et al., 74). The superoxide can then lead to production of hydrogen peroxide or to oxidation of electron donors such as ascorbate (Allen and Hall, 73; Epel and Neumann, 73). It has been proposed that the additional ATP needed for the dark reactions of photosynthetic carbon fixation may be produced in this manner without generation of NADPH (Elstner and Kramer, 73; Heber, 73).

Cyclic photophosphorylation is often the experimental phosphorylation of choice due to its high rates, convenience and superior reproducibility. All photophosphorylation studies undertaken in this thesis research involve cyclic photophosphorylation.

Coupling Factor ATPase Activities

A light activated, magnesium dependent ATPase reaction was discovered in chloroplasts and characterized approximately 15 years ago (Wessels and Baltscheffsky, 60; Avron, 62; Vambutas and Racker, 65; Petrack et al., 65). In contrast to the case in mitochondria where ATP forming and hydrolyzing reactions are freely reversible (Senior, 73), it was found that the chloroplast ATPase rate is very low in the dark (Avron, 62) and must be suitably activated before appreciable rates are observed. The ATPase reaction was immediately recognized as a likely candidate for a reversal of the ATP forming process during photophosphorylation. An active search was initiated for the proteins responsible for the ATPase reaction with the expectation that the photophosphorylation system would prove to be responsible for the ATPase activity and would thus be co-purified.

Early attempts to solubilize the ATPase activity led to the discovery that trypsin digestion of the chloroplast membrane leads to the appearance of a calcium dependent ATPase activity in the soluble phase (Vambutas and Racker, 65). An active research field developed around the Ca^{++}-ATPase which led to the first successful purification of the enzyme to homogeneity in 1970 (Farron, 70; Farron and Racker, 70). The preferred method of isolation became EDTA treatment of the chloroplast membrane (which chelates divalent cations) which causes a soluble latent ATPase enzyme to appear. The soluble enzyme exhibits an ATPase activity following a brief trypsin digestion. The latent ATPase enzyme can be restored to EDTA depleted membranes by incubation along with divalent cations. This restoration is accompanied by a re-coupling of electron transport to photophosphorylation which was lost during the EDTA treatment. For this reason, the protein has been termed the coupling factor of photosynthesis (CF_1 in the literature, CF in this thesis).

Considerable confusion reigns in the early literature on CF and its various ATPase activities. This author is aware of no current reviews which attempt to place all the activities and interconversions in perspective. Since the ATPase and coupling activities of CF are examined and discussed in this thesis, I will attempt to review this body of work. The reader is referred to Figure 1-2 as a guide to understanding these interconversions.

The natural catalytic activity of CF is photophosphorylation which occurs at the membrane surface. When EDTA is added to a preparation of chloroplast membranes, divalent cations are chelated and CF is released from the membrane as photophosphorylation is inhibited (McCarty and

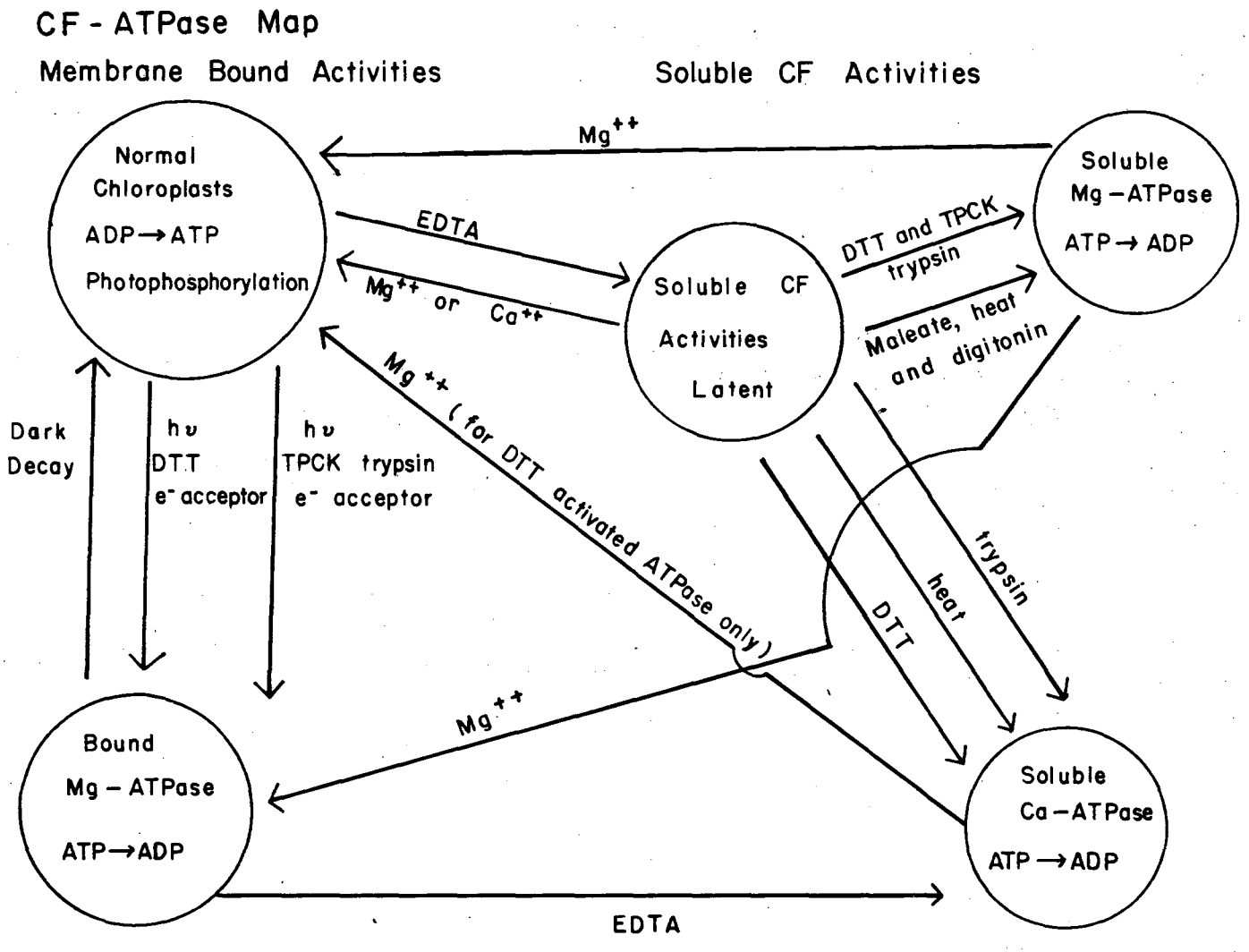

XBL 766-5946

Fig. 1.2

Racker, 66). The attachment of CF to the membrane is reversible since a sample of soluble CF plus divalent cations will substantially restore photophosphorylation activity to EDTA treated membranes. The optimal cation concentration for this reconstitution is approximately 7 mM (Bennun and Racker, 69).

Following the EDTA extraction, CF exhibits no catalytic activities but a short trypsin digestion (Vambutas and Racker, 65), treatment with heat in the presence of ATP (Farron, 70), or incubation with DTT (a sulfhydryl reagent) (McCarty and Racker, 68) activates a Ca^{++}-ATPase activity at rates of 23-47μmoles P_i released/min/mg protein in the purified enzyme (McEvoy and Lynn, 73; Deters et al., 75; Lien and Racker, 71b; Lien et al., 72; Nelson et al., 72a). The soluble ATPase activity can also be induced by direct treatment of chloroplasts with trypsin or heat which both activates the Ca^{++}-ATPase activity and solubilizes the CF (Vambutas and Racker, 65).

The trypsin and heat treatments of soluble CF produce an enzyme which is altered from the native state so that it can no longer bind to the membrane (Bennun and Racker, 69). Thus, the Ca^{++}-ATPase produced by these means is no longer active as a coupling factor for photophosphorylation. By way of contrast, treatment of CF with DTT to activate the ATPase does not lead to loss of the coupling activity (McCarty and Racker, 68). In addition, binding of DTT activated Ca^{++}-ATPase to the chloroplast membrane in the presence of BSA leads to dirct inhibition of the Ca^{++}-ATPase activity (Lien and Racker, 71a).

The Ca^{++}-ATPase activity described above is very sensitive to the metal ion cofactor used in the assay. Calcium is the most active cofactor with other divalent cations such as nickel, magnesium, manganese, cobalt, and strontium producing less than 3% of the ATPase rate observed with calcium (Vambutas and Racker, 65). A very different type of ATPase activity that is maximal in the presence of magnesium but also exhibits an appreciable rate in the presence of calcium can be produced by heating the soluble CF in a digitonin containing maleate buffer. The ATPase rates so obtained are as high as 15 μmoles P_i/min/mg protein (Nelson et al., 72a). The Mg^{++}-ATPase preparation obtained by heat activation is active as a coupling factor for photophosphorylation (Nelson et al., 72a). A soluble Mg^{++}-ATPase activity can also be obtained by a short digestion of soluble, DTT activated Ca^{++}-ATPase by TPCK treated trypsin (trypsin free of chymotrypsin activity) (Lien and Racker, 71a). This TPCK trypsin activated Mg^{++}-ATPase preparation can be returned to the membrane where it exhibits a membrane bound Mg^{++}-ATPase activity. The distinction between these various magnesium and calcium dependent ATPase activities is functionally significant since magnesium rather than calcium serves as the natural cofactor for photophosphorylation (Petrack and Lipmann, 61).

Incubation of chloroplasts with DTT and an electron acceptor during illumination produces a bound Mg^{++}-ATPase activity which can be observed in the dark (Petrack et al., 65; McCarty and Racker, 68). Photophosphorylation inhibitors such as Dio-9, or ammonium chloride severely inhibit the activation of this Mg^{++}-ATPase activity. Since DTT alone will slowly activate the same activity, it has been proposed that illumination merely

serves to accelerate this process (McCarty and Racker, 68). In a subsequent study, Lynn and Straub (69) demonstrated that illumination of chloroplasts in the presence of TPCK trypsin and an electron acceptor also induces this Mg^{++}-ATPase activity. The close association of this activity with the photosynthetic membrane was demonstrated by its sensitivity to DCCD, which does not affect the soluble Ca^{++}-ATPase activity (Lien and Racker, 71a). Further proof was obtained by studies in which the Mg^{++}-ATPase activity remained with the chloroplast membrane through several purification stages which removed the contaminating mitochrondrial fragments and soluble enzyme (Vambutas and Racker, 65). Treatment of membranes exhibiting Mg^{++}-ATPase activity with EDTA leads to inhibition of the Mg^{++}-ATPase activity and the appearance of the Ca^{++}-ATPase in the soluble phase due to release of activated CF from the membrane (McCarty and Racker, 68). The membrane bound ATPase activity will slowly decay in the dark in a process that is accelerated by the presence of magnesium (Bakker-Grunwald and Van Dam, 74).

The complex scheme of activities and membrane associations described above indicates that CF is capable of catalyzing photophosphorylation or its reversal in the form of several ATPase activities. The metal cofactor specificity of the ATPase activity is dependent upon the means of activation and is capable of dramatic alterations when the enzyme interacts with the membrane. The requirement for a sulfhydryl reagent such as DTT to activate so many of the activities has led to the hypothesis that a sulfhydryl-disulfide exchange reaction is involved in the activation since no net change in the SH content of the enzyme is detected upon activation (Farron and Racker, 70).

An equally complex literature exists on the various exchange activities of CF. The patience of both the reader and the author will be spared by avoiding a similar review of the exchange data. Suffice it to mention that these experiments are contained in many of the same references cited above. The ATPase data was dealt with in detail to place into perspective the Ca^{++}-ATPase studies undertaken in this thesis. The trypsin activated Ca^{++}-ATPase activity of CF has been chosen as a representative activity by many researchers (this laboratory included) for its convenience and reproducibility. The review above demonstrates that all of the ATPase activities of CF are closely interrelated and probably represent slight nuances of expression of the same essential biochemical activity.

The ATPase data suggests that an enzyme capable of efficient catalysis of the ATP→ADP reaction may also function in the reverse reaction during photophosphorylation. This has led to the widely held view that CF functions in the terminal step of photophosphorylation whereby ATP is produced from ADP. Perhaps the best evidence for this assignment comes from the work of McCarty and Racker (66) who utilized antibodies to CF and inhibitors of phosphorylation to show that CF is not involved in the production of the energized membrane state following electron transport (as monitored by the pH) but acts at a later step to utilize this energy in the production of ATP. This formulation has so far held the test of time although the important question of the mechanism of CF action and its means of linkage to the energized membrane remains unanswered.

Coupling Factor Subunit Structure

The molecular weight of purified, monomeric CF is 325,000 daltons (Farron, 70). The enzyme contains five different types of subunits labeled alpha through epsilon with the following molecualr weights in kilodaltons: α -(59),β-(56), γ-(37), δ-(17) and ε-(13) (Nelson et al., 73; Adolfson et al., 75; McEvoy and Lynn, 73) with uncertainties of up to ± 25% for the values obtained in these different laboratories. Only antibodies to the α and β subunits elicit a strong agglutination reaction (Nelson et al., 73), suggesting that only these subunits are fully exposed on the surface of the membrane. Anti-γ and anti-α are the only antibodies which strongly inhibit photophosphorylation and the light triggered ATPase reaction. The fact that anti-γ does not agglutinate chloroplast membrane but does inhibit photophosphorylation indicates that this subunit is accessible from the water phase but is located on the membrane side of the protein (Deters et al., 75). No single antibody strongly affects the Ca^{++}-ATPase activity but the combination of anti-α plus anti-γ does produce inhibition (Nelson et al., 73). Coupling factor prepared by heat treatment in the presence of digitonin and then separated from the δ and ε subunits and digitonin on a Sephadex column contains only the α, β and γ subunits and functions as an ATPase but not as a coupling factor for photophosphorylation (Deters et al., 75). It was also shown that prolonged digestion of CF by TPCK trypsin (free of chymotrypsin activity) produces an α,β complex which is active as an ATPase but no longer functions as a photophosphorylation coupling factor (Deters et al., 75). This two subunit ATPase is no longer sensitive to inhibition by the ε subunit, suggesting that the ε subunit binds to the γ or δ subunits but not to α or β (Deters et al., 75). Surprisingly,

anti- α or anti- β alone or together do not inhibit the two subunit ATPase (Deters et al., 75). Finally, we note that covalent labeling of the β subunit with a fluorescent label inhibits 80% of the Ca^{++}-ATPase activity of CF (Deters et al., 75).

In summary, these studies suggest that the α, β, and γ subunits are all accessible from the water phase with the γ subunit partially shielded or facing the membrane phase. Only the α and β subunits are essential for the Ca^{++}-ATPase activity and therefore must contain the catalytically active binding site. In contrast to the original suggestion that the δ subunit may be a tightly bound contaminant (Nelson et al., 73), more recent studies have shown that the δ subunit is essential for the coupling activity of CF (Deters et al., 75) although its precise role remains unclear. It has been proposed that the ε subunit is an inhibitor subunit (in analogy to a similar subunit in mitochondrial F_1) (Nelson et al., 72b). This assignment is based on the observation that removal of the subunit unmasks the ATPase activity of CF and its presence inhibits the activity of activated CF. A strong case can be made against the assignment of such a 'role' for the ε subunit. In contrast to the mitochondrial enzyme, the photophosphorylation coupling factor does not exhibit any ATPase activity in vivo. The discovery that the alteration of a native enzyme by removal of one of its subunits causes a new, unnatural catalytic activity to appear (the ATPase) is not sufficient evidence to assert that the role of the subunit is to inhibit this artificial activity which never appears in the natural state. A much more straightforward interpretation of the data is that alteration of the enzyme by removal of the ε subunit sufficiently disrupts the structure so that a new

reaction, the ATPase reaction, can occur in the active site. No information on the native 'role' of the ε subunit is obtainable from the data. At this point in the research on CF, the function of the ε subunit in the native enzyme remains unclear.

Equilibrium dialysis experiments have revealed the presence of two tight binding sites for ADP or ATP on the coupling factor with dissociation constants of approximately 3 micromolar (Cantley and Hammes, 75a; Roy and Moudrianakis, 71; Livne and Racker, 69). Additional weak binding sites for these nucleotides have also been detected (Cantley and Hammes, 75a) and assigned as the catalytic site by this group. It was suggested that the tight sites represent allosteric conformational switches for the ATPase activity (Cantley and Hammes, 75a). Fluorescence excitation transfer studies have indicated that the tight binding sites are located on each of two copies of the α subunits with the active site located 40 Å away between two copies of the β subunits. (Cantley and Hammes, 75b). These assignments are speculative, however, and more direct studies will be required to establish the locations and roles of these sites.

Chloroplast Membranes

Chloroplasts are intracellular organelles that are bounded by an outer limiting membrane and contain a complex internal network of membranes called the thylakoids. The chlorophyll pigments are contained in the thylakoid membranes which are the site of the light reactions of photosynthesis. The thylakoid membranes are classified into stroma and grana regions. The grana regions consist of tightly opposed stacks of

flattened vesicular discs which are connected to adjoining grana regions by roughly linear stretches of stroma thylakoids. All work on the light reactions of chloroplasts focusses on processes occurring in these internal thylakoid membranes (Muhlenthaler, 71).

Electron microscopy studies using negative staining techniques were the first to identify CF as roughly spherical particles with a 90 Å radius appearing on the surface of the thylakoids (Lien and Racker, 71a; Racker et al., 71; Garber and Steponkus, 74). Subsequent studies using the freeze etching technique confirmed these observations and located CF on the outer surface of the thylakoid discs (Garber and Steponkus, 74; Miller and Staehelin, 76). The ball and stalk structures for CF sometimes observed in negative staining are not seen in freeze etch pictures and have led to the suggestion that the stalk is an artifact of the negative staining technique (Garber and Steponkus, 74). These studies indicate that CF protrudes from the surface of the membranes but do not rule out the possibility that some portions of the molecule may extend into the membrane lipid phase. This concept is in agreement with the antibody studies on CF subunits already discussed in this chapter. Studies on the stoichiometry of CF indicate 860 (Strotmann, et al., 73) or 620 (Girault et al., 74) chlorophyll molecules per CF on the membrane. The CF is asymmetrically distributed over the membrane surface since it is known to be excluded from the tightly opposed stacked regions of the grana thylakoids (Miller and Staehelin, 76).

Treatment of the thylakoids (in broken chloroplasts) with EDTA releases CF from the membranes and causes the 90Å particles to disappear from the membrane surface (Howell and Moudrianakis, 67) (the 90 Å CF

particles were incorrectly termed quantasomes in that study). Silicotungstic acid has also been used as an uncoupler of photophosphorylation which removes CF from the membranes and leads to disappearance of the membrane surface particles (Lien and Racker, 71b). CF is thus a water soluble protein which binds to the membrane surface in the presence of divalent cations and is released during treatment with EDTA or other chelating agents. These properties classify CF as a 'peripheral' or 'extrinsic' membrane protein (Singer and Nicholson, 72; Green et al., 73) in loose association with the membrane surface.

Removal of CF from the membrane leads to a decrease in the extent of proton flux through the membrane during electron transport. In addition the rate of dark decay of the transmembrane proton gradient is accelerated by removal of CF (McCarty and Racker, 67; Neumann and Jagendorf, 64; McCarty and Racker, 66). Both the electrical conductance of the thylakoid membrane and the dark relaxation rate of the light induced transmembrane pH difference increase 100 fold following CF removal (Schmid and Junge, 74). These data indicate that CF removal increases the proton 'leakiness' of the membrane and suggest that CF is situated on a proton conductance channel through the membrane. This information provides significant support for the chemiosmotic theory of phosphorylation which will be discussed later. Further information on this proton conductance channel is provided by experiments with DCCD, a protein crosslinking reagent. Treatment of EDTA chloroplasts with DCCD restores the light induced transmembrane pH gradient and partially restores the lost photophosphorylation capabilities of the membranes (probably due to the ability of residual CF left on the membrane after EDTA treatment to utilize the

restored proton gradient as discussed in Chapter 2) (McCarty and Racker, 67). Lipid soluble DCCD is very effective in this restoration but a water soluble version of the crosslinker does not work (Uribe, 72). It is likely that DCCD is capable of plugging the transmission proton conductance channel which underlies CF following removal of CF from the membrane. This interpretation is strengthened by the observation that DCCD has no effect on the rate constants for the pH rise in the light or its decay in the dark in untreated chloroplasts (McCarty and Racker, 67).

Energy Coupling Mechanisms

One of the major unsolved mysteries of modern biology is the molecular details of the coupling mechanism whereby mitochondria and chloroplasts are able to convert oxidation-reduction energy within the electron transport chains into the production of ATP (a dehydration reaction) during photophosphorylation and oxidative phosphorylation. Research in this area is currently very active and recent developments in the field, which shall be reviewed here, have led to the formulation of an outline of the novel biochemical process responsible for this important energy transduction.

There are three major mechanism of energy transduction which are frequently cited in the current literature. These mechanisms, the Chemiosmotic theory, the Chemical Intermediate theory, and the Conformational Coupling theory, will each be discussed in turn. The chemiosmotic theory is arising as the most widely supported theory and will be reviewed first.

i. The Chemiosmotic Theory

The major tenets of the Chemiosmotic theory are as follows (Jagendorf and Uribe, 66): 1) the photosynthetic (or mitochondrial) membrane is topologically closed in space and defines a separate vesicular internal volume 2) this membrane exhibits a low permeability to protons. 3) electron

transport reactions are obligitorily coupled to the production of an electrochemical gradient across the membrane via a trans-membrane proton pump. 4) the proton electrochemical gradient (consisting of both a membrane potential and a trans-membrane ΔpH is the high energy intermediate between electron transport and phosphorylation which drives ATP production 5) a reversible ATPase system exists in the membrane which utilizes the energy stored in the electrochemical gradient for the production of ATP. These broad proposals on the energy transduction mechanism have been supplemented by detailed biochemical models for several of the steps. For example, Peter Mitchell, who is mainly responsible for the development of this theory, has proposed that of the various components of the electron transport chain, ubiquinone, plastoquinone, and flavoproteins may serve as the proton translocators during electron transport while cytochromes and iron-sulphur proteins serve only to transport electrons (Mitchell, 72). Indeed, an asymmetric distribution of the proposed proton translocators has been observed within the membrane which indicates that they may be preferentially aligned toward the inside or outside face of the membrane in a manner that could facilitate vectorial transport of protons (Trebst, 74; Racker et al., 71). One proposal for a detailed mechanism for this proton pump is found in the work of Walker and Crofts (70).

An example of a detailed model which can explain the linkage of the electrochemical gradient to ATP formation is found in the work of Boyer (75). This model involves the presence of a proton conformational trigger which undergoes cyclical conformational changes while dissipating the proton electrochemical gradient during the production of ATP. The model is of particular interest because it provides a detailed mechanism whereby either the electrical or the chemical nature of the proton gradient can

be used to drive ATP synthesis. At this point in the research, both the proton pump and ATP synthesis models must be regarded as speculative, pending further research.

In the following pages I will review a number of important experimental observations which provide direct support of the Chemiosmotic theory. The first observation involves the discovery that the production of ATP by chloroplasts can be separated into light and dark stages. Shen and Shen (62) and Hind and Jagendorf (63) were the first to observe that illumination of chloroplasts without phosphate brings on the ability to produce ATP when ADP and P_i are added in the post-illumination darkness. The reaction in the light was markedly stimulated when a redox dye was added to stimulate electron flow. X_e was the term used to describe the high energy intermediate produced by illumination which is available for the production of ATP in the dark. Operationally, X_e was measured as the amount of ATP produced during the dark period. The formation of X_e is complete within 30 seconds with pyocyanine as the electron transport cofactor. The yield and dark decay of X_e is highly pH dependent with decay half lives of 2 to 32 sec at 0° C as the pH is varied from 8 to 6 respectively (Jagendorf and Uribe, 66).

Every photophosphorylation uncoupler tested accelerates the dark decay. (An uncoupler is a photophosphorylation inhibitor which also accelerates electron transport). The maximum dark yield of ATP is 270 molecules per 2500 chlorophyll molecules. Since Strotman et al., (73) have determined that there is one CF molecule per 800 chlorophylls, we know that each CF produces 90 ATP molecules on the average during the dark period. The fact that CF turns over many times during dark ATP production

demonstrates that X_e is not a stoichiometric intermediate in ATP synthesis, as most chemical coupling schemes would require. (Jagendorf and Uribe, 66)

If chloroplasts are suspended in an unbuffered medium, a pH rise of up to 1.0 pH units in the bathing medium is detected upon illumination. This pH rise exhibits the same rise time and electron transport cofactor requirements as X_e. Uncouplers decrease the extent of the pH rise and accelerate the dark rate of pH decay. As is discussed later, this pH rise is associated with a transmembrane proton pumping that also leads to an acidification of the internal space of the thylakoids and the formation of a transmembrane ΔpH. From these and other experiments, X_e has been identified as the transmembrane ΔpH. (Jagendorf and Uribe, 66)

It has been observed that the initial rate of X_e formation is only 20% of the rate of ongoing ATP formation. It is likely, however, that a trans-membrane electrical field rather than ΔpH drives this initial ATP formation, as will be discussed. In addition, it must be kept in mind that the data is also consistent with the existence of the ΔpH as a reversible side energy pathway which acts as a storage pool for the high energy intermediate and is not directly on the pathway for ATP synthesis (Jagendorf and Uribe, 66). Thus the membrane electrochemical potential may be an energy linked alternative to phosphorylation (Skulachev, 72).

If chloroplasts are incubated with acid in the dark for approximately 20 sec and then rapidly changed to a basic medium, a transmembrane ΔpH is produced which produces ATP in the presence of ADP, P_i, and magnesium. An inorganic acid buffer which can serve as an internal reservoir of protons is needed for high yields in this process. The normal photophosphorylation uncouplers as well as antibodies to CF inhibit this

acid-base induced ATP synthesis. The dark decay of the acid-base X_e is pH dependent in the same way as X_e produced by illumination. The acid-base ATP synthesis works over a wide range of bathing pH values; only the transmembrane Δ pH is essential for ATP production. (Jagendorf and Uribe, 66)

The magnitude of the transmembrane Δ pH has been estimated by a variety of techniques, such as the absorbance changes at 703 nm by chlorophyll a (Rumberg and Siggel, 69), the uptake of methylamine measured by silicone layer filtration (Heldt et al., 73) and the quenching of 9-aminoacridine fluorescence (Pick et al., 73). In all such studies, a steady state ΔpH of 2.5 to 3.5 pH units has been observed (Hind and Jagendorf, 63; Uribe and Jagendorf, 67; Deamer et al., 67; Portis and McCarty, 73; Jagendorf, 75). The question of the energetic adequacy of this ΔpH for ATP production cannot be answered until the precise ratio of protons consumed per ATP produced is answered (Rumberg and Siggel, 69). Modern estimates center around a value of 3 (Jagendorf, 75) which would provide sufficient energy for ATP production under standard conditions (Mahler and Cordes, 71).

The chemiosmotic theory predicts that illumination generates a transmembrane ΔpH which will decrease as ATP is produced from this energy pool. Several independent laboratories agree in finding that the illumination induced ΔpH decreases by up to 0.4 pH units during phosphorylation (Rumberg and Siggel, 69; Pick et al., 73; Portis and McCarty, 74). This small ΔpH decrease of 0.3 to 0.4 units is consistent with the observed strong dependence of the photophosphorylation rate on ΔpH (Portis and McCarty, 74). Schroeder et al. (71) have demonstrated that the rate

of proton efflux increases on illumination, thus providing evidence that the well known increase in electron flow during photophosphorylation is linked to a decreased internal proton concentration caused by the accelerated proton efflux. Both the level of steady state ΔpH and its decrease during photophosphorylation are strongly pH dependent (Pick et al., 73). It is interesting to note that the addition of ADP alone under non-phosphorylating conditions decreases electron transport but increases ΔpH by inhibiting the dark proton leakage rate (Telfer and Evans, 72; Portis and McCarty, 74). It has been suggested that these nucleotides bind directly to CF to decrease the rate of proton efflux (Teflar and Evans, 72; Portis and McCarty, 74).

The chemiosmotic model states that the full electrochemical potential of protons constitutes the high energy state used for photophosphorylation. Thus the membrane electrical potential as well as the transmembrane ΔpH are expected to contribute to the ATP synthesizing ability. A clear demonstration of this concept is available from studies in which a transmembrane electrical diffusion potential is created from addition of potassium chloride in the presence of valinomycin, a cation inophore. The diffusion potential arises transiently from the different diffusion velocities of the potassium and chloride ions. As discussed above, little ATP is synthesized if the transmembrane ΔpH falls below 2.5. At these suboptimal ΔpH values, addition of potassium chloride in the presence of valinomycin created a membrane diffusion potential that induces ATP synthesis (Schuldiner et al., 73). Thus electrical potentials can couple to ATP synthesis via the proton electrochemical potential. This augmentation of a suboptimal ΔpH has been observed both in acid-base induced

and post-illumination type ATP synthesis (Schuldiner et al., 73). This potassium chloride effect is reduced by decreasing the permeability difference between the cation and its counter-ion, as would be expected for a true membrane diffusion potential. The potential either augments or decreases ATP synthesis depending on whether the potassium ion concentration is greater on the inside or the outside of the thylakoid enclosed space (Uribe and Li, 73).

Investigations of chlorophyll b absorbance changes have shown that a maximum membrane potential of 250 mV is built up within 2×10^{-8} sec of the onset of illumination (Junge and Witt, 68). This rapid rise time suggests that the membrane potential may be connected with charge translocations or ion movements associated with the primary photoact. One model proposes that the membrane is polarized by the initial electron transfer followed by proton binding and release on two sides of the membrane (Schroeder et al., 71). It has been proposed that the membrane potential rather than the Δ pH drives initial ATP formation (Jagendorf and Uribe, 66). In the steady state, however, the membrane potential may be considerably lower (Walker and Crofts, 70). Evidence has been provided that under continuous illumination the proton influx is an active process in an electrogenic pump that leads to a transmembrane electrical potential. Other ion fluxes follow this potential in a passive manner (Schroeder et al., 71). Thus a high membrane potential builds up initially which is transformed into a low membrane potential (5 mV in 10 mM NaCl) and a high Δ pH in the steady state (Schroeder et al., 71).

An interesting set of observations on membrane potentials and ΔpH has been reported by McCarty (69). The inhibition of photophosphorylation by ammonium chloride in sonicated chloroplasts is greatly enhanced by the presence of valinomycin. The same type of enhancement has been observed in normal chloroplasts, but to a much lesser degree. McCarty suggests that uncharged ammonia (NH_3) permeates the membrane but that the ammonium ion (NH_4^+) normally doesn't. Chloroplasts are permeable to chloride ions but sonicated chloroplast preparations are not. In sonicated chloroplasts, ammonium chloride abolishes the Δ pH but photophosphorylation is largely unaffected so a transmembrane electrical potential must exist to drive ATP synthesis. The addition of valinomycin increases the ammonium ion (NH_4^+) permeability but has little effect on proton uptake. The valinomycin induced ammonium ion permeability destroys the transmembrane electrical potential in sonicated chloroplasts and strongly inhibits photophosphorylation. In chloroplasts, a high chloride ion permeability is always present which prevents the formation of a large steady state electrical potential. The addition of ammonium chloride to chloroplasts destroys the Δ pH causing a strong inhibition of photophosphorylation in the presence or absence of valinomycin, since no electrical potential is formed (McCarty, 69).

A series of experiments on the effects of EDTA and DCCD on the proton permeability of chloroplast membranes has been already discussed in this chapter. These experiments demonstrate that CF may be situated directly over a proton permeability channel in the membrane. This result is highly consistent with the chemiosmotic model since it would give CF direct contact with the solutions on either side of the membrane. Such

direct contact could facilitate a direct coupling of the transmembrane protonmotive force to ATP production on CF.

An important experiment has been recently reported in a mixed bacterial and mitochondrial system which lends support to the chemiosmotic theory. Racker and Stoeckenius (74) produced model systems of phospholipid vesicles with added purple membranes containing bacterial rhodopsin that catalyze a net proton uptake upon illumination. ATP synthesis was observed when mitochondrial membrane fragments containing phosphorylation coupling factors were incorporated into the vesicles. The system contains none of the normal electron carriers of mitochondrial phosphorylation, and could not be expected to produce any chemical high energy intermediates that would be associated with electron transport. It appears that proton pumping in the bacterial membrane generated an electrochemical proton gradient which drives remote ATP synthesis on the mitochondrial membrane fragments. This data is difficult to explain with any but the chemiosmotic model.

A large and active body of research has recently developed on the question of identification of the specific sites along the electron transport chain where ATP production is coupled to electron transport. All the novel research on this question has developed from a pioneering paper by Saha et al. (71) in which three classes of electron acceptors were defined based on the nature of the electron transport and photophosphorylation which they catalyze. Since this research area has introduced a fundamental re-evaluation of the concept of coupling sites in a manner that is most consistent with the chemiosmotic theory, the work will be reviewed here in some detail.

Saha et al. (71) have defined three classes of acceptors: Class I acceptors are reduced slowly in the absence of phosphorylation, all members of this class are water soluble ionic compounds, examples are ferredoxin, ferricyanide, and the flavins, the maximum ATP/2e ratio observed in this class is 1.3; Class II aceptors are reduced rapidly in the presence or absence of phosphorylation, little or no ATP is formed with these acceptors, these compounds are lipid soluble weak acids that also serve as uncouplers, an example is the group of phenolindophenol compounds; Class III acceptors are reduced rapidly in the presence or absence of phosphorylation, the maximum ATP/2e ratio is 0.7, all are nonionic, lipid-soluble acceptors; examples are phenylenediamine, oxidized diaminodurene, and dimethylquinone. From these ATP/2e ratios and other evidence, Saha et al. (71) concluded that Class III acceptors catalyze electron transport through one site of phosphorylation, later termed site I, while Class I acceptors catalyze phosphorylation coupled to electron flow through two sites of phosphorylation, termed sites I and II.

An extensive series of experiments using various uncouplers, inhibitors and different classes of electron acceptors by a number of laboratories (this work is reviewed in Trebst, 74) have led to the conclusion that site I is located between the two photosystems, specifically, between plastoquinone and cytochrome f. In a similar manner, site II has been assigned to the oxidizing side of photosystem II. The water oxidation site is the most likely candidate for its location (Gould and Ort, 73).

Phosphorylation sites I and II are defined as the energy conserving sites where electron transport energy is converted to an ATP synthesizing capability. These sites are not necessarily equivalent to two physically

distinct sites for ATP formation. It is possible, and indeed likely, that these sites of energy conservation represent proton pumping sites where redox energy is changed into a transmembrane electrical potential and Δ pH. Since the electrochemical gradient can be tapped anywhere along the membrane, only a single type of CF-membrane protein complex may exist in the membrane which senses the remotely produced proton electrochemical gradient.

In this model, any site of proton pumping becomes identified as an energy coupling site. Cyclic photophosphorylation becomes understood as a nonphysiological process in which an externally introduced electron carrier (such as phenazine methosulfate or PMS) which also shuttles protons across the membrane is used to produce a new, nonphysiological site of energy conservation. The artificial electron carrier produces a transmembrane proton electrochemical gradient as a consequence of reversible oxidation and reduction reactions involving proton uptake or release which it catalyzes on opposite sides of the membrane. (Trebst, 74).

As mentioned previously, site I is most likely the water splitting site of photosystem II. Recent evidence indicates that the water oxidation site is on the interior surface of the thylakoid membrane facing the enclosed space (Trebst, 74; Blankenship and Sauer, 74). In addition, the entire photosystem II is associated with intra-membrane particles which are localized exclusively in the grana regions of the thylakoids (Park and Sane, 71). It is known that CF is located on the exterior face of thylakoid membranes and is excluded from the grana stacks (Miller and Staehelin, 76). Thus, CF is on the wrong side of the membrane and laterally displaced onto the stroma in comparison to the energy conservation

at site I that it couples to, which occurs at the inside face of grana thylakoids. CF at a physically remote site must somehow sense the energy conservation occurring at the distant site I. This action is explained in the chemiosmotic theory where energy conservation sites are proton pumping sites and CF can sense the transmembrane electrochemical gradient at any point along the membrane. The above data is difficult, however, to reconcile with a chemical intermediate model of energy coupling.

Evidence has accumulated from a number of lines of investigation (Trebst, 74) to indicate that electron transport carriers are arranged asymmetrically across the chloroplast thylakoid membrane. This asymmetric distribution leads to the vectorial transport of protons and perhaps to the initial formation of the membrane electrical potential from an asymmetrical charge movement associated with the primary photoact (Trebst, 74). The current view of the distribution of electron acceptors across the membrane offers the surprising conclusion that there is an almost complete parallel between the topological location of electron carriers within the membrane and their electrochemical location on a scale of oxidation-reduction strength (the Z scheme). It appears that the acceptor sides of both photosystems I and II are near the outer membrane surface while the donor sides are near the inner surface with a zigzag scheme of electron flow between them (Trebst, 74; Racker et al., 71).

Since the acceptor side of photosystem I is located on the membrane surface freely accessible to solvent, the ionic class I acceptors catalyze electron flow all the way from water through both photosystems. Lipophilic acceptors of Class III, on the other hand, are able to penetrate into the hydrophobic membrane interior and accept electrons directly from

photosystem II, leading to electron flow only through one phosphorylation site. This explains the observed ATP/2e ratios for these two classes and demonstrates why there is a parallel between classifications of electron acceptors based on their relative hydrophobicities (as Saha et al. (7) have done) and their biological functions in electron transport and phosphorylation.

In the chemiosmotic theory, electron transport is directly coupled to the production of a proton gradient. This direct coupling would be expected to lead to an inhibition of electron flow in the absence of phosphorylation due to a back pressure from the proton gradient which remains at an undissipated high level. The phenomenon has been observed (Jagendorf and Uribe, 66) and the rate of electron transport was shown to be inversely proportional to the transmembrane Δ pH (Bamberger et al., 73). Since the transmembrane electrochemical gradient couples to ATP production, the chemiosmotic theory predicts that an osmotically intact, topologically closed membrane is required for phosphorylation. The need for an intact membrane has been demonstrated by numerous failures to induce photophosphorylation in disrupted membrane systems (Mitchell, 72). It has also been shown that uncouplers act to inhibit energy coupling by increasing the proton permeability of thylakoid membranes and thus dissipating the proton electrochemical gradient (Jagendorf and Uribe, 66; Mitchell, 72). Furthermore, the uncoupling efficiencies of various compounds are proportional to their efficiencies as proton conductors in artificial phospholipid membranes (Skulachev, 72).

Further support for the chemiosmotic theory is provided by work on the ATPase activity of CF. It has been shown that the membrane bound light driven Mg^{++}-ATPase activity of CF drives a proton pump which transports protons uphill energetically in the opposite direction from the proton flow causing dissipation of the ΔpH during phosphorylation (Bakker-Grunwald and Van Dam, 73; Carmeli, 70). The ATPase activity produces a ΔpH of up to 2.9 units. If ATP production is directly coupled to the proton gradient at CF, it is not surprising that the reversal of ATP production (an ATPase activity) leads to a reverse flow of protons at CF.

The extensive body of evidence presented above has made the chemiosmotic theory of energy transduction the most widely accepted theory in this field. Minor problems in stoichiometries (Karlish and Avron, 68) and the absence of a detailed mechanism for the production of ATP from the proton electrochemical potential remain obstacles to its full acceptance. A major remaining problem is that it is possible to reconcile nearly all the data above with the view that the proton electrochemical potential represents an alternative side pathway to the production of ATP. In this case, the electrochemical gradient is seen as a storage pool for the redox energy from absorbed photons. The pool is not directly linked to ATP formation but rather feeds through another energy conserving system (possibly chemical) which is directly linked to ATP formation on CF (Jagendorf and Uribe, 66; Skulachev, 72). Elucidation of the complete details of ATP formation on CF will eventually settle this issue. Evidence favoring the direct linkage of the proton gradient to ATP production on CF has been obtained in this thesis research and will be presented later.

ii. Chemical Intermediate Theory

The chemical intermediate theory of phosphorylation asserts that a high energy phosphorylated chemical species is produced during electron transport reactions and is able to transfer the energized phosphate to ADP in order to form ATP. This theory is modeled after known substrate level phosphorylations which occur in the cell cytoplasm, such as the oxidation of 3-phosphoglyceraldehyde to 3-phosphoglycerate via 1,3 diphosphoglycerate. These reactions are known to couple to ATP formation through a series of phoshate group transfer reactions (Mitchell, 72). A minimal hypothetical reaction mechanism for chemical energy coupling in chloroplasts and mitochondria has been provided (Jagendorf and Uribe, 66; Slater, 71).

Despite extensive research over many years, all efforts to isolate the hypothetical high energy phosphorylated chemical intermediate have failed (Boyer et al., 75). The chemical intermediate model requires direct contact at some stage, between electron transport components and the CF complex. No evidence exists for any such direct influence by electron transport components nor for any direct physical interactions with CF (Mitchell, 72). In fact, the data reviewed in the preceding section which shows that CF is localized to the stroma thylakoids while photosystem II, which contains a coupling site, is localized in the distant grana thylakoids suggests the absence of such direct physical interaction. In addition, the experiments of Racker and Stoeckenius (74) in which bacterial membrane fragments provided a proton pump and separate mitochondrial membrane fragments in the same vesicles utilized the proton gradient for ATP

production are difficult to reconcile with the chemical intermediate theory. For these reasons, the chemical intermediate theory has retained fewer advocates in recent years, though the model must still be considered as current and cannot be ruled out at the present time.

iii. Conformational Coupling Theory

The basic premise in most views of oxidative and photosynthetic phosphorylation has been that energy from the oxidation-reduction reactions serves to form a high energy intermediate that is used for the formation of the terminal covalent anhydride bond of ATP from ADP and P_i. Recent experimental evidence has accumulated that the formation of ATP requires no energy input in the special environment of the ATP forming enzymes, CF in chloroplasts and F_1 in mitochondria. Rather, energy is needed for the release of a tightly bound, preformed ATP from the catalytic site. These concepts have led to the development of the conformational theory of energy coupling. The major tenents of this new theory are (Boyer, 74; Slater, 72; Jagendorf, 75; Boyer et al., 73):

1) Energy input is required for the release of tightly bound ATP from the enzyme active site, not for its synthesis. ATP synthesis occurs with little or no energy input in the special environment of the enzyme active site (of CF). Conditions favorable for energy-free ATP production are facilitated by the presence of a tight binding affinity for ATP at the active site.

2) Release of pre-formed ATP occurs via a protein conformational change. This process is the major energy requiring step of oxidative phosphorylation and photophosphorylation in photosynthetic organisms.

3) The protein conformational change is driven by direct coupling of the phosphorylation enzymes to the components of the electron transport chain which undergo oxidation-reduction induced conformational changes or by coupling to the transmembrane electrochemical potential.

Some of the experiments which have led to the development of these concepts will be reviewed below. It should be pointed out that additional applications of the concept of conformational changes to other biological systems (such as actomyosin in muscle contraction and active transport) have been offered (Boyer, 74).

The insensitivity of the P_i-H_2O exchange reaction to uncouplers can be explained most readily if little energy is needed to form ATP at the catalytic site (Boyer et al., 75), but energy is required for the release of the preformed ATP. Other major evidence supporting these hypotheses comes from the detection of energy linked conformational changes in CF, and from the characterization of tightly bound nucleotides and a novel sequence of nucleotide transformations on the pathway to ATP synthesis. This evidence will be reviewed below. Detailed mechanisms have been offered for the sequence of nucleotide transformations leading to ATP synthesis and the identification of the energy requiring steps (Harris and Slater, 75; Roy and Moundrianakis, 71b; Boyer et al., 75). These mechanisms differ in important details but experimental evidence is lacking

at this time to allow selection of the correct process.

The first indication that CF undergoes an energy linked conformational change was obtained by Ryrie and Jagendorf (71). Chloroplast membranes were illuminated in the presence of tritiated water (^3H_2O) and CF was isolated under dim green light in a tritium free medium. It was found that tritiation of CF occurred in the light but not in the dark and that uncouplers strongly inhibited the light induced tritiation. This tritiation results from the trapping of ^3H_2O or of ^3H on buried regions of the CF that can exchange with solvent under illumination, but not in the dark. Thus, CF undergoes light induced conformational changes which open up buried portions of the protein for exchange with solvent water. The uncoupler sensitivity studies indicate that the conformational change is directly linked to the production of ATP on the enzyme.

In a subsequent study (Ryrie and Jagendorf, 72) it was shown that an acid-base transition or the induction of membrane bound Mg^{++}-ATPase activity was also sufficient to induce tritium uptake. The addition of ADP and P_i to the illumination mixture reduces the extent of labelling. The trapped tritium can be released by re-illumination in normal water. Approximately 45 to 90 atoms of ^3H are trapped per molecule of CF within 45 sec, which makes it likely that most of the tritium is trapped by exchange with hydrogen bonded to oxygen, nitrogen and sulfur atoms in amino acid side chains and peptide bonds in nonhelical regions. It was demonstrated that ATP hydrolysis per se, such as occurs in the Ca^{++}-ATPase activity of soluble CF, does not induce tritiation. The tritium incorporation also functions under conditions in which the net pH gradient is

minimized, which indicates that the membrane potential component of electrochemical gradient may drive the conformational change.

Independent evidence for the conformational change was obtained from an examination of the ratio between the internal hydrogen ion concentration and the rate of electron flow verses pH. At an internal pH of 7.0, the internal proton concentration is a linear function of the rate of electron flow up to saturation. At pH 8.1, the linear relation holds only for values of ΔpH below 2.9 units. It was suggested that the conformation of CF is altered at high external pH values and that this leads to an increased proton efflux from the internal space. (Portis et al., 75).

Treatment of chloroplasts with N-ethymaleimide (NEM) in the light, but not in the dark, leads to a partial inhibition of phosphorylation. NEM is a covalent cysteine label which was shown to react with CF. Uncouplers largely prevent the light induced inhibition. ADP and ATP were shown to partially protect CF from the inhibition. It was suggested that light induces a conformational change in CF which exposes groups for labelling by NEM (McCarty et al., 72). In a subsequent study, it was shown that light induces a labelling of the γ subunit of CF by NEM and that this is the only subunit labelled exclusively in the light. Uncouplers or the presence of ADP with P_i will largely abolish the γ subunit labelling (McCarty and Fagan, 73).

CF can be covalently labelled with the amine label fluorescamine while on the thylakoid membrane. Illumination causes a shift in the emission peak of the label from 500 to 463 nm. This is interpreted as a light

induced change in the label's microenvironment to a more hydrophobic form. This study provides additional evidence for the presence of a light induced conformational change in CF (Kraayenhof and Slater, 74).

Since ADP and P_i are the substrates for photophosphorylation while ATP is the final end product, it has been long assumed that the mechanism for ATP production is a straightforward addition of the terminal phosphate group to ADP. It has been the surprising result of recent experimentation that the reaction mechanism for ATP production is considerable more complex and involves the participation of a number of transformations of the three nucleotides, AMP, ADP, and ATP. The evidence for this viewpoint will be presented below. A re-assignment of the energy requiring step of photophosphorylation to the release of pre-formed ATP has occurred concommitantly with this research, and serves as an important element of the conformational coupling theory.

Most recent papers on these nucleotide transformations and the role of energy input have overlooked the fact that the essential outline of this new picture of photophosphorylation was obtained in an elegant series of experiments by Roy and Moudrianakis (71a, 71b) several years ago. Much of their data has been recently 'rediscovered' with little or no credit to the original work. In their first paper, Roy and Moudrianakis (71a) discovered that purified CF in solution slowly forms tight complexes with ^{14}C-ADP. The bound, radioactive nucleotide was released by complete denaturation of the protein in 10 M urea. Most of the counts were recovered as ^{14}C-ADP, but a significant portion of the radioactivity was recovered as ^{14}C-ATP and as ^{14}C-AMP indicating that a transphosphorylation

reaction of the form: 2 ADP →ATP + AMP had occurred in solution on the enzyme without any energy input. It was discovered that the resulting ^{14}C-AMP was not as tightly bound as the other nucleotides and was slowly released into solution but that denaturation was necessary to destroy the tight complex between CF and ^{14}C-ATP or ^{14}C-ADP. When ADP which is labelled in the β position with ^{32}P is added to CF in solution, enzyme bound ^{32}P-ATP is produced which is labelled to the same extent in both the β and γ positions. This data is again consistent with the transphosphorylation mechanism: 2 AD^{32}P → AMP + AT^{32}P (doubly labelled). Illumination of chloroplast membranes in the presence of labelled AMP and P_i let to the production of labelled ADP which indicates that AMP is the earliest acceptor of P_i in photophosphorylation. In a later work (Roy and Moudrianakis, 71b) the authors demonstrated that the formation of enzyme-bound ADP from AMP and P_i is strictly dependent on photoinduced electron transport. The authors described a model of phosphorylation in which ADP is produced by direct phosphorylation of AMP and the end product, ATP, is produced in a transphosphorylation reaction between two ADP molecules (2 ADP → AMP + ATP).

A recent study by Harris and Slater (75) has repeated many of the observations of Roy and Moudrianakis and supplied several novel observations. It was shown that labelled P_i exchanges with both the β and γ positions of ATP upon illumination of chloroplast membranes in the presence of Mg^{++}, This evidence suggests that AMP is an early phosphate acceptor <u>in vivo</u>. The authors also demonstrated that the major end product of phosphorylation in the presence of ADP and $^{32}P_i$ is γ labelled ^{32}P-ATP. Under these circumstances, however, the presence of β and γ

doubly labelled ATP in a form that was tightly bound to CF and not released into solution was detected (in agreement with the data of Roy and Moudrianakis, 71a). This evidence indicates that direct sequential phosphorylation of AMP, and then ADP cannot be the mechanism for net ATP synthesis.

Strotmann et al. (76) reported that CF is the only tight binding site for ADP in chloroplast membranes and that either a pH jump (acid-base transition) or illumination in the presence of ^{14}C-ADP causes the release of ^{14}C-ADP, ^{14}C-AMP and ^{14}C-ATP into solution. This release is inhibited by DCMU or the presence of uncouplers. Such data is obviously consistent with the assignment of ATP release from CF as an energy requiring step in the Conformational Coupling model. Boyer et al. (75) report that both ADP and ATP show $^{32}P_i$ uptake in illuminated chloroplasts and that at the onset of illumination, AD^{32}P is formed initially at levels greater than AT^{32}P. This evidence also is consistent with the assignment of AMP as the earliest phosphate acceptor during photophosphorylation.

A number of models have been proposed for the mechanism of ATP production based upon these data (Roy and Moudrianakis, 71b; Harris and Slater, 75; Boyer et al., 75) but they all differ in important details. This research area is very active at present and the sequential mechanism for ATP production should soon be established.

The large body of convincing evidence reviewed above for the Chemiosmotic and Conformational Coupling theories should be seen as supporting additive rather than alternative concepts in energy coupling (Strotmann et al., 76). These theories combine into the following current view of energy transduction:

1) Electron transport is coupled to the production of a proton electrochemical gradient across the chlorplast thylakoid membrane.

2) The transmembrane electochemical gradient is coupled to the production of ATP on the Coupling Factor via a protein conformational change which releases tightly bound ATP.

3) Tightly bound ATP is produced on the Coupling Factor in a trans-phosphorylation reaction which requires little or no energy input.

Preliminary views have been provided in the discussions above for the mechanism of the electrochemical proton pump, the nature of the conformational changes in CF and the sequence of reactions leading to net ATP synthesis. The detailed mechanism of these events should be established in the near future. A remaining mystery in this picture of energy transduction is the mechanism by which the transmembrane electrochemical proton gradient induces a conformational change in CF. Some evidence relating to this question has been obtained in this thesis research and will be presented in later chapters.

Fluorescence Probes

Fluorescence probes have long been used as sensitive reporter groups in biological systems (see for example: Stryer, 68; Radda and Vanderkooi, 72; Steiner and Edelhoch, 62; Steinberg, 71). Various physical properties of these probes can be used to extract information about the microenvironment surrounding their binding sites. Fluorescence probes are especially adept at detecting changes in their microenvironment (Radda and Vankerkooi, 72, and as such, they have frequently been used to detect conformational

changes in biological systems.

The primary aim of this thesis research has been to introduce a fluorescent label onto CF in a well defined manner and characterize it to gain insight into the structure, conformational dynamics and biological energetics of CF. A covalent fluorescent label was chosen for this study to avoid any ambiguities about the location of, or changes in, the fluorophore binding site. The use of precisely positioned reporter groups has enabled us to provide information, at the subunit level, of the nature of conformational changes experienced by CF. Such information has not been available with other, low resolution techniques (Ryrie and Jagendorf, 71; 72). In addition, the use of fluorescence lifetime determination has enabled us to extend the accuracy, sensitivity, and resolution of the fluorescence probe technique to gain additional biochemical/biophysical insight. We have constructed a novel single photon counting fluorescence lifetime system for these fluorescence probe studies which has proven to be five times faster than any previous such system (Leskovar et al., 76; Hartig et al., 76). As an introduction to the design and use of this novel system, which is described in later chapters, a brief introduction to the art and science of fluorescence lifetime determination will be provided.

Fluorescence Lifetimes

Excellent review articles exist on the three major methods of fluorescence lifetime determination: the phase shift method (Birks and Munro, 67; Spencer and Weber, 69; Ware, 71), the picosecond mode locked laser method (Alfano and Shapiro, 73; Eisenthal, 75; Netzel et al., 73;

Rentzepis, 73) and the single photon counting technique (Ware, 71; Knight and Selinger, 73; Yguerabide, 72). The interested reader is referred to these articles for a detailed investigation of each lifetime measurement technique. Since single photon counting has been used in this thesis work, a brief description of the methodology will be provided here.

A weak flash of exciting light from a spark gap light source is used to excite fluorescence in a sample. A photomultiplier is placed at right angles to the light source with suitable filters or monochromators to view the fluorescence emitted by the sample. If the fluorescence intensity striking the photomultiplier is attenuated so that on the average only one photon of fluorescence is recorded by the photomultiplier per exciting light pulse, then it is possible to design digital photon counting circuits which will very accurately record the time of arrival of that fluorescence photon at the photomultiplier relative to the starting time of the excitation light pulse. If the exciting light is flashed repeatedly on the sample (approximately 5000-15000 times per second) and the time of arrival of the fluorescence photon is recorded after each flash, then a probability profile in time for the emission of that fluorescence photon following the lamp flash can be built up. The probability as a function of time for the emission of a single photon (built up by repeated determinations of the arrival time of the one photon following a flash) is identical to the probability profile for the emission of the entire cascade of fluorescence photons that are emitted following a single exciting light pulse. Thus, single photon counting will allow us to determine the time profile of fluorescence emission by repeated sampling of the emission time of single photons. It is not possible to measure directly the

time profile of fluorescence emission from all photons following a single flash because the intrinsic response times of the photomultiplier and amplifier circuits involved are too long to yield accurate spectra. Thus the indirect photon counting method is used.

Photon counting offers important advantages in studies of biological fluorescence and biological probes. An extremely high signal to noise ratio is inherent in photon counting and this allows the experimenter to record fluorescence decays accurately over many decades of intensity. This wide dynamic range enables the experimenter to detect the presence of low levels of fluorescence emission that have a lifetime different than the primary emission. This multicomponent lifetime capability is especially suited to biological probe studies where the presence of different binding sites for the probe may reveal themselves by different emission lifetimes in each microenvironment. A multicomponent lifetime analysis permits the experimenter to monitor the activities occurring at each microsite.

The photon counting system built for this thesis research was designed to extend the short lifetime limit of photon counting by a factor of five. This improved time resolution makes the analysis of multicomponent spectra much more accurate. In addition, the short lifetime capability enables the experimenter to study highly quenched fluorophores (such as chlorophyll in situ) that are normally studied by laser techniques which are subject to artifacts from the very high light intensities required. The improved lifetime system will be described in later chapters along with its application to studies on fluorescent labelled CF.

II. ISOLATION AND CHARACTERIZATION OF COUPLING FACTOR

II. ISOLATION AND CHARACTERIZATION OF COUPLING FACTOR

Introduction

A protein fraction enriched in chloroplast coupling factor (CF) was first obtained from an acetone extract of chloroplasts. Vambutas and Racker (1967) isolated a trypsin activated Ca^{++}-ATPase activity from a dried acetone extract of chloroplasts which was resuspended in buffer and fractionated by cycles of ammonium sulfate and protamine sulfate precipitation. Their investigation demonstrated that the coupling factor activity was purified along with the latent ATPase activity in these samples. Soon, other purification procedures were developed, based on the observation that EDTA (a divalent cation chelating agent) caused a preferential release of the ATPase enzyme (CF) from the chloroplasts into the bathing solution (Avron, 1962; McCarty and Racker, 1966; Chang and Kahn, 1966). A highly purified CF preparation was obtained by extraction of broken chloroplasts with 1 mM EDTA followed by precipitation in ammonium sulfate, dialysis against DTT and centrifugation on a sucrose density gradient (Howell and Moudrianakis, 1967; Karu and Moudrianakis, 1969).

The first report of purification of CF to homogeneity was published in 1970 (Farron and Racker, 1970) followed by a detailed report of the purification procedure (Lien and Racker, 1971b). This procedure involved EDTA extraction of washed, osmotically shocked chloroplast membranes followed by ion exchange chromatography of the extract on batch gradient and continuous gradient columns using ammonium sulfate as the gradient ion.

The CF enriched fraction was purified to homogeneity by centrifugation on a linear sucrose density gradient. Ion exchange chromatography and pH precipitation of the EDTA extract was utilized to prepare homogeneous CF in a recent procedure (McEvoy and Lynn, 1973). A significant simplification of these purification procedure resulted from the observation that contaminating proteins (primarily ribulose-1-5-carboxylase)are removed preferentially from chloroplast membrane fragments by repeated washings in dilute sodium pyrophosphate and that a subsequent treatment of the membrane with a hypotonic sucrose solution causes the CF to be released to the supernatant in a highly purified form (Strotmann, Hesse, and Edelmann, 1973). This observation led to our development of an improved large scale technique for the purification of CF that will be described in this chapter.

Isolation of Coupling Factor

Our earliest attempts to isolate the coupling factor were based on the procedure of Lien and Racker (1971b). A block diagram of this technique is shown in Figure 2-1. The isolation requires approximately 6 days and results in a yield of approximately 10 mg of purified CF from 800 mg of spinach leaves (obtained from approximately 2 kg of spinach). All of our isolations utilized fresh, locally obtained market spinach. A detailed description of our procedure appears later in this chapter. The purified CF reamins catalytically active without significant loss of ATPase activity for at least 4 months when it is stored at 4° C in a precipitated form in 2 M ammonium sulfate.

BLANK PAGE

Figure 2-1

CF ISOLATION - EDTA EXTRACTION METHOD

Washed de-veined SPINACH (800 g)

↓ Centrifugations

Isolate CHLOROPLASTS in isotonic tricine, sucrose, NaCl

↓ Osmotic shock

Suspend chloroplasts in 10 mM NaCl

↓ Centrifuge 20,000 g

Suspend in 0.75 mM EDTA

↓ Centrifuge 20,000 g

Retain supernatant as CF EXTRACT

↓ Bind to DEAE Sephadex A-50 in 80 mM $(NH_4)_2SO_4$

↓ Wash the bound CF with 100 mM ammonium sulfate

↓ Elute with 280 mM ammonium sulfate

Precipitate CF in 50% saturated ammonium sulfate as COLUMN I CF

↓ Centrifuge and re-dissolve in 80 mM ammonium sulfate

↓ Bind to second DEAE Sephadex A-50 column

↓ Wash with 0.12 M ammonium sulfate

↓ Elute in a linear gradient of 0.12 M to 0.30 M ammonium sulfate

Precipitate CF in 50% ammonium sulfate, add ATP, store as COLUMN II CF

↓ Centrifuge in 5-20% sucrose linear gradient for 12 hr

Retain electrophoretically homogeneous fraction as SUCROSE GRADIENT CF (20 mg)

Fig. 2-1. Coupling factor isolation--block diagram of the EDTA extraction procedure. Details are provided in the text.

To obtain high yields in the isolation, careful attention must be paid to certain experimental details. The upper layers of the chloroplast pellets obtained during the centrifugations tend to be soft and oily in nature and can be easily resuspended if they are disturbed. For this reason, all supernatants are removed by careful vacuum pipetting. In addition, the centrifuge rotors are often subject to vibrations at low rotor speeds during deceleration. To minimize this effect, the rotors must be clean and dry, and the bottles carefully matched and equilibrated by weight before each run.

The yields of protein obtained at various stages during a typical isolation by this EDTA extraction procedure are shown in Table 2-1. The isolation stages correspond to the underlined fractions in Figure 2-1. For purposes of comparison, the yields reported by Lien and Racker (1971b) are shown in an adjacent column. Our yields by this method are generally about 50% lower than the values reported by the Cornell group.

While this investigation was in progress, a report appeared in the literature of a new isolation technique based upon a simple sequence of washes in buffers of different compositions (Strotmann et al., 1973). In this study, the authors claimed that a small amount of coupling factor could be obtained in homogeneous purity if chloroplasts were subjected to a sequence of four washes in dilute sodium pyrophosphate solution followed by suspension of the pellet in a dilute buffer solution containing 300 mM sucrose. The pyrophosphate acts as a chelating agent for divalent cations which will extensively remove divalent cations from the pellet during four washes, but the CF is prevented from leaving the membrane surface by the high concentration of sodium counterions present in the

Table 2-1 Yield data for the various CF isolation procedures. The isolation stages coincide with the various fractions described in Figures 2-1 and 2-2. The Lien and Racker data was obtained from Lien and Racker 1971b.

	YIELD		
ISOLATION STAGE	LIEN and RACKER	EDTA Extraction	Pyrophosphate Wash
Chloroplasts	200 mg chlorophyll	149 mg chlorophyll	184 mg chlorophyll
CF Extract	162 mg protein	83 mg protein	157 mg protein
Column I CF	63 mg protein	28 mg protein	39 mg protein
Column II CF	39 mg protein	17 mg protein	--------
Sucrose Gradient CF	23 mg protein	11 mg protein	19 mg protein

pyrophosphate buffer. When the sodium counterions are removed by the final wash in the sucrose and buffer solution, the coupling factor is released from the chloroplast thylakoid membrane and appears in the supernatant. The authors also state that the major contaminating protein, RuDP carboxylase, is removed from the pelleted membrane fraction during the pyrophosphate washes and is retained in the membrane fraction during the sucrose and buffer wash.

In an attempt to speed up the isolation procedure and increase the yields, we developed a large scale isolation procedure for coupling factor based upon this pyrophosphate wash procedure. In contrast to the studies of Strotmann, et al. we did not find that CF was released in homogeneous purity following this procedure. It must be pointed out, however, that the German group does not report concentrations of chloroplasts or volumes of buffer used in the washes so that our procedure may be quite different. In addition, significant contamination of the CF-rich supernatant with chloroplast fragments was always obtained, as indicated by a slight green color in the supernatant. A batch-gradient anion exchange chromatography step was introduced at this point to remove the contaminating chloroplast fragments and further purify the CF extract. Following this step, CF was obtained in high yield and with a purity equivalent to the Column II CF fraction from the EDTA extraction isolation procedure. This purified CF fraction was further purified by a final sucrose gradient centrifugation to yield nearly homogeneous (> 95% pure) CF. This overall pyrophosphate wash method can be performed in 4 days which represents a significant savings in time (and thus a lesser degradation of CF during the isolation) over the EDTA extraction procedure.

A block diagram of this pyrophosphate wash procedure is shown in Figure 2-2 and the detailed procedure is presented later in this chapter. All experiments reported in this thesis were performed with, or verified by, CF which had been isolated by this pyrophosphate wash procedure.

In Table 2-2 we present data on the yield of protein released to the supernatant during the sequential pyrophosphate washes. Strotmann et al. (1973) reported that no further protein was released after two sequential washes. We find that large amounts of protein are released during the first wash and a twenty-fold lower amount of protein is released at a constant level in each of the following washes. The amount of CF which is released during the sucrose extraction which follows the fourth wash is approximately 10-fold higher than the level of impurity proteins (primarily RuDP carboxylase) which are released in the fourth wash. Thus, we find that continued washings of the chloroplast pellet does not lower the level of contaminating proteins below that obtained after one or two washings, and that this represents the limit on the purity of coupling factor which can be obtained by pyrophosphate washes alone.

The protein yields obtained at various stages of the pyrophosphate wash isolation procedure are shown in the last column of Table 2-1. As the table demonstrates, the yields obtained by this procedure are much higher than the yields obtained by the EDTA extraction procedure in our hands. Our yields from the pyrophosphate wash procedure are quite comparable to the yields obtained by Lien and Racker (1971b).

Fig. 2-2

CF ISOLATION-PYROPHOSPHATE WASH METHOD

Spinach

↓ Wash, devein, grind

↓ Centrifugation, washes

Retain chloroplast pellet

↓ Wash 4 times in 10 mM sodium pyrophosphate, pH 7.4

Retain CF-rich pellet, discard RuDP carboxylase-rich supernatants

↓ Suspend in 0.3 M sucrose, 2 mM tricine, pH 7.4

↓ Centrifuge

Retain supernatant as CF Extract

↓ Bind to DEAE Sephadex A50 in 80 mM ammonium sulphate

↓ Wash with 100 mM ammonium sulphate

↓ Elute with 280 mM ammonium sulphate

Retain Column I CF eluant

↓ Centrifuge on 5-20% sucrose density gradient for 12 hours

Retain pure fractions (> 95% pure) as Sucrose Gradient CF

Fig. 2-2. Coupling factor isolation--block diagram of the pyrophosphate wash procedure. Details are provided in the text.

BLANK PAGE

Table 2-2 Protein released to the supernatant during sequential washes of chloroplasts in pyrophosphate buffer. The buffer contained 10 mM sodium pyrophosphate pH7.4. Immediately following the fourth wash, 157 mg of protein was obtained as the "CF extract" when the washed pellet was resuspended in 0.3 M sucrose, 2 mM Tricine-NaOH pH7.4.

PROTEIN RELEASED IN PYROPHASPHATE WASHES

Wash Number	Milligrams of protein released
1	390
2	21
3	23
4	17

Purity of Coupling Factor

The final stage in both isolation procedures is a linear sucrose density gradient centrifugation. This centrifugation separates CF from a faster moving band of impurity proteins. Following the run, the gradient is separated into a number of fractions by puncturing the bottom of the tubes and collecting drop fractions. A rough estimate of the amount of proteins in each fraction can be obtained by monitoring the intensity of the fluorescence emission between 300 and 350 nm in the region of emission by aromatic amino acids. Figure 2-3 shows the fluorescence emission intensity in the fractions obtained from a typical sucrose gradient run. The separation of the sample into a pure CF sample from fractions 5 to 10 and an impurity fraction from fractions 1 to 3 is clearly seen.

The difference in composition between the impurity fractions and the pure CF sample is clearly seen from the data presented in Figures 2-4 and 2-5. In Figure 2-4, the distinctive difference between the protein fluorescence emission spectra of the two samples is recorded. The impurity fractions show a broad transition which peaks at 328 nm. This type of emission spectrum is observed from a majority of proteins and is characteristic of any protein which contains tryptophan residues, which tend to dominate the emission characteristics. The pure CF sample shows an unusual protein emission spectrum with a narrow bandwidth and a peak at 303 nm. This type of emission spectrum is characteristic of tyrosine residues and is generally observed only in those proteins which contain no tryptophan (Konev, 1967). An amino acid analysis of CF has been performed (Farron, 1970, Farron and Racker, 1970) which shows that this protein contains approximately 84 tyrosine residues but no tryptophanes. This unusual, tryptophan-free emission spectrum of CF has been incorporated

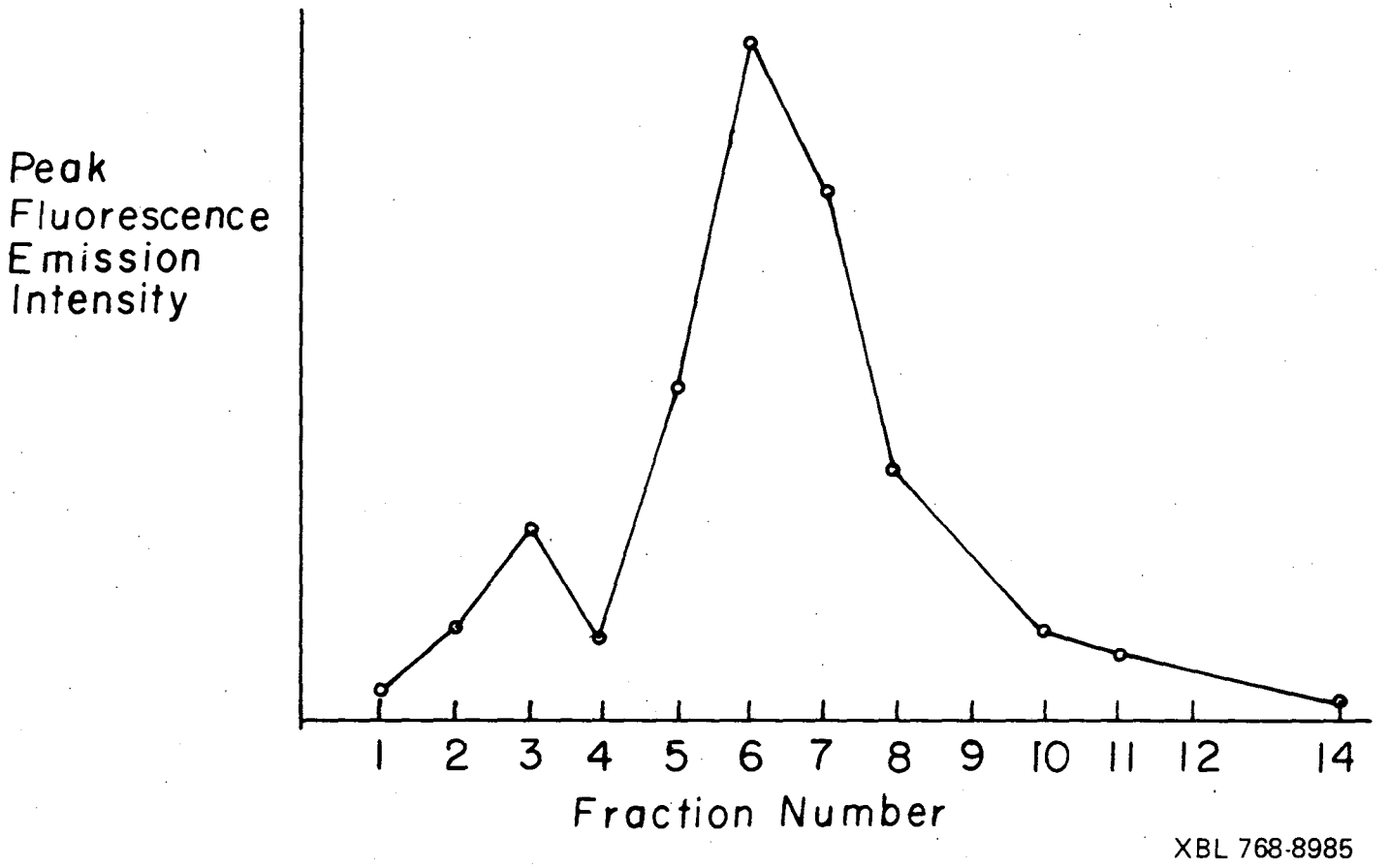
Peak
Fluorescence
Emission
Intensity
1 2 3 4 5 6 7 8 9 10 11 12 14
Fraction Number
XBL 768-8985

Fig. 2.3

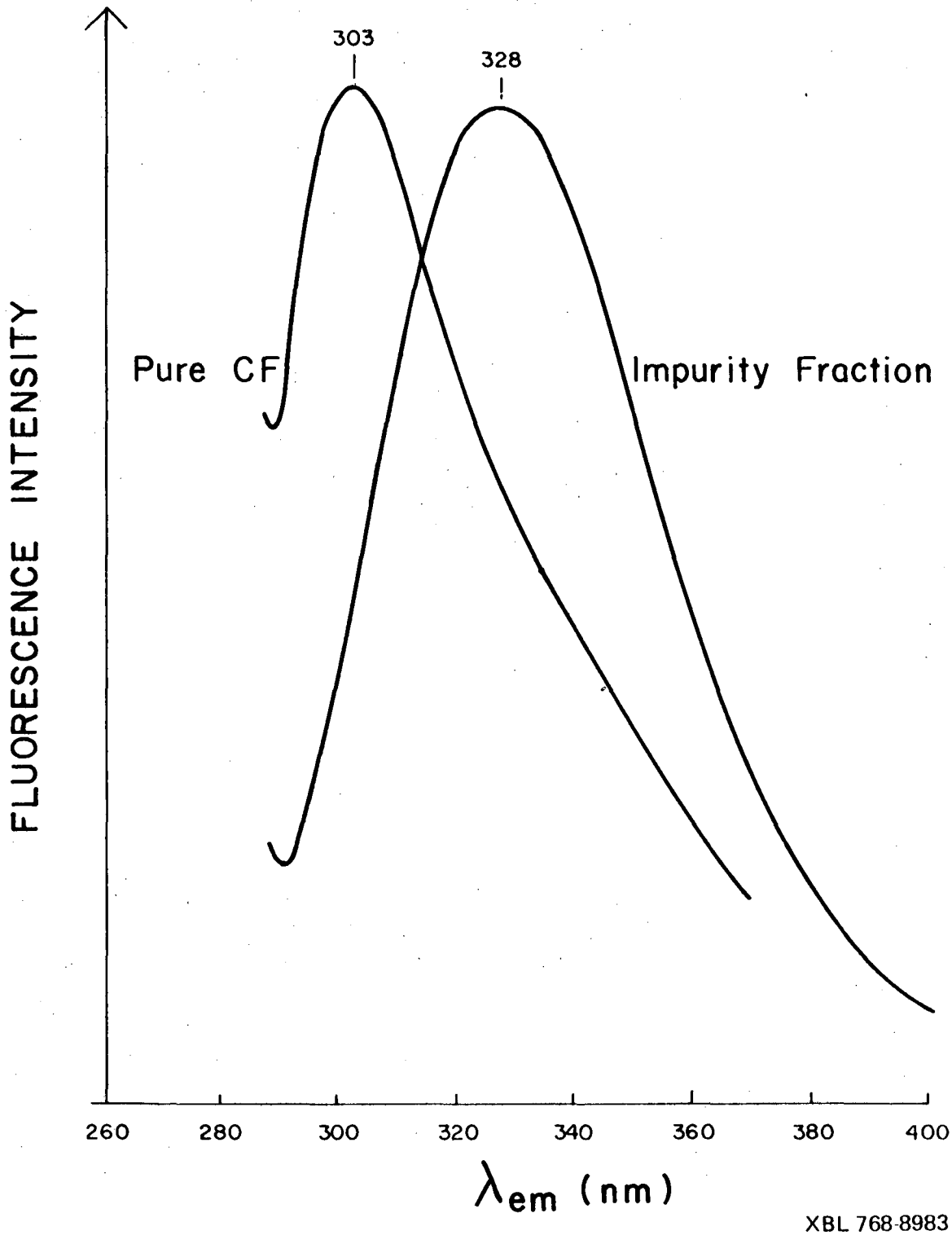
303
328
Pure CF
Impurity Fraction
FLUORESCENCE INTENSITY
260
280
300
320
340
360
380
400
λem (nm)
XBL 768-8983

Fig. 2.4

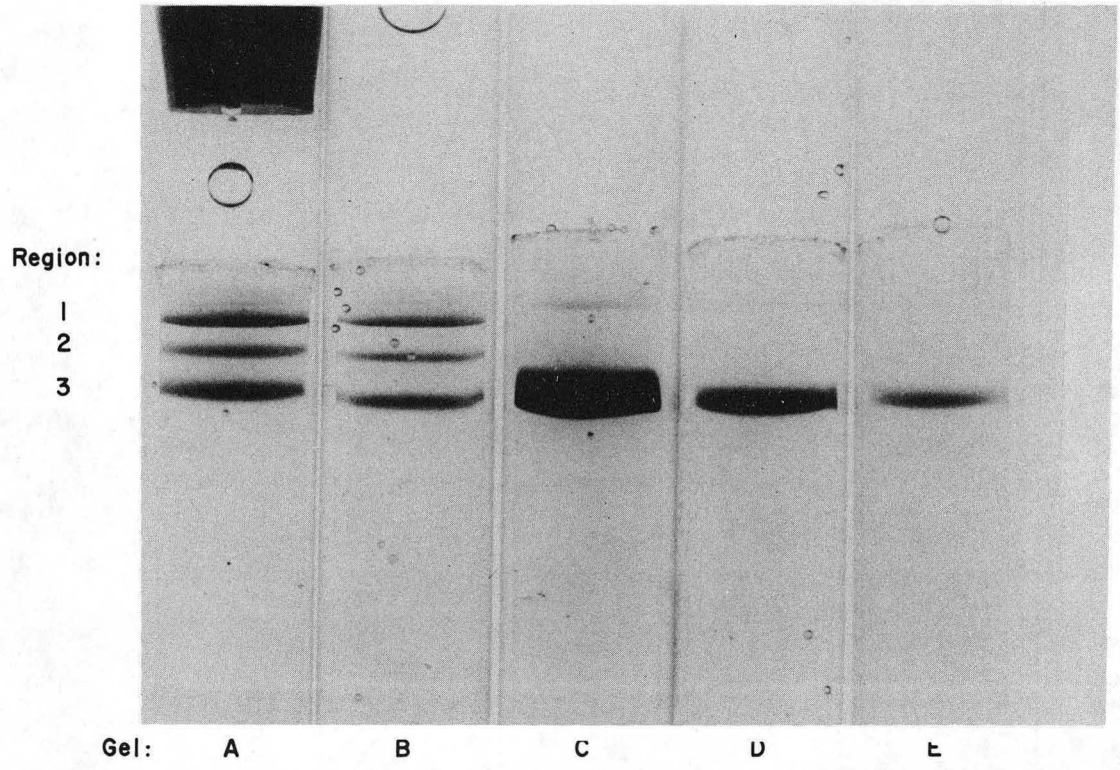

XBB 732-1503

Fig. 2.5

into a convenient assay for the purity of CF which measures the ratio of the emission intensity near 303 nm where tyrosine emission dominates to the emission intensity at 350 nm where tryptophan dominates (Lien and Racker 1971b). Unfortunately, the authors do not provide any information on the fluorometer, light source, or photomultiplier that they used to measure the emission ratio of purified CF. Since the measured fluorescence intensity will strongly depend on the wavelength sensitivity characteristics of the particular photomultiplier used and on the spectral emission properties of the excitation light source, we cannot compare our data to theirs for purified CF. Instead, we have developed a well defined fluorescence emission assay (described later in this chapter) and calibrated our assay against polyacrylamide gel electrophoresis assays of the purity of CF which provide an independent test of purity.

Figure 2-5 shows the staining pattern of a nondenaturing gel electrophoresis run on samples of pure CF and of impurity fractions. Gels A and B contain impurity fractions and gels C, D and E contain pure CF samples. Coupling factor appears in region 3 of the gels. Gel C, which contains a heavy loading of pure CF, shows a trace of a weak secondary band near region 1. This slow moving band has been seen in other reportedly 'homogeneous' preparations of pure CF and has been attributed to an aggregate of CF (Farron, 1970). In our case, at least, the minor band is more likely an impurity. The highest fluorescence emission ratio (E_{303}/E_{350}) that we have recorded was 2.7 which was obtained from several fractions on the trailing edge of the main CF peak in the sucrose gradient centrifugation. The fluorescence emission ratio of the pure CF sample used for Figure 2-5 was approximately 2.5, which is a typical value obtained from an isolation. Since the fluorescence emission ratio is lowered

by the presence of tryptophan-containing proteins, we believe that 2.7 is the fluorescence emission ratio of absolutely pure CF and that the 'pure CF' samples from the sucrose gradient runs contain a small amount of other proteins.

The absolute purity of the pure CF fractions can be estimated by taking a densitometry scan of the stained bands from the gel electrophoresis run. A densitometry scan of the pure CF gels from Figure 2-5 shows that the main band contains approximately 95% of the staining density. For this reason we estimate the purity of this sample to be approximately 95%. The CF samples used for all experiments reported in this thesis were generally 95% or better in purity as demonstrated by gel electrophoresis and/or fluorescence emission ratios.

Activity of Coupling Factor

i. ATPase Activity

Coupling factor, as isolated from chloroplasts, exhibits no independent catalytic activities. In this native state, CF can be added to membranes which have been partially stripped of the photophosphorylation enzyme by uncoupling agents to yield a restoration of the ATP generating capability of the photosynthetic membranes (Vambutas and Racker, 1965; Lien and Racker, 1971a). The soluble enzyme exhibits an ATPase activity if it is briefly exposed to trypsin (Vambutas and Racker, 1965). This exposure to trypsin, which unmasks the ATPase activity, simultaneously destroys the ability of CF to couple to the membrane to restore photophosphorylation (Bennun and Racker, 1969). It has been shown that the

ε subunit of CF is very sensitive to trypsin digestion and that the presence of this subunit will inhibit the ATPase activity of CF. (Nelson et al., 1972). The ε subunit is not, however, necessary for the coupling activity of CF (Nelson et al., 1972) so its destruction is not responsible for the failure of the activated ATPase to restore photophosphorylation.

Trypsin activation of the ATPase activity of CF provides a convenient, albeit somewhat indirect, assay for the catalytic integrity of CF. Early work on purified CF indicated that the specific activity of the purified enzyme is in the range of 23 to 34 micromoles of ATP hydrolized/min/mg of protein (McEvoy and Lynn, 1973; Deters et al., 1975,; Lien and Racker 1971b) when the enzyme is activated by trypsin digestion. If the enzyme is activated by heating in the presence of DTT, then specific activities in the range of 34 to 47 micromoles ATP/min/mg protein are recorded (Lien et al., 1972; Nelson et al. 1972a). For convenience, we have used the trypsin activation method for our ATPase assays.

Table 2-3 shows the specific ATPase activities of CF obtained from a number of different isolations, The specific activities of our best preparations compare quite favorably with the literature values. The specific activities of CF obtained during other isolations by essentially the same method as was used for the most active preparations show an appreciably lower range of values. In reviewing these data, the only systematic variation which separates the isolations which yielded highly active CF from the lower activity isolations was the season of the year during which the isolation occurred. It appears that CF isolated from summer harvested spinach always yielded a higher specific activity. The

Table 2-3 Coupling factor trypsin-activated ATPase rates from various isolations. The activation and assay methods are described in the text. The best ATPase rates obtained are reported for each isolation.

SEASONAL VARIATION OF THE CF ATPase RATE

Date Isolation Began	ATPase rate in μmoles P_i/min-mg protein
Nov. 9, 1973	18.0
Jan. 31, 1974	18.6
June 26, 1974	29.3
Jan. 8, 1975	14.1
June 25, 1975	25.3

data are not extensive enough to prove this contention, but it is consistent and highly suggestive. There is precedent in the literature for seasonal variations in biological activities in chloroplasts. Walker (1971) found that summer chloroplasts contain much higher levels of ascorbate than winter chloroplasts. Jagendorf and Uribe (1971) found that the specific yield of ATP produced by an acid to base transition is much higher in summer chloroplasts than in winter chloroplasts. Winter chloroplasts yield 130 micromoles of ATP/mg chlorophyll while summer chloroplasts yield 240 micromoles ATP/mg chlorophyll. This ATP production obviously involves CF, and may represent another manifestation of the lower winter specific activity that we observe for the ATPase function of CF.

ii. Photophosphorylation Activity

The natural catalytic activity of CF is photophosphorylation. It was observed that CF could be added to chloroplast membranes which were uncoupled by EDTA treatment to restore partially the photophosphorylation activity (Vambutas and Racker, 1965). The restoration of photophosphorylation by CF is a rather involved and lengthy procedure and is not routinely used as the standard assay for activity. In addition, the restoration is not highly reproducible from day to day. We have conducted photophosphorylation studies with several CF preparations, however, and the results are quite comparable to data published in the literature, as will be shown.

The extent of recovery of photophosphorylation that can be obtained when CF is added back to uncoupled membranes correlates with the photophosphorylation activity retained by the uncoupled membranes (McCarty, 1971). For example, Shoshan and Shavit (1973) reported that chloroplasts

which lost approximately 99% of their photophosphorylation activity upon EDTA treatment exhibit a reconstitution of only about 10% when they are reconstituted with CF. Girault et al. (1971) observed that chloroplasts which lost 99.7% of their activity upon EDTA treatment show a reconstitution of only 12% upon incubation with CF. On some occasions a high loss of activity is followed by a moderate restoration of photophosphorylation. Girault et al. (1974) reported experiments in which a 99.7% loss was followed by a 29% restoration and a 99.0% loss was followed by a 23% restoration. These values fall in the range of typical reconstitutions reported in the literature. Lesser degrees of loss of activity during the EDTA treatment will lead to a stronger reconstitution of photophosphorylation during reconstitution. Girault et al. (1971) report that a 93% loss leads to a 35% restoration while an 83% loss leads to a 90% restoration of activity. These findings have also been verified by photophosphorylation studies on chloroplasts which have been uncoupled by treatment with silicotungstic acid (Lien and Racker, 1971a).

We have also observed this dependence of the success of reconstitution upon the degree of loss of activity during EDTA treatment. In Table 2-4 we give the photophosphorylation rates and reconstitution efficiencies from several experiments. The rates that we observe agree with the literature values both in their absolute values and in the dependence of the reconstitution on the degree of activity loss upon EDTA treatment. These photophosphorylation studies complete the demonstration that the CF which we isolate and have used for the experiments in this thesis is extremely pure and highly catalytically active.

Table 2-4 Reconstitution of photophosphorylation by purified coupling factor. Chloroplasts are uncoupled by treatment with EDTA and photophosphorylation is restored by addition of purified coupling factor and Mg^{++}. Typical experimental values are shown. The extent of reconstitution that can be obtained increases as the extent of loss of activity upon EDTA treatment decreases.

PHOTOPHOSPHORYLATION RATE in μmoles ATP/hr/mg chlorophyll

Chloroplasts	EDTA treated chloroplasts	% loss upon EDTA treatment	Reconstituted with CF	% Reconstitution
587	0.3	99.9%	23	4%
484	7.2	98.5%	96	20%
467	11.6	97.5%	134	29%

On rare occasions, reports have appeared that nearly complete reconstitution of activity can be achieved with EDTA chloroplasts which have lost nearly all of their activity. Lynn and Straub (1969) reported nearly 100% reconstitution but the absolute rates of their chloroplast samples were not reported and only sketchy experimental details are provided. Shoshan and Shavit (1973) reported a 98% restoration of activity following a 96% loss during EDTA treatment. These authors reported that rapid processing of the samples and use of high concentrations of chlorophyll during the incubation were the essential conditions which allowed them to achieve these high reconstitutions. This report is the only well documented study in the literature claiming high rates of reconstitution following extensive loss during EDTA treatment. Unfortunately, no verification of these findings has appeared in the literature. In addition, a report has appeared which fails to confirm their findings (Girault et al., 1974). Experiments in our laboratory have also failed to reveal any improvement in the extent of reconstitution when high chlorophyll concentrations are used during the EDTA incubation. In light of these findings, we must conclude that it is not possible reproducibly and extensively to deplete the chloroplasts of CF and restore full photophosphorylation activity by reconstitution with CF. A possible explanation for this annoying failure will be discussed later.

It has been observed both in the literature and in our laboratory that an experiment will occasionally yield high rates of reconstitution following extensive loss during EDTA treatment. Unfortunately, the conditions necessary for this achievement have not been identified, and it

remains an occasional, uncontrolled occurrence. The experiment is important, however, because it demonstrates that CF remains fully catalytically active during its isolation, and it is the sole protein factor needed to restore full photophosphorylation to chloroplasts which have been extensively inactivated by EDTA treatment, which removes most of the CF from the membrane. Girault et al. (1974) report one experiment in which they observed a 79% restoration of activity following a 99.0% activity loss upon EDTA treatment. In the best experiment obtained in our laboratory, an 86% restoration of activity was observed following a 97.2% activity loss upon EDTA treatment.

Treatment of chloroplast membranes with EDTA causes approximately 50-70% of the CF to be released from the membranes into the supernatant (McCarty and Racker, 1967). Associated with this partial loss of CF during EDTA treatment we find a nearly complete (90-99%) loss of photophosphorylation activity, as the data above have shown. The lack of proportionality between the extent of loss of CF from the membrane and the extent of inhibition of photophosphorylation may arise from a secondary effect of the removal of CF. Studies on the rate and extent of proton flow across the photosynthetic membrane indicate that extraction of CF opens a conductance channel for protons which effectively collapses the pH gradient across the membrane produced by electron transfer (McCarty and Racker, 1967; Schmid and Junge, 1974). This increased proton leakiness will effectively dissipate the storage of electron

transport energy in the form of a proton gradient.* In the chemiosmotic theory, the proton gradient (or another membrane potential) provides the energy for ATP synthesis. Dissipation of the pH gradient thus effectively uncouples the residual CF on the membrane from the electron transfer reactions even though the residual CF remains fully biochemically active. This dual effect of removal of CF can explain the lack of proportionality between the extent of CF removal and the extent of inhibition of photophosphorylation.

Recently, evidence has been obtained that EDTA treatment of chloroplast membranes does more than simply remove CF from the membrane. A second effect of EDTA seems to be an irreversible damaging of membrane functions (Girault et al., 1974). In light of these findings, we expect that incubation of EDTA treated membrane with fully active CF will not lead to a full restoration of photophosphorylation. Indeed, the level of photophosphorylation obtained after EDTA treatment may be sensitive to the EDTA damage suffered by the membranes as well as to the extent of removal of CF. In this case, we expect the extent of restoration of photophosphorylation activity upon reconstitution with CF to decrease as the extent of inhibition of photophosphorylation by EDTA treatment increases. This has been the situation observed in chloroplast membranes, as discussed

*Further support for this idea is provided by experiments with dicyclohexylcarbodiimide (DCCD). It was found that low concentrations of DCCD markedly stimulate photophosphorylation in EDTA treated chloroplasts. This stimulation is associated with an inhibition in the rate of pH decay, indicating that DCCD may act by blocking a proton pore exposed by removal of CF (McCarty and Racker, 1967; Uribe, 1972) thus activating the residual CF left on the membrane.

above. Thus, all of the observations on photophosphorylation activities mediated by CF that are presented in this section can be understood in terms of currently held views on the nature of energy conversion in chloroplasts.

Assays and Techniques

1. EDTA Extraction Procedure

This isolation procedure closely follows the technique outlined in Lien and Racker (1971b) with the following alterations:

A. The DEAE Sephadex beads were not pre-cycled by washing in acid and base. Sephadex literature indicates that this step is unnecessary. Furthermore, the concentrations of acid and base suggested by Lien and Racker could lead to partial hydrolysis of the beads (Pharmacia, 1971a; Lien and Racker, 1971). Pre-cycling should be initiated however, if difficulties are encountered with the flow rate, release of unpolymerized dextran from the beads, or the elution of other impurities from the beads.

An alternative gel preparation procedure was developed as follows: 27 g of dry Sephadex A 50 are swollen in 600 ml of 0.4 M Tris-SO_4, 0.5 M $(NH_4)_2SO_4$, pH 7.1, for 1 day at room temperature or 2 hr on a boiling water bath. This procedure effectively changes the gel counterion from chloride to sulfate. The gel is then agitated and fine particles are decanted from the rapidly sedimenting bulk of the gel, if necessary. The gel is rinsed with 20 mM Tris-SO_4, 2 mM EDTA, 80 mM $(NH_4)_2SO_4$, pH 7.1, and suspended in the same buffer. After 30 min, the buffer is drained to the level of the bed and approximately 1 bed volume of fresh buffer is

added. This cycle of suspension and drainage is repeated for a total of four suspensions.

The gel slurry is de-aerated under vacuum for 15 min with occasional gentle agitation. Vigorous stirring with a magnetic bar and the use of sintered glass bed supports are avoided to prevent damage to the beads. The slurry is carefully poured down a glass tube along the edge of the column to fill a 4.5×20 cm column and a 2.5×25 cm column. The gel is allowed to settle for 10 min after which a flow of the suspension buffer is initiated under a pressure head of approximately 30 cm. After the gels have settled under flow, the pressure drop is adjusted to an operating pressure of about 50 cm to yield a flow rate of approximately 1.5 ml/min and 1 ml/min for the large and small columns, respectively. After packing, each column is washed with two bed volumes of 20 mM Tris-SO_4, 2 mM EDTA, 1 mM ATP, 80 mM $(NH_4)_2SO_4$, pH 7.1, before use.

B. During the linear gradient elution of CF from the second DEAE Sephadex A 50 column, the CF is detected by its fluorescence emission rather than by the colorimetric method of Lowry et al. (1951). Since CF contains no trypophan residues (Farron, 1970), the bulk of its fluorescence emission arises in the tyrosine residues which emit maximally at 302 nm when excited at 280 nm (Lien and Racker, 1971). By contrast, most other proteins contain some tryptophan and show a fluorescence emission which peaks in the range of 320-350 nm. Thus, CF can be detected by its fluorescence emission at 302 nm, and the purity of the enzyme can be assayed by calculating the ratio of its fluorescence emission at 302 nm to the emission at 350 nm. Moderate degrees of scattering can be present

during these assays. Care must be taken to demonstrate that the Raman line from the excitation light does not interfere with the assay of protein fluorescence which occurs in the same spectral region. Using the Perkin Elmer MPF 2A fluorometer with a Hamamatsu R 106 phototube, the purest CF fraction attained to date (over 95% pure) exhibited a fluorescence emission ratio E_{302}/E_{350} of 2.7 (uncorrected) when excited at 280 nM.

C. The final purification step consists of a linear sucrose density gradient centrifugation. To improve the separation, the run is performed at a higher rotor speed and with smaller samples for a shorter centrifugation time than is recommended in Lien and Racker (1971b).

Column II CF is centrifuged for 15 min at 10,000 g at 20° C. The pellet is retained and resuspended in 2 ml of 20 mM Tris-SO_4, 2 mM EDTA, 1 mM ATP, pH 7.1. The resuspended CF is clarified by centrifugation in a desk top clinical centrifuge for 10 min. The supernatant is applied to a Sephadex G 50 column (0.7×15 cm). Desalted CF is collected in a volume of 3 ml, and 500 λ samples are carefully applied to the top of each of 6 sucrose gradient tubes.

The gradients are prepared in 1.3×9 cm cellulose nitrate tubes by the application of 500 λ of 70% sucrose in 20 mM Tris-SO_4, 2 mM EDTA, 1 mM ATP, pH 7.1 (7 g of sucrose is mixed with sufficient buffer to make 10 ml of solution) to the bottom of each tube as a cushion followed by a 5-25% linear sucrose gradient. The gradient is produced by introduction of 5.75 ml of 5% sucrose in 20 mM Tris-SO_4, 2 mM EDTA, 1 mM ATP, pH 7.1, to the reservoir chamber of a gradient generator (Martin and Ames, 1961)

which is fed into the mixing chamber containing 5.75 ml of 25% sucrose in the same buffer. The mixing chamber is swirled by a mechanical or magnetic bar stirrer and gradients are formed at the rate of about 1 ml/min by allowing the output solution of the gradient mixer to flow smoothly down the side of the cellulose nitrate tube. The pre-formed gradients are stable for 2 days in the cold (Martin and Ames, 1961) and are equilibrated to ± 0.1 g before application of the samples. The gradient tubes with CF samples applied are placed in the buckets of an SW 41 rotor and the buckets are sealed with Spinkote and rubber gaskets as recommended by the manufacturer. The rotor is run at 40,000 rpm for 12 hr at a temperature of 20° C.

At the termination of the run the tubes are individually removed and attached vertically to a clamp. The tube bottom is cleaned, punctured with a needle, and fractions collected in 15 drop increments (about 1 ml each). The fluorescence emission of each sample is checked, using a narrow cuvette, and a clear separation of a faster migrating impurity band emitting maximally at 320 nm from the CF band emitting at 302 nm is observed. Samples with a fluorescence emission ratio (302/350) of over 2.4 are pooled and added to an equal volume of 20 mM Tris-SO_4, 2 nM EDTA, 1 mM ATP, pH 7.1, which is made 4 M in $(NH_4)_2SO_4$ by addition of the dry salt. This pooled sample is stored at 4° C as Sucrose Gradient CF.

ii. Pyrophosphate Wash Procedure

This method was developed from the isolation technique outlined in Strotmann et al. (1973). Supernatants are removed by suction pipetting to avoid disturbing the soft pellets. All pellets are resuspended by serial additions of the suspension buffer with stirring of the slurry by a rubber policeman (a small rubber tipped glass rod) to achieve uniform resuspension.

Rinse and de-vein 5 bunches (approximately 4.5 pounds) of market spinach to obtain approximately 800 grams of leaves. Fifty grams of leaves are chopped and placed in a Waring blender with 75 ml of isolation buffer (0.3 M sucrose, 10 mM sodium pyrophoshate, 20 mM tricine-NaOH pH 7.8). The blender is run for 15 sec and the homogenate is filtered through 8 layers of pre-rinsed cheese cloth. The process is repeated for all of the leaves and the liter of filtered homogenate is placed in 4 centrifuge bottles for the Sorval GSA rotor. All stages of the preliminary isolation (up to the extraction of CF in sucrose-tricine buffer) are performed in a cold room at 4° C or with the samples kept on ice.

Centrifuge the filtered homogenate at 4° C and 300 g (1400 rpm) for 2 minutes. Pour the supernatant into clean GSA bottles, discard the pellet.

Centrifuge the supernatant at 3000 g (4200 rpm) for 10 min. Discard the resulting supernatant and resuspend the pellets in a total of 500 ml of isolation buffer.

Centrifuge the suspension at 3000 g (4200 rpm) for 10 min. in two GSA bottles. Pipette and discard the supernatant. Resuspend the pellet in 500 ml of cold 10 mM sodium pyrophosphate pH 7.4. Stir the suspension

in the dark in the cold room (4° C) for 10 min with a magnetic stirring bar.

Centrifuge the suspension at 20,000 g (11,100 rpm) in two GSA bottles for 20 min at 4° C. Pipette and discard the supernatant. Resuspend the pellets in a total of 500 ml of cold 10 mM sodium pyrophosphate and repeat the centrifugation, supernatant removal and resuspension for a total of 4 washes in pyrophosphate. The supernatant should appear pale yellow following each centrifugation.

Following the last centrifugation and supernatant removal, resuspend the pellet in 500 ml of 0.3 M sucrose, 2 mM tricine-NaOH pH 7.4. Use room temperature sucrose-tricine buffer and perform all subsequent steps at room temperature, because CF in solution is cold labile (McCarty and Racker, 1966). The suspension is stirred in the dark at room temperature for 10 min with a magnetic bar.

Centrifuge the suspension at 20,000 g (11,100 rpm) for 30 min at 20 C. The supernatant is retained as the source of CF. It is noticeably green from contaminating chloroplast fragments, which are removed by the ion exchange column step which follows. Appropriate aliquots of 1 M Tris-SO_4 pH 7.3, 2 M ammonium sulfate, and 0.1 M ATP pH 7 are added to the supernatant to make it 20 mM in Tris-SO_4, 80 mM in ammonium sulfate, and 1 mM in ATP.

An ion exchange column is prepared in advance (5 cm×12 cm) from 11 g of Sephadex G-50 beads which are swollen for 2 or more hours in de-ionized water and pre-cycled in acid and base as described below. The beads are transferred to a large Buchner funnel and rinsed with 1.5 1 of 0.1 N HCl.

The beads are immediately rinsed by passage of 4.5 l of water through the slurry. The rinsed beads are then washed with 1.5 l of 0.1 N NaOH and rinsed again with 4.5 l of water which brings the pH below 8.0. The base treatment causes a small fraction of the beads to denature and float on the surface during subsequent rinses. The majority of these floating beads are removed by adhesion to cheese cloth carefully laid on the surface during the rinses. The gel is washed with 500 ml of column buffer (20 mM Tris-SO_4, 2 mM EDTA, 80 mM ammonium sulfate pH 7.1) and left overnight in 500 ml of fresh column buffer. The equilibrated gel is then de-aerated under vacuum for 15 min and poured into a 5 cm diameter column. The column is prepared for use by passage of 400 ml of column buffer to which has been added 4 ml of 0.1 M ATP pH 7.

The buffered CF supernatant (CF extract) is introduced into the Sephadex column under a 30 cm pressure head. The column bound CF is washed by application of 400 ml of column buffer to which has been added 4 ml of 0.1 M ATP pH 7 and 1.06 g of ammonium sulfate (to yield 100 mM). The wash buffer is applied under a 12 cm pressure head to yield a flow rate of 1.5 ml/min.

The CF is eluted by application of 400 ml of column buffer to which is added 4 ml of 0.1 M ATP pH 7 and 10.6 g of ammonium sulfate (to yield 280 mM). The eluant is collected in 4 ml aliquots, and each aliquot is mixed with an equal volume of precipitating buffer (column buffer which is mixed with saturating amounts of dry ammonium sulfate and made 2 mM in ATP, the final pH is adjusted to 7.1). Fractions which contain CF exhibit a cloudy white precipitate. These fractions are combined and stored at 4° C as Column I CF. The final purification is performed by a linear

sucrose gradient centrifugation of Column I CF which is executed as described in the section on the EDTA extraction procedure.

iii. Fluorescence Emission Purity Assay

The fluorescence emission properties of most proteins are dominated by the contributions of tryptophan residues. Since the vast majority of proteins contain some tryptophan, their fluorescence emission spectra usually consist of a broad, structureless peak centered between 328 and 342 nm (Konev, 1967). The minority of proteins which contain tyrosine residues but no tryptophan exhibit a fluorescence emission spectrum which peaks near 303 nm, due to the tyrosine emission (Konev, 1967). Both amino acid analysis and the observed emission spectrum indicate that CF is free from tryptophan and exhibits a pure tyrosine emission spectrum (Farron, 1970; Farron and Racker, 1970; Lien and Racker, 1971b). This unusual property provides a convenient assay for the purity of CF. The ratio of the fluorescence emission intensity at 303 nm to the emission intensity at 350 nm provides a number whose value increases to a characteristic limit as the percentage of CF in a protein sample increases.

Most fluorescence spectrometers are not absolute instruments. The fluorescence intensity recorded at various wavelengths is not directly proportional to the quantum yield of the sample being measured since the intensity of the excitation light source will, in general, vary with wavelength and the spectral sensitivity of the photomultiplier will also depend on the wavelength under observation. To compare data observed in various laboratories on such uncorrected instruments, it is necessary to specify carefully the instrumental parameters involved in the measurement.

Unfortunately, the data on fluorescence emission of CF presented by the Cornell group lacks this information and thus cannot be compared to our data (Lien and Racker, 1971b).

The following conditions have been used in our laboratory in a fluorescence emission purity assay for CF. A Perkin-Elmer, Hitachi MPF 2A Fluorescence Spectrophotometer was used for the measurements. The protein samples were at room temperature at a concentration of approximately 1 mg/ml in the sucrose-Tris buffer used for the sucrose gradient centrifugation as previously described. The excitation wavelength was 280 nm and both the excitation and emission slits were set for 6 nm spectral bandwidth. The instrument sensitivity was adjusted to yield an approximately full scale signal for the peak emission. To obtain efficient spectral sensitivity in the blue region, a Hamamatsu R106 photomultiplier was used. Under these conditions, the fluorescence emission ratio is defined as the ratio of the observed emission intensity at 303 nm to the intensity at 350 nm. As previously discussed, the maximum fluorescence emission ratio observed in our laboratory for purified CF was 2.7.

We have chosen 0.2 g/l biphenyl in cyclohexane as a reference solution for the comparison of data obtained on other spectrometers to ours. When this solution is excited at 280 nm with both excitation and emission slits set for 6 nm spectral bandwidth and an R106 photomultiplier is used, the ratio of the observed emission intensity at 300 nm to the intensity at 350 nm is 5.06. As an absolute reference, the corrected emission spectrum of this solution can be found in Berlman (71). This reference data should permit other laboratories to compare the emission spectrum of CF to our purified sample.

iv. Protein Assays

In solutions which exhibit interfering absorbance at 280 nm or high levels of light scattering, the sensitive colorimetric assay of Lowry et al. (1951) is preferred although there are a number of problems in its use which are discussed below. The protein assay proceeds in two stages. The first stage is similar to the classic Biuret reaction (Gornall, et al., 1949). The second stage involves the reduction of a phosphomolybdo-phosphotungstic reagent by the copper-protein. In the first stage, an aliquot of protein is treated with $CuSO_4$ and potassium tartrate in a basic bicarbonate buffer to denature the protein and form a complex between the copper atoms and the amide nitrogens of the peptide backbone. Each copper atom complexes with four amide nitrogens (Lowry et al. 1951). A faint purple color develops, which is dependent on the amount of protein present and is rather independent of the nature of the particular protein used.

In the second stage of the assay, an aliquot of Folin reagent is added to the reaction mixture and the copper-protein complex reduces the phospho-metal complex producing an intense blue color. In this stage, the color developed is a sensitive indicator of the amount of protein present but the specific absorbance developed can vary by a factor of three, depending on the particular protein used.

It is common practice to use standard solutions of BSA in the calibration of the assay. It is important to realize that the particular protein under analysis will likely have a different sensitivity to the assay than does BSA.

It has been shown that the color intensity developed during the assay is highly dependent on the particular amino acids present in the protein (Chou and Goldstein, 1960), thus it is not surprising that a wide variation is observed among various proteins. The Cornell group has determined that the value obtained in the Lowry assay for CF with BSA as the standard must be multiplied by a factor of 1.15 in order to obtain the true dry weight of CF present (Farron and Racker,1970). In our laboratory, under the assay conditions described below, we find that the Lowry assay value obtained for CF must be multiplied by 0.74 to obtain the true dry weight value for CF. This correction factor was obtained from a comparison of the Lowry values for purified CF to the values obtained in the absorption assay for CF which is described below. As a verification of this determination, samples of CF of known absorption assay and Lowry assay values were dried and carefully weighed. Good agreement is obtained among these three independent protein assays only if the factor 0.74 is used.

A number of substances are known to seriously interfere with the Lowry assay (Lowry et al., 1951). Ammonium sulfate, which is used in the isolation and storage of CF is one example. For this reason, CF must be carefully desalted before each protein assay. Tris buffer is also known to interfere with the assay. I have noted that Tricine buffer and EDTA in mM concentrations also seriously lowers the sensitivity of the assay. EDTA interferes by complexing the copper ions used in the Biuret stage of the assay. The interference by Tricine can be tolerated so long as the standard curve is run in the same Tricine buffer as is used for the assay.

A typical BSA standard curve obtained for the calibration of the Lowry assay is shown in Figure 2-6. This standardization was run in the buffer used for the Lowry assay of CF. The high degree of linearity and reproducibility obtained in these standardizations indicates that the interference by buffer can be readily tolerated when the same buffer is used for standardizations and the assay. The standardization remains highly reproducible as long as fresh reagents are used in the assay and the intervals between various steps in the assay are carefully time and exactly reproduced for each sample.

The samples to be assayed are first desalted on Sephadex G-50 column in 40 mM Tricine-NaOH, 2mm EDTA pH 8.0 to assure that all samples are free from contaminating ions and suspended in the same buffer.

The assay begins with 2% (w/v) Na_2CO_3 in 0.1 N NaOH, 100 λ of 1% (w/v) $CuSO_4$ and 100 λ of 2% (w/v) potassium tartrate. One ml of alkaline copper solution is added to 10 to 150 micrograms of protein in 500 microliters of 40 mM Tricine-NaOH, 2mM EDTA pH 8.0. After 10 minutes, 100 microliters of 40 mM Tricine-NaOH, 2mM EDTA pH 8.0. After 10 minutes, 100 microliters of 1N Folin reagent is added quickly with rapid mixing. After 30 minutes, the absorbance at 740 nm above a buffer blank is determined.

The potassium tartrate and copper sulfate are stored in separate stock solutions. If the two reagents are stored in a single solution, as Lowry et al. (1951) recommend, the reagent deteriorates in a matter of days forming a white precipitate. The Folin reagent should be refrigerated when not in use and it should be replaced when it first develops a slight green tinge from reduction of the phospho-molybdic phospho-tungstic reagent. The Folin reagent must be added with rapid and continuous stirring to

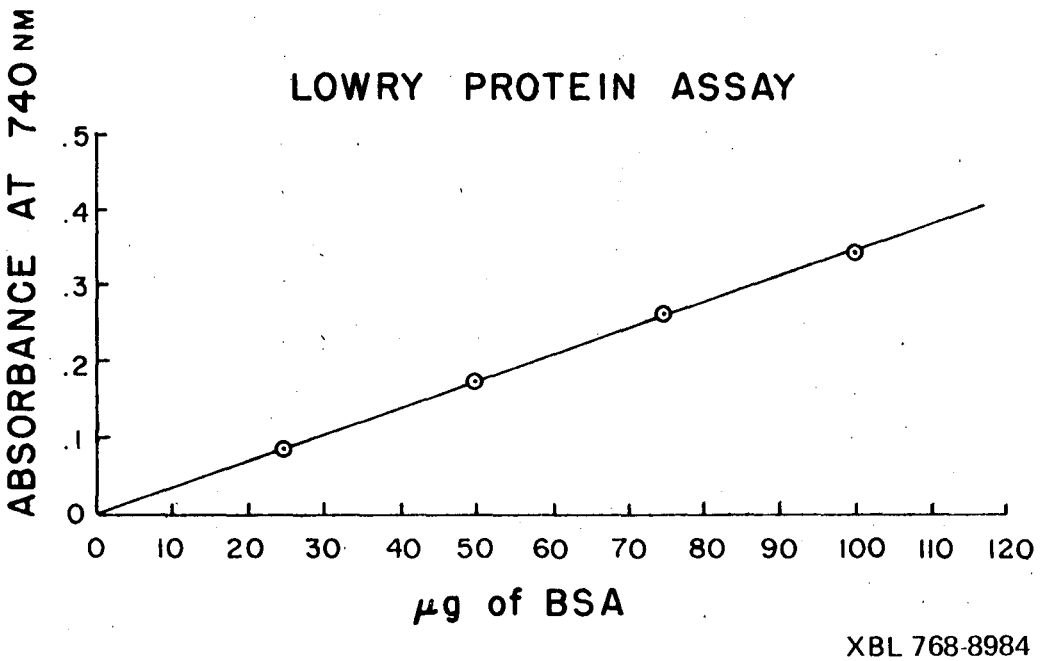
LOWRY PROTEIN ASSAY
ABSORBANCE AT 740 NM
.5
.4
.3
.2
.1
0
0 10 20 30 40 50 60 70 80 90 100 110 120
μg of BSA
XBL 768-8984

Fig. 2.6

assure reaction with all the copper-protein before it is inactivated in the alkaline reaction mixture.

If the sample is free from interfering absorbance and light scattering, a rapid and convenient protein assay is obtained from the absorbance of the protein (minus the buffer blank) at 280 nm. The typical, distinctive absorption spectrum obtained for purified CF is shown in Figure 2-7. The protein concentration is determined from the fact that a 1 mg/ml solution of CF exhibits an absorption of 0.54 at 280 nm (Farron, 1970).

v. Native Gel Electrophoresis

The purity of CF is assayed by gel electrophoresis on a 7.5% polyacrylamide gel at pH 8.3. The gel solution is prepared from 3.568 g of recrystallized acrylamide, 0.188 g of N,N'-methylene-bis-acrylamide, and 15 λ of N,N,N', N'-tetramethylenediamine (TEMED) suspended in sufficient Gel Buffer to make 50 ml of solution. The Gel Buffer is made from 9 g of Trizma Base and 43.2 g of glycine suspended in sufficient de-ionized water to make 3 liters of buffer. The recrystallized acrylamide is prepared in chloroform by a procedure on p. 34 of Maurer (1971). A beaker of overlayer water is prepared by bubbling argon through glass distilled water. Immediately before use the gel solution is de-aerated for exactly 30 sec by bubbling with argon and 0.02 g of ammonium persulfate is added with gentle swirling. The gel solution is carefully pipetted into the gel tubes to avoid bubble formation and each gel is immediately overlayered with the de-aerated water. The gel sets up in approximately 15 min, forming a slightly hazy gel which is characteristic for this gel formula. The haziness gradually diminishes over several days. After 30 min the gels are

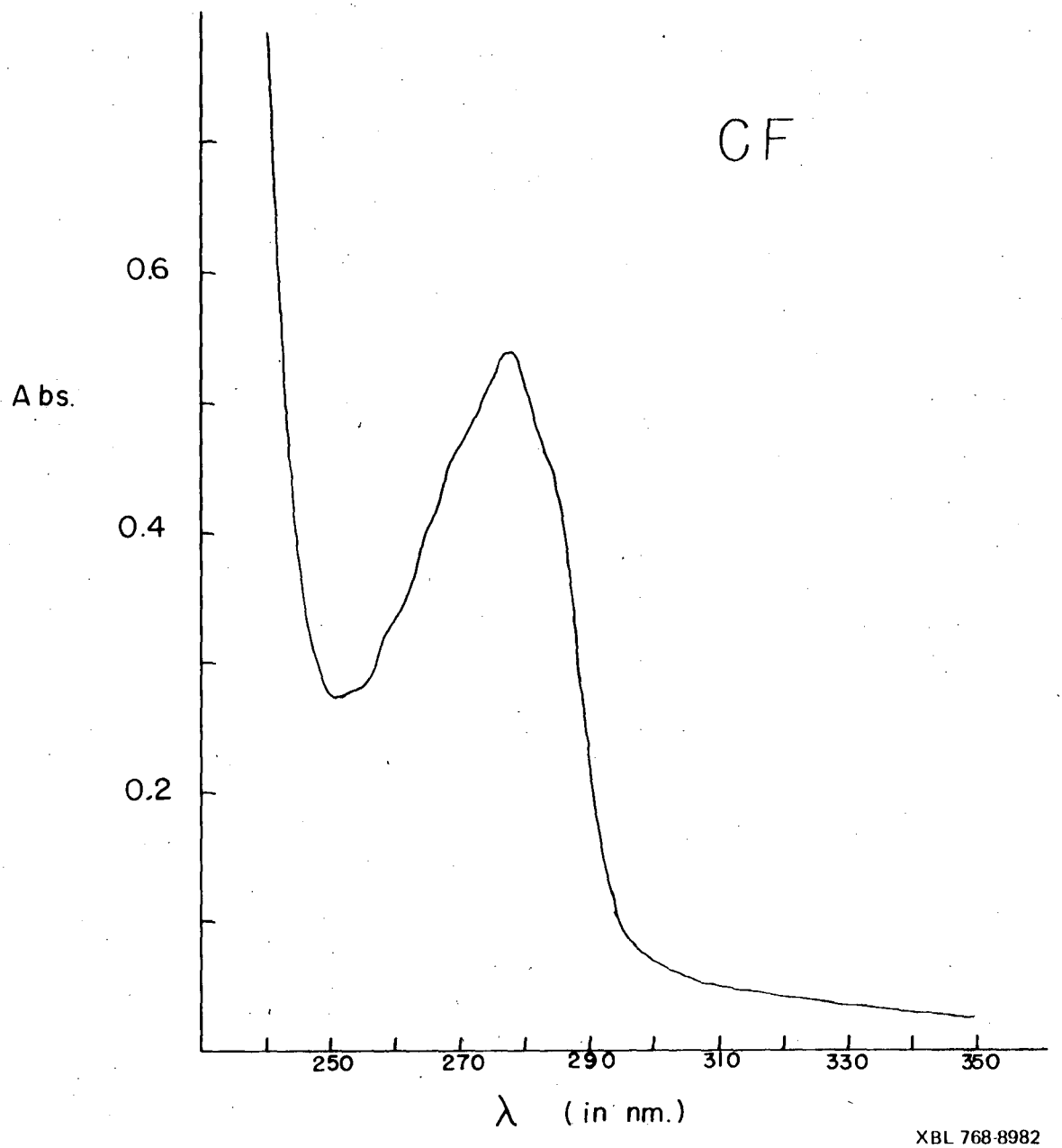

Fig. 2.7

transferred to the electrophoresis apparatus and pre-electrophoresed at 1 mA per tube for 2 min, followed by 3 mA per tube for 2 hr. Gel Buffer is used in both the upper and lower buffer reservoirs during pre-electrophoresis. The initial voltage level during pre-electrophoresis is approximately 200 volts which rises to about 250 volts after 2 hr.

Following the pre-electrophoresis, both the upper and lower buffers are replaced with fresh Gel Buffer. Approximately 100 μg of desalted CF is then prepared. Coupling Factor is desalted by centrifuging a sample at 5000 g for 10 min, resuspending the pellet and passing the solution through a 0.7×4 cm Sephadex G 50 column. An aliquot of desalted protein is assayed for protein (see below) and samples containing 5-25 μg of CF are carefully applied to the top of the gels after addition of 0.05 g of sucrose per ml of sample to increase the sample density and a few crystals of bromophenol blue to one sample as a marker dye. The gels are run at 1 mA per gel for 1 min, then at 3 mA per gel in a cooling bath at 20° C until the marker dye reaches the end of the gel (about 30 min). Following the run the gel tubes are gently cracked open using a vise, the gels are removed, and stained in 1% (w/v) Amido Black 10B in 7% (v/v) acetic acid for 2-3 hr. The stain is poured off and the gels are rinsed several times in 7% acetic acid. The gels are de-stained by diffusion in a hot room (100° F) in 7% acetic acid with constant stirring and frequent changes of the acetic acid. De-staining is completed in approximately 10 hr. The gels may also be electrophoretically de-stained in about 30 min without loss of bands but with a decrease of approximately 50% in the band intensity. An approximate percent purity is calculated from a densitometry scan of the gels.

vi. Chlorophyll Assay

The chlorophyll concentration is determined spectrophotometrically. A small aliquot of chloroplasts is suspended in 80% acetone (v/v with water) and the light scattering membrane fragments are removed by filter paper filtration or by centrifugation on a desk top clinical centrifuge. The absorbance at 652 nm is determined and the chlorophyll concentration is obtained from the formula: $(A_{652}) \cdot (29)$ = chlorophyll concentration in micrograms per milliliter in the acetone (Arnon, 1949).

vii. Photophosphorylation Assay

The following technique for measuring photophosphorylation rates of chloroplasts, EDTA-treated chloroplasts and reconstituted chloroplasts was developed in our laboratory with reference to the work of Shoshan and Shavit (1973) and McCarty (1971) and the assistance of Richard Chain, Department of Cell Physiology, University of California, Berkeley. It is important to adhere to the temperature, sequence of operations and time interval information contained in this method to obtain accurate, reproducible results.

The photophosphorylation activity of freshly isolated chloroplasts decays rapidly, so it is essential to prepare the solutions and instrumentations in advance whenever possible. The following solutions are prepared before the isolation: STN Buffer consisting of 20 mM Tricine-NaOH, 10 mM NaCl, 0.4 M sucrose pH 8.0; NaCl-Sucrose consisting of 10 mM NaCl, 40 mM sucrose; Salt Buffer consisting of 20 mM Tricine-NaOH, 10 mM NaCl pH 8.0 and all of the solutions mentioned during the procedure. An illumination

chamber consisting of four 150 watt incandescent flood lights with sample holders and a circulating water bath set at 20-23° C is prepared. The samples are connected to an agitator which insures continuous stirring during the illumination. 25-50 g of fresh spinach leaves are stored in a dark, moist environment at 4° C. A series of round-bottom flasks are prepared for the illumination. For each chloroplast sample add 0.39 ml of water, 3 µl of 0.2 M EDTA pH 8.0 and 5 µl of 1 M $MgCl_2$ to each flask. For each EDTA Chloroplast or Reconstitution sample add 0.39 ml of water, and 3 µl of 0.2 M EDTA pH 8.0 to each flask. Prepare a Photophosphorylation Solution from 205 µl of water, 125 µl of 0.4 M Tricine-NaOH pH 8.2, 50 µl of 1 mM Phenazine Methosulfate (freshly prepared and stored in the dark) and 40 µl of 50 mM $KH_2P^{32}O_4$ (approximately 10^6 cpm per µ mole, from 20 µl of 20 mCi/ml $H_3P^{32}O_4$ plus 5 ml of 50 mM KH_2PO_4 pH 8.2) for each sample.

Desalt approximately 1 mg of CF on a Sephadex G-50 column in 40 mM Tricine-NaOH, 2mM EDTA pH 8.0. Measure the absorbance at 280 nm and determine the protein concentration. To each reconstitution sample add 50 µg or more of CF and enough water to bring the volume of the added CF to 0.39 ml. This makes the total volume of the samples 1 ml during illumination.

Wash and remove the midribs from 25-50 g of fresh spinach leaves. Place the torn leaves in a blender and add 100 ml of STN buffer. Grind for approximately 5 sec to produce a slurry and grind the slurry for 10 sec more. Pour the homogenate into 4 layers of rinsed cheesecloth in a funnel and filter into two Sorvall SS-34 tubes on ice. Do not apply any pressure to squeeze the filtrate through the cheesecloth. Work in dim

light whenever possible.

Centrifuge the filtrate at 5000 rpm for 1 min. To speed the rotor decelerations, the rotors are slowed by hand friction below 3000 rpm in all runs. Discard (pour off) the supernatant.

Resuspend the pellets in a total of 40 ml of Salt Buffer. All resuspensions are performed as follows. The pellet is stirred with an equal volume of buffer by a rubber policeman on a glass rod to generate a homogeneous, thick slurry. The slurry is diluted up to volume by sequential addition of small aliquots of buffer and careful gentle stirring after each addition. In this manner, a homogeneous solution is obtained with minimal damage to the pellet.

Remove 1 ml of the suspension and add it to 9 ml of 8 to 1 (v/v) acetone with water and mix. Transfer this extract to a small stoppered test tube and remove light scattering particles by mild centrifugation. The chlorophyll concentration in the original salt buffer suspension is $(0.29)\times(A_{652})$ in mg/ml.

Transfer 3 mg of chlorophyll to each of two centrifuge tubes. Centrifuge up to 8000 rpm in an SS 34 rotor and immediately turn off the centrifuge when this speed is reached. Carefully remove the supernatant by pipette taking care not to disturb the soft pellet.

Resuspend one pellet in 5 ml of 0.4 mM EDTA pH 8.0 and immediately centrifuge the suspension up to 10,000 rpm and turn off the centrifuge when this speed is reached. (All centrifugations up to this point are performed at 0-4° C and all pellets are stored on ice in the dark when not in use). Carefully remove by pipette as much supernatant as possible from the soft pellet.

Resuspend the pellet in 4 ml of room temperature Salt Buffer. Transfer 100 µl of this EDTA Chloroplast solution to each Reconstitution and EDTA Chloroplast sample. Store the EDTA Chloroplast solution in the cold for a later chlorophyll assay.

Add 5 µl of 1 M $MgCl_2$ to each Reconstitution and EDTA Chloroplast sample and incubate for 10 min at room temperature under dim illumination.

Resuspend the chloroplast pellet from the 8000 rpm centrifugation in 4 ml of Salt Buffer at room temperature to create the Chloroplast solution. Transfer 100 µl to each chloroplast sample and incubate at room temperature under dim illumination. Store the Chloroplast solution in the cold for later chlorophyll assay.

Add 500 µl of Photophosphorylation Solution to all samples, flush each flask with nitrogen for 15 sec and tightly cap. Illuminate each flask for 2 min on the illumination chamber. To terminate the illumination, add 500 µl of ice-cold 1 M trichloroacetic acid to each flask and store on ice.

Assay each sample for AT^{32}P using the following technique which is derived from the method of Avron (1960). Centrifuge each photophosphorylation mixture on a clinical, desk-top centrifuge to remove the denatured protein. Place 1 ml of the supernatant in a 10 ml glass-stoppered flask. Add 1 ml of water saturated with 1 to 1 isobutanol-benzene and mix. Add 5 ml of 1 to 1 isobutanol-benzene and mix by vigorous inversions for 30 sec. After phase separation, add 500 µl of 10% ammonium molybdate in 10 N H_2SO_4 along the side of the flask and gently mix by inversion (maintain phase integrity). Wait for 1 min. Mix the layers by vigorous inversions for 30 sec and wait for complete phase separation. Suck off all of the

upper organic layer with a pipette removing some of the water layer if necessary. Add 20 µl of 20 mM KH_2PO_4 and mix. Add 5 ml of 1 to 1 isobutanol-benzene and mix the layers for 30 sec. Remove all of the upper organic layer taking some of the water layer if necessary. Remove 100 µl of the final water layer, place it in the center of a metal planchette and dry it down under a heat lamp. Count each sample in a planchette counter. The specific count rate for the ^{32}P is determined from the average of several 100 µl samples of the initial organic layer. Each sample is counted for 10 min which is repeated 3 times to yield an average count rate. The final photophosphorylation rate in moles ATP formed per hr per mg of chlorophyll is determined for each sample.

The various steps in this procedure are performed as rapidly as possible so that less than 1 hour elapses between the grinding of the leaves and the completion of the illuminations. We have observed that the chloroplast sample maintains a high rate of photophosphorylation for at least 1 1/2 hrs following the grinding. The incubation of chloroplasts with EDTA is maintained for the minimum possible time interval because we have observed that longer incubation leads to a stronger inhibition of the photophosphorylation activity. We have performed experiments with incubations in EDTA solutions varying from 0.2 to 1.5 mM with similar results in all cases, although the extremes of concentration tend to produce less extensive inhibition of the photophosphorylation activity. This result coincides with the data reported by McCarty and Racker (1966).

Control experiments were performed in which a sample of $KH_2{}^{32}PO_4$ in the presence or absence of cold ATP was analyzed for $AT^{32}P$ by the method described above. Less than 0.2% of the ^{32}P was detected in the final

water layer in agreement with the findings of Avron (1960). This contamination by inorganic ^{32}P would lead to an apparent photophosphorylation rate of less than 1μ mole/hr/mg of chlorophyll in a typical experiment. In addition, we demonstrated that the ammonium molybdate which is present along with $AT^{32}P$ in the final water layer (yielding a blue solid on the planchette) does not significantly quench the ^{32}P counts.

viii. ATPase Activity Assay

The ATPase activity of CF is determined following trypsin activation of the enzyme by a modification of the procedure of Lien and Racker (1971b). Solutions of 2 mg of trypsin in 400 μl of 5 mM Tricine-NaOH pH 6.9, and of 0.0623 g of ATP-$4H_2O$ (99% pure) in 1 ml of 0.2M NaOH (final pH-7) are prepared. A sample of CF (0.2 mg or more) is desalted on a column of Sephadex G-50 fine equilibrated with 40 mM Tricine-NaOH, 2 mM EDTA, pH 8.0, and the protein concentration is determined.

The desalted CF is activated by trypsin. Combine 30 μl of 1 M Tricine-NaOH pH 8.0, 20 μl of 0.2 M EDTA pH 8.0, and 20 μl of 0.1 M ATP with enough water so that the volume of the CF sample plus water is 870 μl. Add 30-50 μg of desalted CF. Add 20 μl of the 5 mg/ml trypsin solution and note the time. Divide the sample into 4 aliquots of 240 μl each. At the end of the desired activation time, add 10 μl of 5 mg/ml trypsin inhibitor to each aliquot.

The activated CF is assayed as follows. Combine 40 μl of 1 M Tricine-NaOH pH 8.0, 75 μl of 0.1 M $CaCl_2$, and 760 μl of water. Add 50 μl of activated CF to each sample. At timed intervals, add 75 μl of 0.1 M ATP to each sample and insert the sample in a 37°C water bath.

After 10 min, add 500 µl of ice cold 1 M trichloroacetic acid to each sample and place the sample on ice. Assay 500 µl of each sample (out of the 1.5 ml total) for inorganic phosphate using the method described below.

An assay for the inorganic phosphate derived from ATP hydrolysis was developed from the method of Martin and Doty (1949) (see also Lindberg and Ernster, 1956). The phosphate assay of Taussky and Schorr (1953) which is frequently used, did not prove acceptable owing to residual ATP hydrolysis in the highly acidic assay medium. We observed that the color developed in the assay does not remain stable over long time intervals in contrast to the claims of the authors. To 1-20 µg of phosphorus (in the form of phosphate) in 1 ml add 2 ml of 1 to 1 isobutanol-benzene saturated with water. Add 200 µl of 10% ammonium molybdate in 10 N H_2SO_4 and immediately shake for 15 sec. After the phases separate, remove 1 ml of the organic (upper) layer, which exhibits a yellow color. Add 2 ml of 4% (v/v) H_2SO_4 in absolute ethanol to the 1 ml sample of the organic layer and mix. Add 30 µl of $SnCl_2$ solution (prepared fresh daily from 50 µl of 10% $SnCl_2$-$2H_2O$ in concentrated HCl diluted to 10 ml with 0.5 M H_2SO_4), mix and cover the test tube. After 10 min measure the absorbance at 730 nm and compare the reading to a standardization curve based on samples of KH_2PO_4. A typical phosphate standards curve is shown in Figure 2-8. The standards curve can be run in water because we have observed that the ATPase solution has no interfering effects on the phosphate assay. The ATPase activity is calculated from the observed release of inorganic phosphate in excess of the value obtained for a sample of water which was subjected to the trypsin treatment and assay procedure as described above.

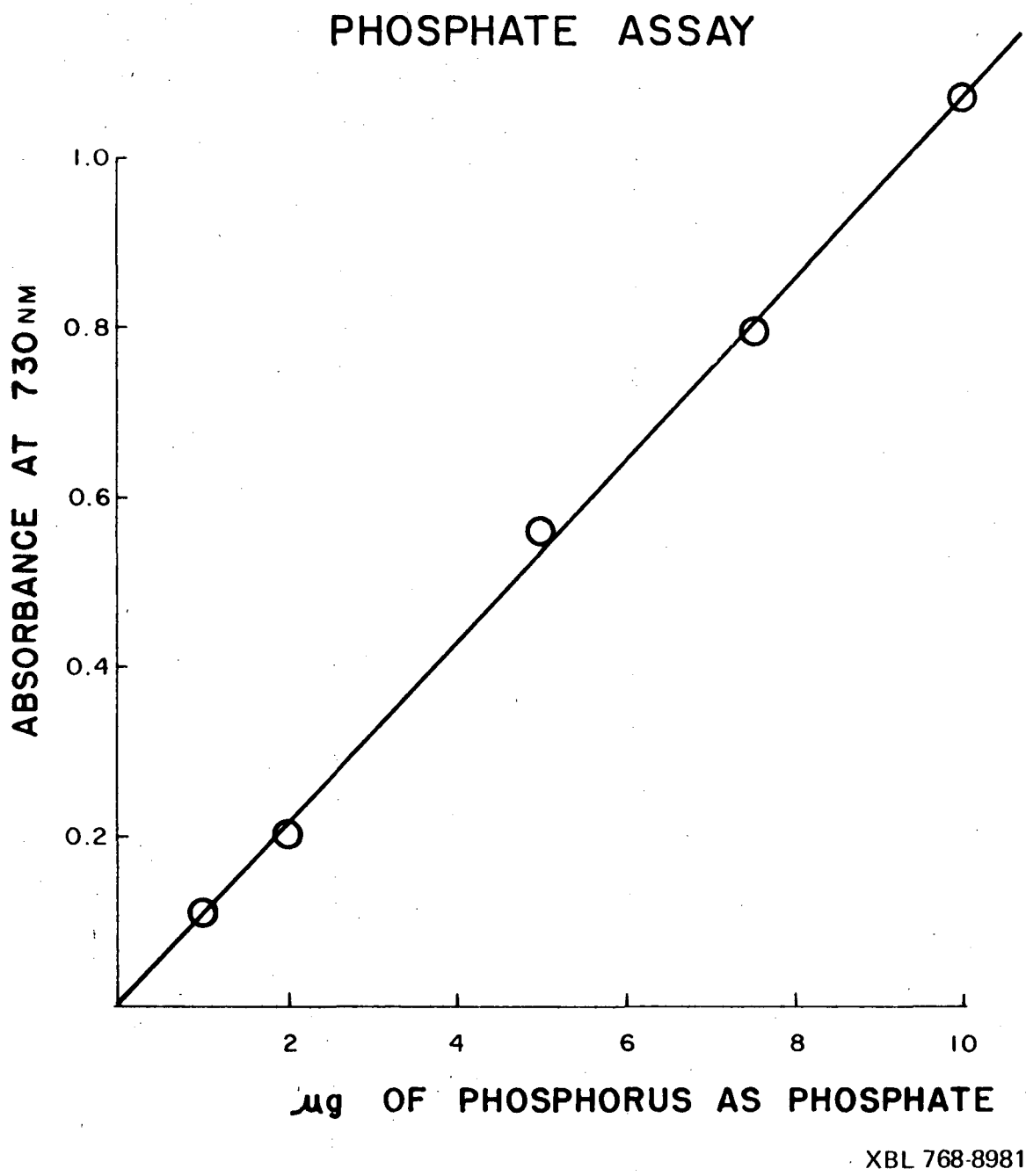
PHOSPHATE ASSAY
ABSORBANCE AT 730 NM
1.0
0.8
0.6
0.4
0.2
2
4
6
8
10
µg OF PHOSPHORUS AS PHOSPHATE
XBL 768-8981

Fig. 2.8

The ATPase activity of CF before trypsin activation was reported to be negligible (Vambutas and Racker, 1965). We have verified these findings in our preparations. When an aliquot of CF was treated as described above except that trypsin was omitted, we found that the color developed by the trypsin-free sample of CF was the same as the color developed by the water blank (A_{730} = 0.08 for a 1 cm path length) indicating no intrinsic ATPase activity. The color developed in the colorimetric assay for phosphate when a water sample is assayed was A_{730}= 0.04 for a 1 cm path length so the water blank value is small compared to the A_{730} values of 0.4 or more which are encountered for a 1 cm path length in a typical ATPase assay.

Trypsin activation durations of 4 to 12 minutes were commonly used in our laboratory with a preparation of trypsin from Sigma Chemical Company that was reported to have a specific activity of 12,000 BAEE units per mg. To avoid self-hydrolysis, the trypsin solution is prepared immediately before use. All reagents used in the assay (especially the $CaCl_2$) must be obtained from very pure sources to avoid contamination with magnesium. Vambutas and Racker (1965) report that the presence of 3% Mg^{++} in the Ca^{++} solution used for the ATPase assay causes a 50% inhibition of the ATPase rate.

III. A NOVEL PROTON COUNTING SYSTEM FOR MEASUREMENT OF VERY SHORT FLUORESCENCE LIFETIMES

III. A NOVEL PHOTON COUNTING SYSTEM FOR MEASUREMENT OF VERY SHORT FLUORESCENCE LIFETIMES

Introduction

Fluorescence lifetime measurements are commonly performed using single photon counting systems, (Yguerabide, 1972; Knight and Selinger, 1973) phase shift instruments, (Ware, 1971; Spencer and Weber, 1969) or mode-locked laser systems. (Mourou and Malley, 1974; Porter et al., 1974) Phase shift instruments provide good speed and accuracy but they offer limited capabilities for the resolution of multiple component spectra. Laser systems provide time resolution in the picosecond time domain but suffer from poor signal to noise ratios and diminished multiple component capabilities. Photon counting systems operate with excellent signal to noise ratios which result in a wide dynamic range in the time and intensity intervals over which the fluorescence can be recorded. This wide dynamic range makes possible an accurate analysis of multiple component fluorescence data.

The single photon counting technique of lifetime measurement is based on the concept that the probability distribution for the emission of a single photon of fluorescence following a single exciting light pulse is identical to the intensity-time profile of the cascade of all the photons which are emitted following a single flash of exciting light (Yguerabide, 1972). Thus, to record the total fluorescence emission in the short time interval following an exciting flash of light one can record the time of arrival of single photons of fluorescence following the

exciting flash. The sample is repeatedly excited with such flashes and the fluorescence photon arrivals are recorded to obtain the frequency of photon emission in each of a number of preset time intervals following the exciting light flash. Only one fluorescence photon arrival can be electronically processed per exciting light flash so it is important to attenuate the fluorescence intensity reaching the photomultiplier so that less than one photon is detected per excitation flash. The experimenter's record of the number of photons emitted in each of a series of time intervals following the excitation flash is then equivalent to the intensity of emission verses time which follows a single excitation pulse (the ensemble average is equivalent to the time average).

Figure 3-1 shows a block diagram of our photon counting system. A short duration pulse of exciting light is generated by the light pulser and illuminates the sample. A reference photomultiplier views the light pulse through a light pipe and sends a voltage pulse to the discriminator. The amplitude of the reference photomultiplier pulse varies greatly from flash to flash. The discriminator converts the varying input pulses from the reference photomultiplier into a constant shape output pulse which is required by subsequent modules. In addition, the discriminator has a pulse threshold setting which rejects the low amplitude noise pulses generated in the reference photomultiplier. This ability to discriminate between noise and signal pulses is responsible for the high signal to noise ratio characteristic of photon counting.

The discriminator pulse from the reference photomultiplier side is applied to the START gate of a time to pulse height converter. The time to pulse height converter generates an output voltage pulse whose amplitude is proportional to the time delay between a pulse received at the

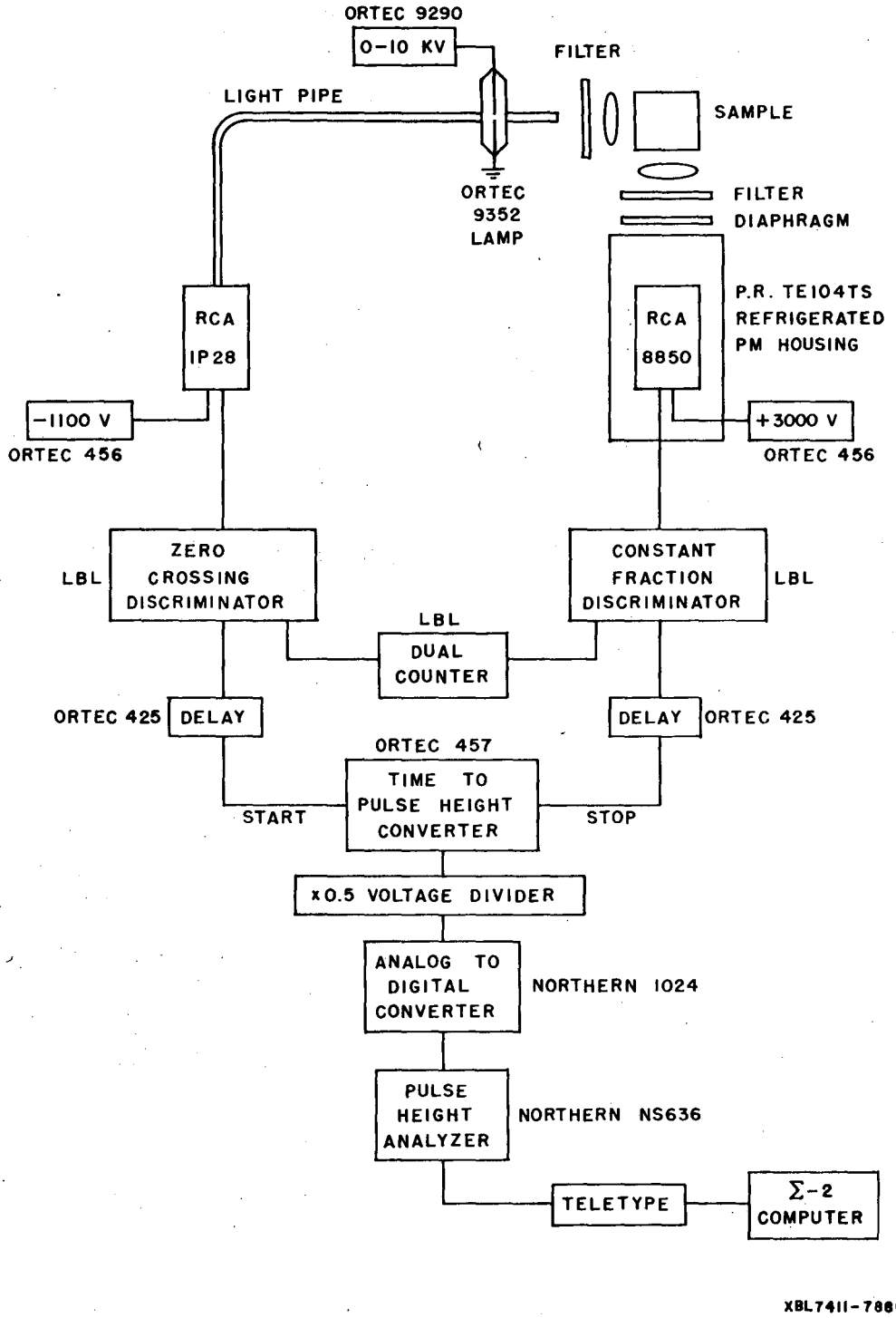

Fig. 3.1. Block diagram of the photon counting system for sub-nanosecond fluorescence lifetime measurements.

START gate and a separate pulse received at the STOP gate. The STOP pulse is generated by a photon of fluorescence which strikes the RCA 8850 or 8852 photomultiplier and is accepted by the discriminator as a true photon event. Thus, the time to pulse height converter output is a pulse whose amplitude is proportional to the time delay between the exciting light pulse and the emission of a fluorescence photon by the sample. The two delay lines are used to adjust the START to STOP time delay so that if falls within the operating range of the time to pulse height converter.

The time to pulse height converter output pulse is registered by an analogue to digital converter and pulse height analyzer combination which stores a count in the analyzer memory in a channel corresponding to the time delay (pulse amplitude) detected by the time to pulse height converter. A series of channels are set up in the analyzer to cover the entire time interval of interest for fluorescence emission following the excitation pulse. By repeated flashing of the light pulser and recording of the arrival time of the resulting fluorescence photons, a fluorescence intensity verses time profile is built up in the analyzer memory.

Due to the finite width of the light pulse, the time resolution limitations of the photomultiplier, and the electronic signal processing system the experimental fluorescence lifetime curve is significantly distorted. In order to extract the true value of lifetime parameters from the experimental data, itis necessary to solve the convolution integral (Brody,1957). Generally, the convolution procedure is more accurate if experimental data are measured under identical experimental conditions, particularly concerning variations of photomultiplier and electronic circuitry parameters, as well as variations of the time profile of the light pulse.

Our measurements have shown that in situations where a subnanosecond lifetime must be accurately measured, the fundamental limitations on the precision of measurements are imposed by the following conditions: the fluctuations in the light pulse waveshape, the single-photoelectron time spread of the photomultiplier, the measuring system dependence on the excitation and emission wavelengths, and the timing error introduced by the discriminator used in the system. Consequently, a high-precision measuring system operate with the shortest possible light pulses, because the time spread in the light pulse waveshape is in absolute amounts smaller for narrower pulses. Also, the fastest photomultipliers with adequate gain and optimized operating conditions (Leskovar and Lo, 1975; Leskovar,1975) are used, since they generally exhibit a relatively smaller value of the single-photoelectron time spread. To minimize the measuring system wavelength dependence, (Wahl et al., 1974) the same optical filter for excitation is used in recording both the excitation and fluoresecence emission profiles, and the difference between excitation and fluorescence wavelengths is chosen to be as small as practically possible.

According to our knowledge, fluorescence lifetime measurements using a single-photon counting system for substances with lifetimes smaller than 480 psec have not been reported in the literature. Our system, which uses the above-mentioned components with optimized operating conditions, can measure fluorescence lifetimes as short as 90 psec. In this short time domain, the inherent wider dynamic range of photon counting provides important advantages in measurements on chemical and biological systems where highly quenched fluorescence is observed from multiple chemical

species or physical environments. In addition, this increased time resolution can improve the accuracy of multiple or single component lifetime determinations in longer time domains.

Lifetime System Design

An Ortec Model 9352 nanosecond light pulser, with operating conditions adjusted to minimize the light pulse waveshape spread, is used as the light source. The light pulser operates as a relaxation oscillator and generates light pulses by a spark discharge between tungsten electrodes.

The sample is placed in the cuvette and repetitively excited with short duration pulses of light. Colored glass or interference filters are used to isolate the proper wavelength of excitation and fluorescence emission for each individual sample. The fluorescence light is detected at 90° to the exciting light. The sample lenses, focal lengths 15 mm each, focus the exciting light onto the sample and the fluorescence light onto the photomultiplier photocathode, respectively. Both lenses have a diameter of 25 mm. The fluorescence light is attenuated with the variable diaphragm to a low intensity so that the detection system is in the single-photoelectron mode. This mode is obtained when about 10% of the exciting light pulses result in an output pulse from the photomultiplier. The variable diaphragm aperture is typically 20 mm. The photomultipliers used are RCA's 8850 or 8852. The former has a 116 spectral response, and the latter has a 119 ERMA III spectral response which extends into the near-infrared region.

The choice of photomultiplier for a particular experiment depends upon the wavelength of the fluorescent light. In either case the photomultiplier is placed in a thermoelectric cooling chamber to reduce the dark pulse counts. The reference (START) pulse is obtained from an RCA 1P28 photomultiplier, operating 1.2 kV, which is optically coupled by means of a 12-in.-long American Optical LG 3 light guide to the light pulser. The sample cuvette, the fluorescence and reference photomultipliers, the thermoelectric cooler, the interference filters, the diaphragm, and the shutter are all mounted in a metal compartment that is light tight and electrically shielded. The aperture of the variable diaphragm is adjustable from outside of the compartment. The fluorescence signal photomultiplier output pulses are processed in a specially designed constant-fraction discriminator, with upper and lower level adjustments, which has a time walk less than ±35 psec over a 50-mV to 5-V input pulse amplitude variation (Leskovar et al., 1976). The constant-fraction discriminator output is applied to the STOP input of a time-to-pulse height converter via an adjustable delay line, used for calibration purposes. The reference channel photomultiplier output pulse is processed in a constant-fraction discriminator and is applied to the START input of the time-to-pulse height converter via a second delay line. The second output channel from the reference channel discriminator is applied to the first input of a two-channel counter with a dual display. Whenever a pulse appears at the STOP input of the time-to-pulse height converter, following a START pulse within a preset time window, an output pulse will be produced at the output channels of the time-to-pulse height converter. This pulse is applied to the second channel of the dual counter, and it is counted as a single photon event.

A direct percentage readout of the measuring system counting efficiency is readily available from the dual counter. The time-to-pulse height converter is followed by an analog-to-digital converter whose output pulses are applied to a 1024 channel pulse-height analyzer.

After many excitations, the number of counts versus channel number on the multichannel analyzer gives the decay time function of the fluorescence intensity. The relation between channel number and time is established by calibrated variable delay lines. Since the analysis of fluorescence decay data requires corrections for the shape of the light pulse and evaluation of complex decay functions, the multichannel analyzer memory contents are transferred to the Sigma 2 computer for further numerical analysis. The multichannel analyzer is interfaced with the computer by means of the LBL analyzer-to-computer interface.

Light Pulser Considerations

A critical evaluation of the photon counting system shows that the spread in the light pulse waveshape is one of the fundamental limitations on the precision of the measurements. For an accurate measurement of fluorescence lifetimes and the necessary mathematical corrections, the spread in the light pulse waveshape should be as small as possible in comparison with the value of the sample decay time. This is particularly important in situations where operating conditions of the photomultipliers are optimized to obtain a minimum value of the photomultiplier single-photoelectron time spread.

For the relaxation-type nanosecond light pulser in air, such as Ortec Model 9352, which uses two tungsten electrodes to form a spark gap, our measurements show that the optimum operating voltage for a minimum light pulse waveshape spread is 5 kV. In this case the full width at half maximum of the light pulse is less than 800 psec. Values of 2.5 to 3.3 nsec have been reported for the measured FWHM of the light pulses from air gap spark lamps (Knight and Selinger, 1973; Schuyler et al., 1972; Lewis et al., 1973). The measured FWHM of 800 psec on our system represents a considerable improvement over previous instruments. This value approaches the practical limit of 500 psec which is the FWHM of the light emission from the air lamp (Yguerabide, 1965). We believe that this improvement reflects the reduction of the timing jitters and the faster response time of our system rather than a shorter light emission process in our air lamp.

The tungsten electrode spacing, which is adjustable between 0 and about 2 mm by means of a collar on the light pulser barrel, is adjusted to a value which gives a light pulse rate of 14×10^3 pulses/sec. Under these operating conditions, the photon yield is approximately 2.8×10^6 photons/pulse over visible and uv wavelengths through the output window. Also, to obtain stable performance of the light pulser with respect to the light pulse and waveshape spread, it is necessary to gently and continuously flush the spark gap chamber with a flow of dry air during operation. The electrode tips have to be cleaned after every 10 hours of operation and the electrode spacing reset. Also it is necessary to resharpen the pointed electrode into a conical tip after significant erosion has occurred. The maximum photon yield of approximately 1.2×10^7

photons/pulse is obtained by using a nonoptimum operating voltage of 9 kV. Under these conditions, the FWHM of the light pulse is 2.2 nsec, and the light pulse waveshape spread is about five times worse than in the case when the spark gap is operated with optimum operating voltage. Also, the light pulser performance is significantly degraded at pressures above 1 atmosphere.

Optimization of Photomultiplier Operating Conditions for a Minimum Transit Time Spread

The total electron transit time spread of the photomultiplier is defined as the variation in the time of travel of photoelectron packets through the photomultiplier electron amplification stages (dynodes). The photoelectron packets begin as a single photoelectron emission following photon absorption by the photocathode, and grow to an electron cascade as they transit through the dynode chain. The total electron transit time spread is expressed as the full width at half maximum of the transit time interval probability distribution (generally a Gaussian distribution). The transit time interval is the time interval between the absorption of a photon by the photocathode and the appearance of the peak of the output pulse at the anode. This transit time spread represents the second major limitation on the precision of the decay time measurements. The transit time spread of an electrostatically focused photomultiplier consists of the photoelectron transit time spread between the photocathode and the first dynode of the photomultiplier, the electron transit time spread in the electron multiplier, and the spread between the electron multiplier and the anode. The major causes of transit time spreads are the distribution of

initial emission velocities of photoelectrons and secondary electrons, unequal electron path lengths between different electrodes, and nonuniform electric fields. Generally, the initial stages of a photomultiplier contribute predominantly to the total transit time spread. The transit time spread resulting from the initial velocity distribution is decreased by increasing the voltage between the photocathode and the first dynode. Similar considerations are valid for the secondary-electron initial velocity in an electron multiplier.

Optimization of operating conditions of the RCA 8850 and 8852 photomultipliers for a minimum transit time spread is performed using the procedure and measuring system described in Leskovar et al. (1976). Design of a dynode voltage divider network to optimize the response of selected photomultiplier tubes is a unique feature of our instrument which contributes to our improved time resolution. Furthermore, anode positive voltage is applied to the voltage-divider network so that the photocathode is at the ground potential during operation. This voltage-divider configuration is essential to reduce the number of noise pulses generated by electroluminescence in the photomultiplier glass envelope and in the face plate of the cooling housing because the thermoelectric cooling chamber components surrounding the photomultiplier are at ground potential.

Constant-Fraction Discriminator Design

The time resolution of the photon counting system, which depends on the spread in the light pulse waveshape and the photomultiplier electron transit time spread, is also determined by the time-walk and resolution characteristics of the constant-fraction discriminator. The discriminators

used in this system are developed with improved time-walk and resolution characteristics. The circuit diagram, and performance characteristics of the special discriminators used in our system are described in Leskovar et al. (1976) along with a description of its operation. The unique design of these discriminators has enabled us to obtain a time walk of ± 35 psec over an input pulse amplitude range from 50 mV to 5 V. The intrinsic time resolution of the discriminator with a constant 2nsec risetime pulse is 70 psec at 50 mV, decreasing exponentially to 20 psec at 800 mV.

Experimental Conditions

For all measurements reported in this thesis the RCA 8850 photomultiplier was used at an operating temperature of 0°C and a dynode supply voltage of 3000 V. All fluorescence lifetime measurements were performed with the samples at room temperature.

The light pulser was operated in air at 1 atmosphere. The light pulser voltage was 6,000-9,000 V which yielded a detected flash rate of 13,000-26,000 flashes per second. The data collection rate [(time-to-amplitude-converter rate)/(light pulser flash rate)] was 10% or less for all measurements.

The excitation and emission wavelengths were selected by optical filters. The filters used in each experiment were: Erythrosin--Optical Industries 4900 Å and 5500 Å interference filters; Diphenyl Butadiene--Corning 3-72 and 3-74 in series for emission, Optics Technology 330 nm interference filter for excitation; Anthracene--Corning 3-72 and 3-74 in series for emission, Kodak 18A for excitation. The diaphragm was adjusted

to an opening of 2 mm to 20 mm diameter in these studies. The light pulser profile for the anthracene and diphenyl butadiene experiments was recorded using a polished metal front surface reflector from a Perkin-Elmer MPF3L fluorescence spectrometer. The light pulser profile for the erythrosin experiment was obtained using distilled water in a 1 cm × 1 cm fluorescence cuvette as the scatterer. Additional details are provided in the experimental section for each compound investigated.

Colored glass or interference filters are used in our system to isolate the proper wavelengths of excitation and fluorescence emission for each sample. Filters permit recordings with high collection efficiency and with a broad bandpass, which increases the system sensitivity. Glass filters also introduce significant fluorescence and phosphorescence artifacts into lifetime measurements. Exposure of colored glass filters to bright room lights introduces phosphorescence emission which can be detected by the photomultiplier as an increase in the background count rate for more than 1 hour after light exposure. In addition, the filters capture scattered or incident exciting light or fluorescence photons and convert them into filter fluorescence arising in the glass. Filter fluorescence can add a low intensity ($\sim$0.5%) lifetime component to each spectrum taken. This system artifact has a significant effect on lifetime measurements, especially when the filter and sample lifetimess are very different. Examples and discussion of this problem appear in the Experimental section of this chapter.

Pulse Pileup Rejection

The single photon counting technique of lifetime measurement is based upon the concept that the probability distribution for the emission of a single photon of fluorescence following a single exciting light pulse is identical to the intensity-time profile of the cascade of all the photons which are emitted following a single flash of exciting light. The single photon emission probability distribution is built up by repetitive exposure of the sample to short bursts of exciting light and recording of the time of arrival of the first photon of fluorescence following each exciting pulse. If more than one fluorescence photon arrives at the photomultiplier following a single excitation flash, only the first photon will be recorded because only one fluorescence photon stop pulse can be processed at the time-to-amplitude-converter per excitation start pulse. The loss of later fluorescence events will distort the recording of the probability distribution by artificially enhancing the early portion of the fluorescence spectrum. To avoid this problem, several techniques for the prevention of this pulse pileup have been developed.

The simplest method for the prevention of multiple photon events is to attenuate the light intensity reaching the photomultiplier so that multiple photon events are extremely rare. Under these circumstances, the multiple photon contribution to the spectrum will result in a distortion of only a few percent in the data, which can usually be tolerated. The limited rate of data collection associated with this approach increases the time required to record a spectrum. This can be an important limitation when labile biological samples are under investigation. There is a

theoretical correction for multiple photon events which allows higher data collection rates and shortens the recording time (Davis and King,1970; Coates, 1968; Donohue and Stern, 1972). Certain experimental uncertainties make the correction difficult to apply accurately, however (Davis and King, 1970).

Pulse pileup rejection can also be accomplished electronically by utilizing a digital inhibit circuit. If the output of the time to pulse height converter is delayed by a suitable length of cable, then a pulse counter can be used to gate the input of the analogue to digital converter. The pulse counter will inhibit storage of the fluorescence event if more than one photon of fluorescence is detected following a single lamp flash (Knight and Selinger, 1973; Davis and King 1970). With this technique, data collection efficiencies [(time to amplitude converter rate)/(light pulser flash rate)] of up to 20% can be utilized (Davis and King; 1970). It is important to note, however, that this method suffers from a frequently overlooked 'blind spot'. The discriminators used in our lifetime system and in other systems require a reset time of at least 50 nanoseconds before they are able to process a second fluorescence photon. During this period the pulse counter will fail to detect the arrival of subsequent photons. Since the probability for photon emission peaks sharply and falls off exponentially or as a sum of exponentials (for short light pulser flashes), if multiple photon events occur, they will most likely occur with a small time separation. This method will be blind to precisely those multiple photon events which are most likely to occur, especially when short fluorescence lifetimes are being measured.

An alternative electronic pulse pileup rejection scheme is available. If two photons are captured by the photomultiplier within a very short time interval, then their resulting photoelectron cascades will overlap. This overlap will cause the amplitude of the photomultiplier output pulse to be outside the normal range of single photon output pulse heights. An upper limit threshold can then be built into the photomultiplier's discriminator, in addition to the lower limit threshold for noise rejection, in order to reject all pulses of large amplitude, originating from multiple photon events. The excellent multiple photon resolution of the RCA 8850 lends itself to this mode of pileup rejection (Schuyler and Isenberg, 1971; Leskovar and Lo, 1972). We have incorporated this method of pulse pileup rejection in our lifetime system.

This method also has its characteristic 'blind spot'. If the separation in time between photons is much larger than the FWHM of the output signal of the photomultiplier, then the electron cascades will be resolved from each other and the amplitude of the output pulse will not be significantly different than for single photon events, although two separate peaks will be seen. In this case, the pulses will pass through the discriminator window but only the first photon event will be recorded in the analyzer. This problem will be particularly severe when long fluorescence lifetimes are measured, since the multiple photons are more likely to be separated by longer time intervals. Most single photon counting photomultipliers exhibit a FWHM output of 2-3 nsec in response to a single photon event. Thus, multiple photon events will not be detected by this pulse pileup method if the two photons are separated by more than approximately 2 nsec.

We have seen that pileup rejection based on a digital inhibit circuit exhibits a blind spot if the photons are separated by less than about 50 nsec. Pileup rejection based on discriminator windows is ineffective for photons separated by more than approximately 2 nsec. Even a combination of these electronic methods will be unable to detect all multiple photon events. A modified discriminator window method of pulse pileup rejection has been designed, however, which can effectively record all multiple photon events. (Shuyler and Isenberg, 1971) This method utilizes a single channel analyzer with upper and lower thresholds and an appropriately slow time constant to stretch the input pulses from an intermediate dynode of the photomultiplier. Events occurring within the measuring time interval of the system will overlap and the window in the single channel analyzer can select for single photon events. The analyzer produces a gating pulse that inhibits recording of the photon event whenever multiple photons are detected.

It is important to be aware of these deficiencies of pulse pileup rejection when making lifetime measurements. If the simple electronic pulse pileup rejection system is chosen, it should be supplemented by an attenuation of the data collection rate and/or the application of appropriate theoretical corrections for multiple photon events. In our lifetime system, the simple discriminator based pileup rejection system is supplemented by an attenuation of the TAC count rate to 10% or less of the lamp firing rate. This method was used for all measurements reported in this paper.

Data Analysis

The fluorescence emission from a set of identical fluorophores in response to a delta pulse of exciting light is given by the relation:

$$f(t) = \sum_{i=1}^{N} \alpha_i \, e^{-t/\tau_i}$$

where N is the number of fluorescence components, and α_i and τ_i are the relative intensity and lifetime respectively of the i^{th} component. The best fit values for α_i, τ_i and N must be determined for each sample investigated. Whenever the exciting light pulse has an appreciable time width on comparison to the fluorescence signal, a convolution integral must be solved in order to extract the lifetime parameters (Brody, 1957). A number of theoretical approaches have been developed to extract the amplitude and lifetime values from the experimentally determined excitation and fluorescence profiles (Ware et al. 1973; Munro and Ramsay, 1968; Gafni et al. 1975). We have utilized the method of moments technique (Isenberg and Dyson, 1969; Isenberg et al. 1973) for all data analysis reported in this thesis. The technique involves the calculation of the moments in time of the experimental fluorescence and excitation profile followed by solution of a matrix for the lifetime values and intensities. In principle, the method is capable of deriving the number of lifetime component as well as their values in a given experimental spectrum without prior assumptions. In addition, it has been extensively documented in a number of model and real systems and certain modifications have been offered which increase its applicability to complex fluorescence systems

Table 3-1 These count rates in single photon counts per second were obtained on the fluorescence lifetime system.

PHOTOMULTIPLIER DARK CURRENT

Tube Temperature	RCA 8850 (blue sensitive)	RCA 8852 (red sensitive)
21°C	520	55,000
10°C	390	9,800
0°C	250	1,600

XBL 761-5639

(Isenberg, 1973; Isenberg, 1975).

Photomultiplier Dark Counts

To obtain high signal to noise ratios in photon counting, it is essential to minimize the dark current in the signal photomultiplier. Thermal emission processes within the phototube contribute substantially to this dark current. By cooling the photomultiplier, a significant reduction in the dark current is often obtained. In Table 3-1 we see the dark currents of the photomultipliers that are used in this system as a function of the tube temperature. The RCA 8850 photomultiplier exhibits a two-fold decrease in dark counts as the tube is cooled from room temperature to 0 deg C. The red sensitive RAC 8852 shows a dramatic 34-fold decrease in dark counts upon cooling to 0 deg C. It is important to use photomultiplier cooling when the red sensitive photomultiplier is used in the single photon counting mode.

Results

1. All published excitation and fluorescence decay curves from single photon counting instruments exhibit secondary peaks of low intensity which occur before and after the primary peak (Leskovar et al.,1976; Schuyler and Isenberg, 1971; Lewis et al., 1973). If the photomultiplier dynode string is poorly adjusted, then further peaks will appear (Lewis et al., 1973). An expanded profile of the light pulser flash as measured on our instrument can be seen in Figure 3-2. Both the early and late peaks exhibit approximately 0.35% of the intensity of the primary peak. The early peak occurs 7 nsec before the main peak, the late peak

Fig. 3.2. Expanded view of the lamp flash profile; the effect of the region of photomultiplier illumination on the early and late spectral peaks. The main peak in each curve is approximately 21,500 counts. A) The front surface of the RCA 8850 photomultiplier was covered by an opaque mask with a central 5 mm diameter opening. B) The entire 50 mm diameter of the front surface of the photomultiplier was exposed.

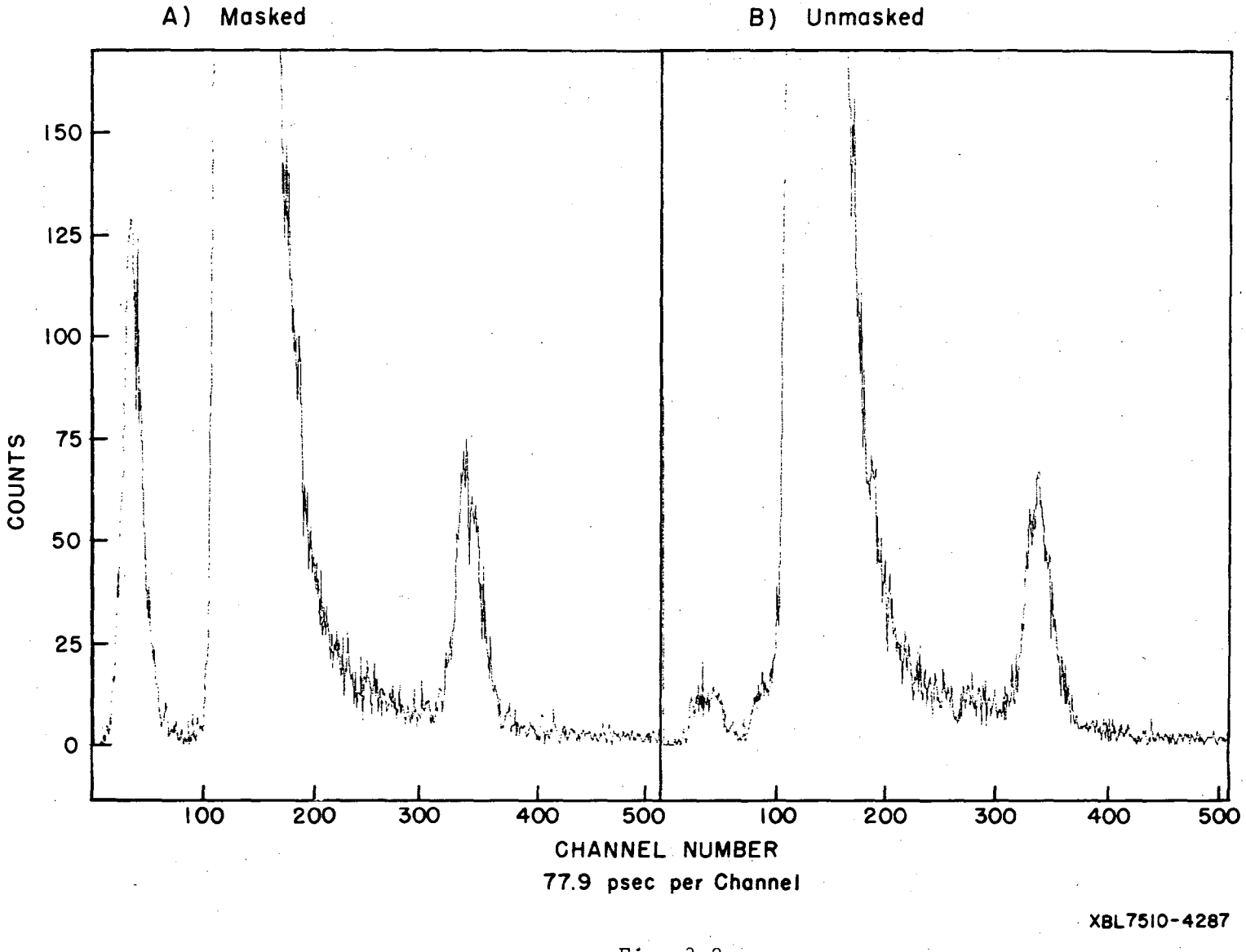
A) Masked
B) Unmasked
COUNTS
150
125
100
75
50
25
0
100
200
300
400
500
CHANNEL NUMBER
77.9 psec per Channel
XBL7510-4287

Fig. 3.2

occurs 16 nsec after the main peak. It has been proposed that these supplemental peaks arise from internal processes in the photomultiplier (Yguerabide, 1972; Stevens and Longworth, 1972). Our findings confirm this interpretation. The peaks do not arise from light reflections in the sample chamber because the profile is unchanged if a light pipe is used to channel light pulser flashes directly into the photomultiplier. The peaks are not a function of the light source because they are also seen in the record of the flash profile using a light emitting diode as the emission source. The intensity of the early peak is, however, sensitive to the area of illumination of the photomultiplier. In Figure 3-2, we have observe that restricting the illumination to the center of the photocathode causes the early peak to increase in intensity while the late peak is unaffected. The dynode structure underlies the center of the photocathode and is preferentially illuminated in this case. Apparently, the early peak arises from photons which are not absorbed by the photocathode, but rather pass through this surface and directly strike the first dynode causing an early electron cascade. The origin of the late peak is uncertain. It appears to result from an internal electron reflection of some sort since it is unaffected by variations in the illumination of the photocathode. One possibility is that electrons from the first dynode travel back up to the photocathode, initiating a late starting secondary electron cascade (Stevens and Longworth, 1972).

If excitation and fluorescence spectra are not recorded under identical conditions, the amplitudes of the early and late peaks can differ between spectra. These differences can lead to problems when a deconvolution analysis of the lifetimes is attempted. The variation in early

peak amplitude can be minimized if the emitting volumes of the samples used for excitation and fluorescence spectra are equalized. Equalization of emitting volumes will also reduce variations in photo-multiplier response characteristics associated with illumination of different photocathode areas (Lewis et al., 1973).

ii. Total System Time Resolution

The time resolution characteristics of this system are indicated by measuring the time profile of the excitation light flash. The sample is replaced by a polished metal front surface mirror at an angle of 45 degrees to the symmetry axis of both the light pulser and photomultiplier. The total system time resolution is defined as the FWHM of the light pulse measured by a particular photomultiplier. With the RCA 8850 operated at the supply voltage of 3000 V and cooled to 0°C, the system total time resolution is 800 psec FWHM, as shown in Fig. 3-3. No colored glass filters were used during the measurement. The spark gap was cleaned and adjusted before the measurement. The resolution decreases to approximately 1 nsec in 30 hours of operating time if a gentle stream of dry air is used for flushing of the spark gap. Without dry air flushing, the resolution decreases to 1 nsec in 15 hours of operating time. The total system resolution is 1.48 nsec when using the 8852 photomultiplier. The 8852 is operated at the supply voltage of 2800 V, after the photomultiplier is kept in the dark for 24 hours and cooled to 0°C. During the measurements a Corning glass filter, No. CS 3-66, is used at the output window of the light pulser. The CS 3-66 is a short wavelength cutoff filter with a 0.02% transmittance at 540 nm and a 50% transmittance at 575 nm. The

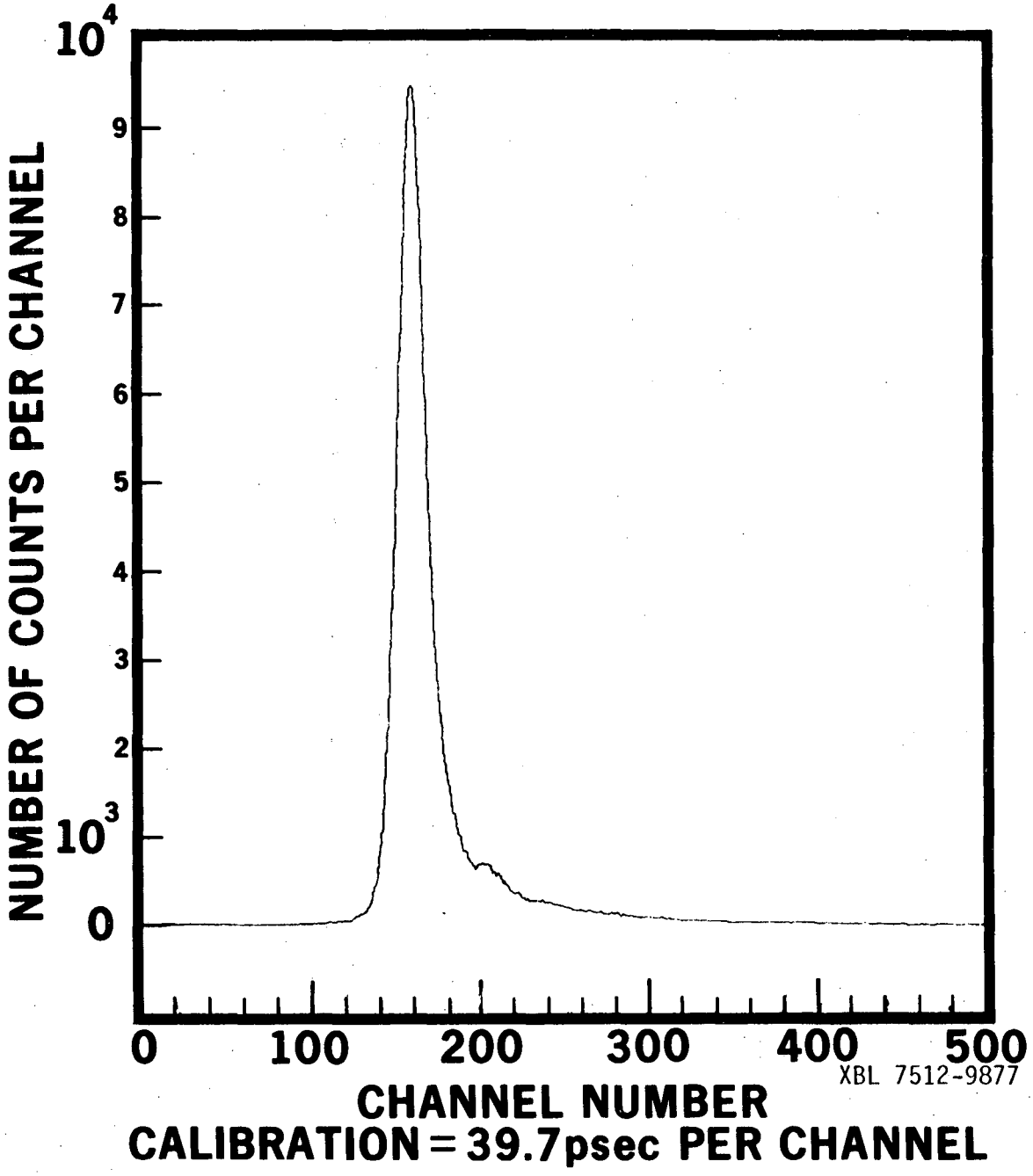

Fig. 3.3. Light pulse waveshape from the nanosecond light pulser with optimized operating conditions.

system resolution falls to 1.08 nsec when a Corning CS5-58 blue glass filter is used instead of CS3-66. The CS5-58 filter has transmittance of 0.02% at 340 and 480 nm, and a peak transmittance of 40% at 415nm.

iii. Anthracene in cyclohexane

To demonstrate the accuracy of lifetime measurements provided by this system we have chosen to investigate pure compounds with well established fluorescence lifetimes. Anthracene is commercially available in high purity and there is agreement in the literature on its fluorescence lifetime in cyclohexane. Values of 4.9 nsec (Berlman, 1971) and 5.0 nsec (Greenberg et al., 1966) have been reported. The fluorescence of deoxygenated anthracene in cyclohexane is shown in Figure 3-4. The sample consists of 0.3 mg/ml anthracene (99.99 mol%, Materials Ltd., Inglewood, N.J.) in cyclohexane (Chromatoquality 99+ mol%, M.C.B., Norwood, Ohio) which is deoxygenated by bubbling with nitrogen gas for 15 min inside a nitrogen-filled glove box. The best-fit analysis, shown in Figure 3-4, yields an anthracene lifetime of 4.94±0.07 nsec with a minor component [$\alpha_2/(\alpha_1+\alpha_2) = 4\times10^{-3}$] of 21 ns.

The minor lifetime component is seen in all spectra from a variety of compounds that we have investigated. It appears to be a system artifact which arises primarily from two sources. In many spectra the system artifact represents a true background system fluorescence which arises primarily from the glass adsorption filters used to isolate the excitation and fluorescence light. This is the case with anthracene because the same low intensity long lifetime fluorescence is observed when cyclohexane, or any other scatterer, serves as the sample in the setup used

Fig. 3.4. Fluorescence of anthracene in cyclohexane (1.7×10^{-3}M). A) Lamp excitation progile; B) Experimental and calculated fluorescence profiles; the noisy curve is the experimental fluorescence response and the smooth curve is the calculated response generated from the excitation profile best fit intensities and lifetimes: $\alpha_1 = 0.0419$, $\tau_1 = 4{,}94$ nsec; $\alpha_2 = 0.00016$, $\tau_2 = 21.2$ nsec.

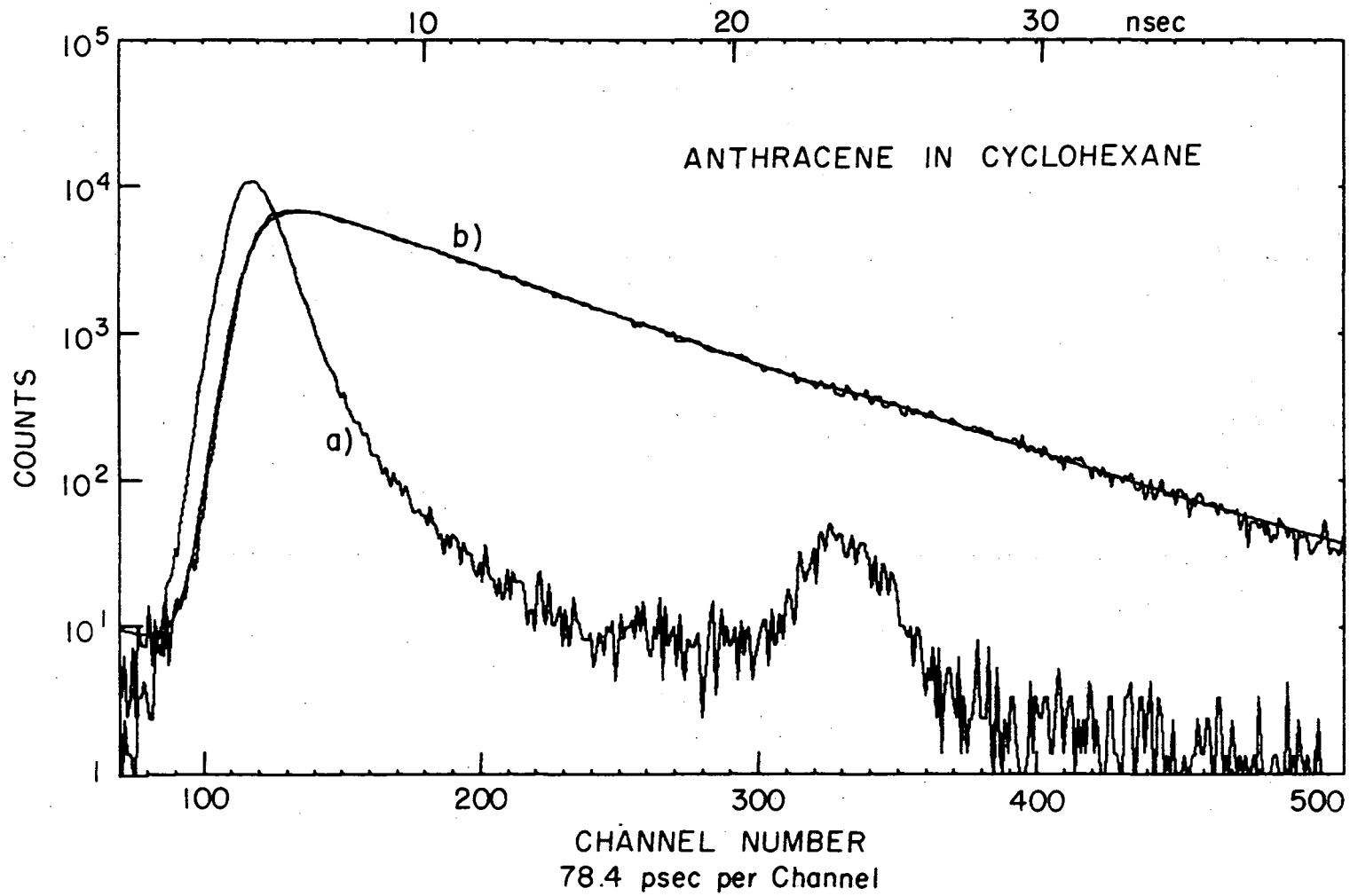

Fig. 3.4

XBL754-5153

to record the anthracene fluorescence. An additional factor that contributes to the system artifact is the sensitivity of the lifetime analysis, especially in the tail region where long lifetime components dominate, to the size and distribution of the scattering or emission volume within the sample. In the case of excitation spectra, the use of a large diffuse scatterer such as the sample solvent in a cuvette, will yield a broader excitation spectrum with a more pronounced tail component than is obtained from a small, focussed scattering image from a polished metal surface. If the image size and intensity distribution properties are not exactly matched in the fluorescence and excitation samples, then different areas of the photomultiplier surface are illuminated and an artifactual small intensity, long lifetime fluorescence component will be observed in the analysis.

The presence of the system artifact can be demonstrated in any particular set of data by the improved fit that a multi-component lifetime analysis will yield. The method of moments program contains a number of objective fit tests which permit the experimenter to choose the best-fit analysis of his data from the one component , two component or three component analyses that the program allows. In addition, a visual examination of the experimental and calculated fluorescence curves will often reveal the presence of the small amplitude long lifetime system artifact in the data.

The measurement of a relatively long fluorescence lifetime, such as 5 nsec for anthracene, is not seriously complicated by the presence of the system artifacts. In the anthracene experiment, a one component analysis yields a value of 5.02 nsec compared to the best-fit two component

value of 4.94 nsec. The removal of dissolved oxygen is, however, an important requirement. Since molecular oxygen normally exists in a triplet state, it can serve as an effective fluorescence quencher. The lifetime of anthracene in air saturated cyclohexane (without deoxygenation) was determined to be 4.0 nsec. Control of solution oxygen levels is important for accurate lifetime determinations.

iv. Diphenyl Butadiene in Cyclohexane

Accurate subnanosecond lifetimes have been reported for very few compounds. One of the fastest, well characterized chemical systems is trans, trans-1,4-diphenyl-1, 3-butadiene in cyclohexane. A lifetime of 0.63 nsec has been reported for this system using a quantum counter to minimize photomultiplier wavelength effects (Lewis et al., 1973). The emission of this compound measured on our lifetime system is shown in Figure 3-5. The sample contains 1.0×10^{-5} M trans, trans-1,4-diphenyl-1,3-butadiene (M.C.B., Norwood, Ohio; twice recrystallized from carbon tetrachloride before use) in cyclohexane (chromatoquality 99+ mol%, M.C.B.) which had been deoxygenated in a stream of nitrogen gas as described for anthracene. The best fit analysis yielded two lifetime components. The observed lifetimes were 0.64±0.03 nsec for diphenyl butadiene and 15 nsec for a minor [$\alpha_2/(\alpha_1+\alpha_2) = 1.8\times10^{-3}$] system artifact component. In this case the presence of the very minor level of system artifact fluorescence has a significant effect on the lifetime analysis. If the presence of this minor component is ignored, and a one component lifetime analysis is attempted, the result is an apparent lifetime of 0.96 nsec. To obtain accurate analysis of short lifetime samples, it is

Fig. 3.5. Fluorescence of 1,4-diphenyl-1,3-butadiene in cyclohexane (1.0×10^{-5}M). A) Lamp excitation profile. B) Experimental and calculated fluorescence profiles; the noisy curve is the experimental fluorescence and the smooth curve is the calculated response generated from the excitation profile; best-fit intensities and lifetimes: $\alpha_1 = 0.111$, $\tau_1 = 0.642$ nsec; $\alpha_2 = 0.0002$, $\tau_2 = 14.9$ nsec.

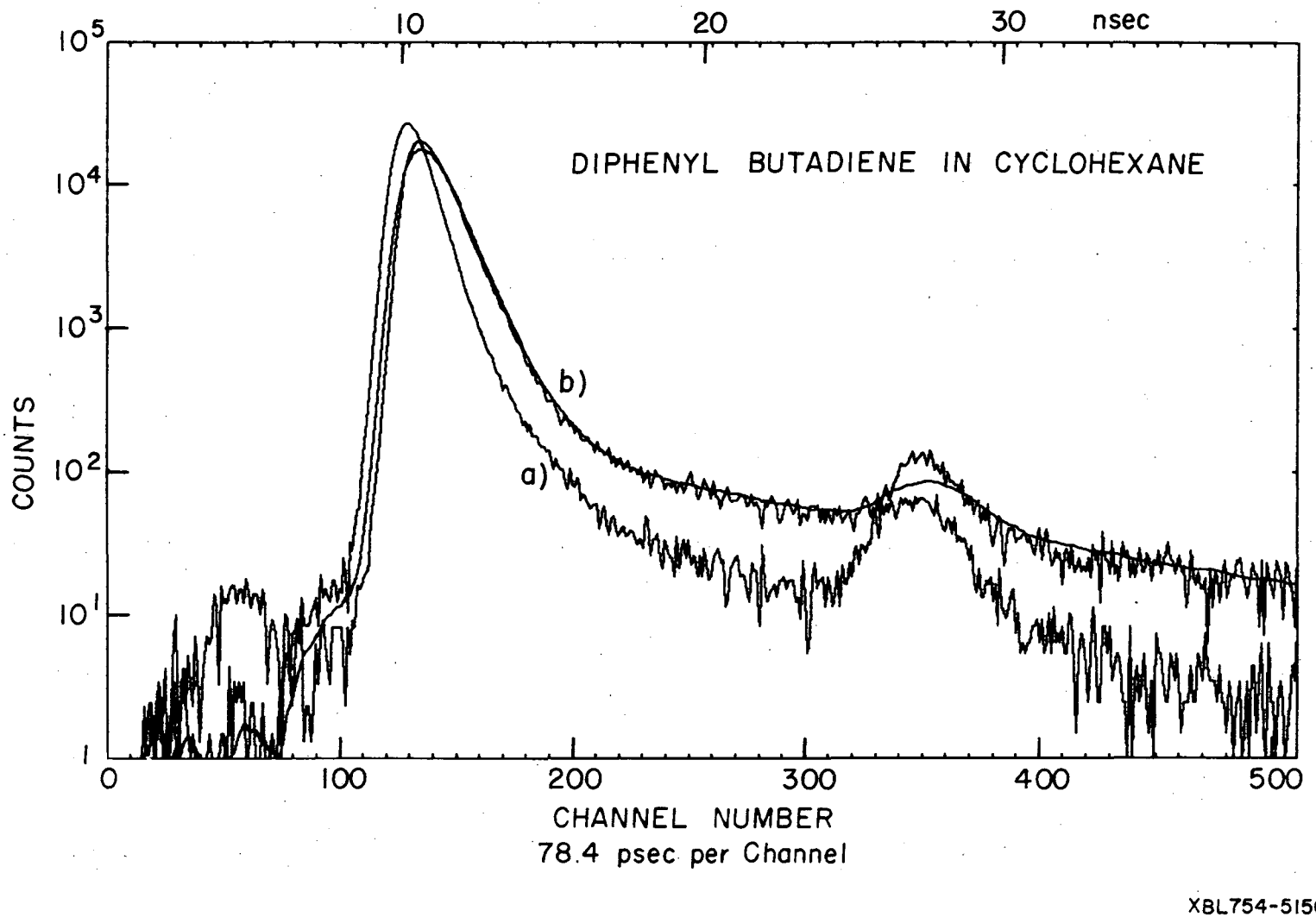
10
20
30
nsec
10^5
10^4
10^3
10^2
10^1
1
COUNTS
DIPHENYL BUTADIENE IN CYCLOHEXANE
b)
a)
0
100
200
300
400
500
CHANNEL NUMBER
78.4 psec per Channel
XBL754-5156

Fig. 3.5

important to use a two component analysis whenever even minor contamination from long lifetime sources is encountered. In the absence of multicomponent capabilities in the analysis, the results may be quite inaccurate.

v. Erythrosin in Buffer

To our knowledge, lifetime measurements on compounds with lifetimes of under 480 psec (Schuyler et al., 1972) have not been reported in the literature from single photon counting systems. To test the limits of our measurement capabilities, we examined the lifetime of erythrosin fluorescence. Values of 57 psec (Munro and Ramsey, 1968), 90 psec (Alfano and Shapiro, 1972), and 110 psec (Porter et al., 1974) have been reported for the lifetimes of erythrosin and erythrosin B (the disodium salt of erythrosin) in water. These measurements were obtained with mode-locked laser systems. Our sample of erythrosin (Eastman, Rochester, N.Y.) was purified by passage through a silica gel-methanol column and suspended in a buffer solution of 40 mM Tricine-NaOH, 2 mM EDTA, pH 8.0. We determined the lifetime of this erythrosin solution to be 90±30 psec for fluorescence emission at 550 nm that is excited at 490 nm, with a minor system artifact component of 4.7 nsec, $[\alpha_2/(\alpha_1+\alpha_2) = 4\times10^{-4}]$. The experimental and predicted lifetime curves are shown in Figure 3-6.

To obtain accurate measurements of very short lifetimes, certain experimental conditions must be carefully controlled. The most critical problems arise from slow drifts that occur in the light pulser time profile and from the wavelength dependence of the system response. To obtain stable, optimal performance from the air gap light pulser, we have

Figure 3.6. Fluorescence of erythrosin ($2.8\times1-^{-5}$M) in 40 mM Tricine-NaOH, 2 mM EDTA pH 8.0. The lamp excitation profile closely resembles the fluorescence profiles and is deleted for purposes of clarity. The noisy curve is the experimental fluorescence spectrum, the smooth curve is the calculated fluorescence response generated from the excitation profile best fit lifetimes and intensities: $\alpha_1 = 0.429$, $\tau_1 = 88$ pdrv; $\alpha_2 = 0.00017$, $\tau_2 = 4.71$ nsec. Note that the fit of the data to the predicted profile deviates by less than the width of the pen trace over several orders of magnitude.

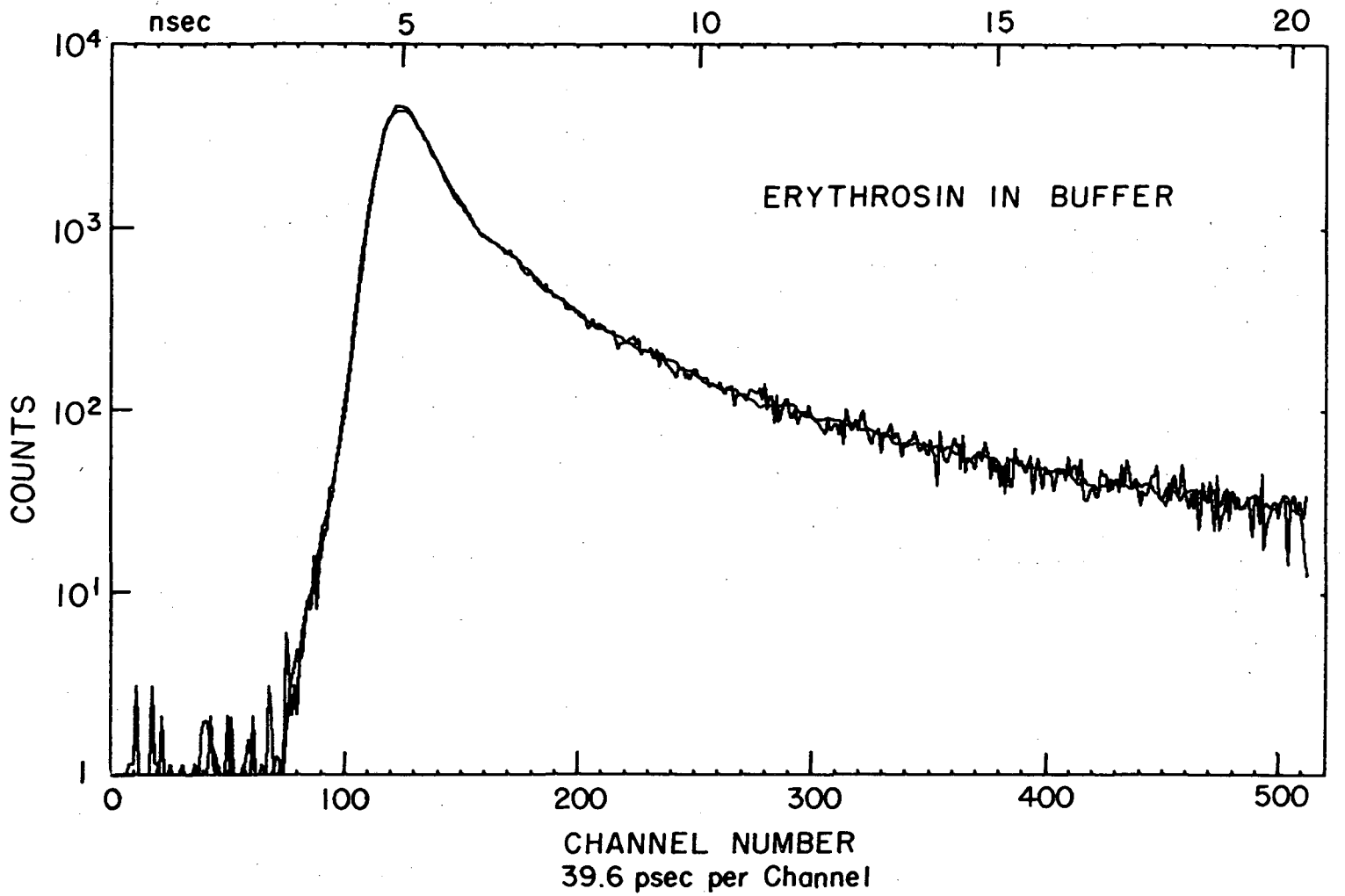

XBL7510-4279

Fig. 3.6

found it necessary to flush the chamber continuously with a flow of dry air during operation, to clean the electrode tips after every 10 hours of operation and to resharpen the pointed electrode into a conical tip after significant erosion has occurred. The remaining drift which occurs in the excitation profile can be minimized by recording excitation and emission profiles alternately (Hazan et al., 1974). We find that drift problems in our system are significantly decreased by recording half the excitation profile before the fluorescence measurement and half afterwards. In the case of erythrosin, we recorded the fluorescence response for one hour. An excitation profile recorded only before the fluorescence yields a lifetime that differs by up to 40% from the value obtained from an averaged excitation profile.

The presence of a significant wavelength dependence in the system response function can complicate lifetime measurements (Ware et al., 1973; Wahl et al., 1974). This dependence arises in part in the photomultiplier, from the dependence of the kinetic energy of the photoelectrons on the wavelength of the incident photons (Wahl et al., 1974). If the fluorescence of a sample is observed at a constant emission wavelength as the excitation wavelength is progressively blue shifted, then the peak of the fluorescence response time profile remains at a constant position, but the peak of the excitation profile is increasingly shifted towards earlier times. When very short lifetimes are extracted from excitation and emission profiles recorded at widely separated wavelengths, this artifactual peak shift leads to the indication of an anomalously long fluorescence lifetime in the analysis. For example, if purified erythrosin in buffer is excited near 360 nm and the fluorescence is recorded at 550 nm a

lifetime of 470 psec is indicated, with a poor fit of the observed and calculated fluorescence curves. If the same sample is excited at 490 nm and fluorescence recorded at 550 nm, then a lifetime of 90 psec is observed. Inspection of the fluorescence profiles reveals that this is a curve fitting artifact rather than a change in lifetime with changes in the excitation wavelength.

The presence of a wavelength dependence in the light pulser emission profile also contributes to the system wavelength dependence. The fluorescence emission from a compound whose lifetime is much shorter than the FWHM of the excitation light pulse closely resembles the excitation profile, as can be seen from an examination of the convolution integral. If a series of fluorescence profiles are recorded from a short-lifetime sample at a constant emission wavelength as the wavelength of excitation is varied, then symstematic variations occur in the emission profile which arise solely from the wavelength dependence of the light pulser emission. In this manner, the wavelength dependence of the light pulser emission is revealed, independent of any contributions from the wavelength dependence of the photomultiplier response. This technique requires that the sample lifetime be independent of the exciting wavelength. Using this method, we have observed that the red emission from the air gap discharge is slightly broader in time (10% broader at 490 nm than at 360 nm) and has a significantly larger tail component than the ultra-violet emission. In our judgement, the best way to minimize the system wavelength dependence, which arises from both photomultiplier and lamp effects, is to use the same light pulser filter recording both the excitation and fluorescence profiles and to minimize the difference between the excitation and emission

wavelengths.

Accuracy

Estimation of the accuracy of a lifetime determination is a complex problem. A number of parameters must be considered individually in the error estimate for each specific experiment. The spread in the light pulser profile, the single photoelectron time spread of the photomultiplier, the timing error introduced by the discriminator and the stability of the measuring system over the time span of an experiment contribute to the instrumental experimental uncertainty. In addition, the lifetime value is determined by an iterative computer de-convolution whose convergence is somewhat sensitive to the input parameters in the program. The time axis calibration for the multi-channel analyzer can provide another source of error. Other factors in the error determination are common to all experimentation, such as repeatability of the experiment, and sensitivity of the analysis to slight, reasonable variations in the experimental conditions (such as the choice of excitation and emission filters). In each experiment, the primary source of error must be identified and estimated.

In our anthracene studies, the largest source of error seems to be drifts in the system electronics which can be observed in the repeatability of the calibration of the analyzer time axis. The calibration of the time axis can be repeated to an accuracy of approximately 1.5%. For this reason we estimate the random errors in the 4.94 nsec lifetime determination to be ± 0.7 nsec. In the erythrosin and diphenyl butadiene experiments, the major error factor seems to be the uncertainty in the computer determination of lifetime. In these cases, the FWHM of the lamp

spectrum is equal to or larger than the lifetime under investigation. As a result, the shape of the fluorescence profile is relatively insensitive to the lifetime value over a significant range, and the error between the observed and the hypothesized fluorescence profiles varies little as the hypothesized lifetime is changed. In the erythrosin experiment, for example, the reliability of the 90 psec lifetime determination was tested by assigning other values to the decay constant and comparing the quality of the fit of the experimental to the hypothesized fluorescence profile. If a lifetime of 120 psec is assumed, a distinctly poorer fit of the curves is visually obvious (root mean square residual of 59 versus 35 for the 90 ps fit). Determination of a lower limit to the lifetime from visual examination of the calculated fluorescence response curves is insensitive to lifetimes below 90 psec. The method of moments program (Isenberg and Dyson, 1969) does, however, contain objective fit analysis parameters that demonstrate that lifetimes below approximately 60 psec provide a poorer fit to the data than the observed value (root mean square residual of 60 for 60 psec versus 35 for the 90 psec fit). For these reasons, we assign an uncertainty of ± 30 psec to the erythrosin result and a like value for diphenyl butadiene where the same considerations dominate.

Discussion

We have demonstrated that it is possible to make accurate fluorescence lifetime measurements down to 90 psec with single photon counting systems. Short lifetime measurements require a photon counting system with a very fast time response, such as the system we have developed, (Leskovar et al., 1976) and attention to a number of experimental conditions. The light pulser output must be optimized by the use of clean, sharp electrodes and the stability enhanced by continuous flushing with dry air. The lifetime analysis can be further improved by time averaging of the excitation profile. The emitting volumes of the excitation and fluorescence samples must be equalized to assure the same distribution of illumination on the photocathode. If the sample-solvent system under investigation is susceptible to oxygen quenching, the solution oxygen level must be carefully controlled. Small amplitude lifetime components from a number of sources may appear as artifacts in the results. Multicomponent lifetime analyses are required to separate the sample lifetime from these system artifacts. The presence of photomultiplier and light pulser contributions to the wavelength dependence of the system response function must be considered in the design of the experiment. When these criteria are fulfilled, it is possbile to extend the wide dynamic range and multicomponent advantages of single photon counting to chemical, physical and biological systems which exhibit highly quenched fluorescence emissions.

PHOSPHORYLATION COUPLING FACTOR FROM CHLOROPLASTS LABELED WITH 5-IODOACETAMIDOFLUORESCEIN: BIOPHYSICAL CHARACTERIZATION OF THE LABELING SITE

INTRODUCTION

The chloroplast coupling factor (CF) is a water soluble protein which is associated with the thylakoid membrane surface, where it catalyzes the terminal step of ATP production during photophosphorylation. It contains five different subunit types ranging in size from 13,000 to 59,000 daltons (Nelson et al., 1973). Two tight binding sites for ATP or ADP have been characterized (Livne and Racker, 1969; Roy and Moudrianakis, 1971; Cantley and Hammes, 1975a) along with other, weaker sites (Cantley and Hammes, 1975a). These sites have been tentatively assigned to the α and β subunits (Cantley and Hammes, 1975a). This assignment is verified by the observation that an α and β subunit complex derived from CF is active as an ATPase (Deters et al., 1975).

In a previous investigation, covalent labeling of the β subunit with a fluorescent label led to 80% inhibition of the enzyme activity (Deters et al., 1975). We have used a new sulfhydryl-specific fluorescent label, 5-iodoacetamidofluorescein (5-IAF) to label CF with minimal decrease in the enzyme activity. The label binds preferentially to the β subunit. Investigation of the fluorescence emission spectrum, the fluorescence polarization, and potassium iodide quenching of the label enables us to explore the microenvironment at the 5-IAF binding site on the β subunit. The effects of substrate addition and trypsin treatment (which activates an ATPase activity) on the fluorescent label are investigated.

EXPERIMENTAL

5-Iodoacetamidofluorescein

The 5-IAF was synthesized by Dr. Richard Haugland (Hamline University, St. Paul, Minn.) and generously provided to us as a gift. 5-IAF has recently become available from Molecular Probes, 1775 Maple Lane, Roseville, Minn. 55113. It was used without further purification. An apparent molar absorptivity of 60,000 was measured at the 491 nm absorption peak in water buffer (40 mM Tricine-NaOH, 2 mM EDTA), at pH 8.0. The material migrates as a major band with several minor components when examined by reverse phase thin layer chromatography using Eastman # 13181 silica gel sheets impregnated with 5% (v/v) Dow Corning 200 silicone fluid (10 cs. viscosity) in anhydrous ethyl ether and run in a solvent of 90% acetone 10% water saturated with the silicone fluid. The solid 5-IAF was stored at -25°C in the dark. In solution it is relatively stable when refrigerated in the dark, but it undergoes a slow degradation in the light. Illumination of the parent fluorophore, fluorescein, can lead to free radical formation (Niizuma et al, 1974) and superoxide production (Balny and Douzou, 1974). For these reasons the dye and labeled proteins are kept in the dark or under dim illumination, when possible.

Coupling Factor

Coupling Factor was purified by a method adapted from the pyrophosphate wash procedure of Strotmann et al. (1973). In contrast to their findings, we obtained appreciable protein contamination in the CF samples following this method. However, when the washes are supplemented by subsequent batch gradient ion exchange chromatography on DEAE Sephadex A-50 followed by sucrose gradient centrifugation (Lien and Racker, 1971b), then CF is obtained in high yield and purity. We have used this method (Hartig, 1976) to obtain yields comparable to the method of Lien and Racker (1971b). The purity of isolated CF was demonstrated to be greater than 95% by polyacrylamide gel electrophoresis. The fluorescence

emission ratio of the purified CF (E_{303}/E_{350}) was typically 2.4 or greater when measured using a Perkin Elmer MPF 2A fluorometer with a Hamamatsu R106 photomultiplier, excitation wavelength-280nm, emission and excitation slits- 6nm spectroscopic bandwidth.

5-IAF Labeling of CF

We have adopted a labeling technique in which the fluorescent dye is first adsorbed onto Celite (diatomaceous earth) before being introduced into the protein solution (Rinderknecht, 1960, 1962). Approximately 0.6 g of Johns-Manville acid washed Celite is heated to 350° C for 45 min and allowed to cool to room temperature. A solution of 0.06 g of 5-IAF in 30 ml of methanol is added to the Celite and the solvent is removed at room temperature on a rotary evaporator. The dried yellow powder is stored in the dark at - 25° C. A suspension of 30 mg of Celite containing adsorbed 5-IAF in 0.2 ml of 40 mM Tricine-NaOH, 2 mM EDTA, pH 8.0 is brought to approximately pH 7 be addition of K_3PO_4. Forty microliters of 0.1 M ATP, pH 7 is added to the suspension. A solution containing 0.5 to 5 mg of CF in 1 ml of the same buffer is added and the pH of the reaction mixture is adjusted to 7.5 with K_3PO_4 and KH_2PO_4. The mixture is placed in a room temperature shaker bath and incubated in the dark for approximately 2 hr with constant agitation to keep the Celite suspended. Following the incubation, the mixture is centrifuged on a clinical centrifuge and the supernatant is applied to a 0.7 x 15 cm Sephadex G-50 column. The labeled protein is collected in the void volume, free from unreacted label. It is stored at 40°C after precipitation in 2 M $(NH_4)_2SO_4$. The same results are obtained if the Celite is removed from the labeling mixture, leaving behind a millimolar 5-IAF solution for the labeling reaction. The primary role of Celite in this case is to provide a convenient means of producing a concentrated solution of the label.

The extent of labeling is determined from the protein concentration and the absorbance of the attached dye at 498 nm. A correction for light scattering, which is observed in the labeled protein, is made by subtracting an interpolated light scattering curve from the 5-IAF-CF absorption. The scattering curve is drawn between points at 600 nm and at 400 nm where the 5-IAF absorption is known to be 0% and 6% respectively of the absorption peak of the attached dye at 498 nm. The attached label has a molar absorptivity of 42,000 at the 498 nm absorption peak (see Results). The stability of the covalent labeling is verified by a constancy in labeling ratio following successive desaltings on Sephadex G-50 and precipitations in 2M $(NH_4)_2SO_4$ over several days.

Protein Assay

The protein concentration of CF preparations is determined from a specific absorptivity of 0.54 at 280 nm for a 1 mg/ml solution (Farron, 1970). In the presence of light scattering or interfering absorbance the protein concentration is determined by a Lowry assay in 40 mM Tricine-NaOH, 2 mM EDTA, pH 8.0 (Lowry et al., 1951). When bovine serum albumin in the same buffer is used as a standard, the value obtained in the Lowry assay for CF must be multiplied by a correction factor of 0.74 to obtain the true dry weight. This is in contrast with the result obtained by the Cornell group (Farron and Racker, 1970). The buffer used by the Cornell group was not specified. We have observed a strong buffer dependence in the Lowry assay sensitivity. Our value was calibrated against both the CF absorption assay and a direct dry weight measurement of CF. A molecular weight of 325,000 has been used in all calculations (Farron, 1970).

ATPase Assay

The ATPase activity of CF or 5-IAF-CF is determined following trypsin

activation of the enzyme by a modification (Hartig, 1976) of the procedure of Lien and Racker (1971b). ATP hydrolusis was detected by a modification of the inorganic phosphate assay of Martin and Doty (1949; Lindberg and Ernster, 1956). Trypsin activation times of 4 to 12 min, depending on the sample, were used.

Photophosphorylation Assay

The photophosphorylation assay was derived (Hartig, 1976) from the methods of Shoshan and Shavit (1973) and McCarty (1971). Rapid processing of the chloroplasts and strict adherence to the protocol are essential for high rates and reproducibility. ATP^{32} production was monitored by the method of Avron (1960).

SDS Gel Electrophoresis

We used the procedure of Laemmli (1970) without a stacking gel for 9% polyacrylamide gels at pH 8.8 with 0.1% SDS. The gels were stained with Coomassie blue using the procedure of Fairbanks et al., (1971).

Absorption and Fluorescence Measurements

We recorded spectra at room temperature using a Cary model 118 absorption spectrometer, steady state fluorescence spectra using a Perkin-Elmer MPF 2A spectrofluorometer at ambient temperature, and corrected fluorescence spectra with a Perkin-Elmer MPF 3 Spectrofluorometer. Fluorescence polarization measurements were obtained on the MPF 2A fluorometer with the standard polarization accessory. Fluorescence lifetime measurements were obtained on a novel single photon counting system which has been described elsewhere (Hartig et al., 1976; Leskovar et al., 1976).

Fluorescence polarization P and the limiting polarization in the absence of molecular motion P_o were determined in 40 mM Tricine-NaOH, 2 mM EDTA pH 8.0. The excitation wavelength was 490 nm and the emission wavelength was 520 nm with an 8 nm bandpass in the excitation and emission slits. P_o was determined from polarization measurements in 95% glycerol at different temperatures extrapolated to infinite viscosity.

RESULTS

The structure of 5-iodoacetamidofluorescein (5-IAF) is shown in Figure 1. The absorption peak observed at 491 nm in water solution (40 mM Tricine-NaOH, 2 mM EDTA, pH 8.0) shifts to 495 nm in methanol and 505 nm in isopropanol. This corresponds to similar solvent shifts observed for fluorescein (Seybold et al., 1969; Martin and Lindqvist, 1973). Solutions in certain solvents, such as acetone and dimethylsulfoxide are colorless and non-fluorescent. Similar observations for fluorescein have been ascribed to the formation of a non-fluorescent lactone form (Davies and Jones, 1954).

The corrected emission maximum occurs at 518 nm in water solution (40 mM Tricine-NaOH, 2 mM EDTA, pH 8.0) and is shifted to 519 nm in methanol and 525 nm in isopropanol. Similar results have been obtained for fluorescein (Martin and Lindqvist, 1973). The apparent molar absorptivity for 5-IAF in 40 mM Tricine-NaOH, 2 mM EDTA, pH 8.0 is 60,000 at 491 nm. The true value may be slightly higher due to the presence of contaminants in our sample.

The extent of reaction of CF with 5-IAF is shown in Table I. It appears that a single labeling site is saturated after approximately 2 hr reaction time in the presence of a 1000-fold excess of label. By comparison with the absorption of urea-denatured 5-IAF-CF, the peak molar absorptivity of 5-IAF in native 5-IAF-CF was determined to be 42,000. A correction was made based on the absorption change of unreacted 5-IAF upon addition of urea. The molar absorptivity also includes a correction for 10% decay in the absorption owing to instability in the dye during the labeling reaction and subsequent measurements.

The labeling site can be localized on a particular subunit by separation of the subunits on SDS polyacrylamide gels. Figure 2 shows a photograph of the Coomassie blue staining pattern of the subunits in the two gels on the left. The photograph of the gel on the right was taken from an unstained gel

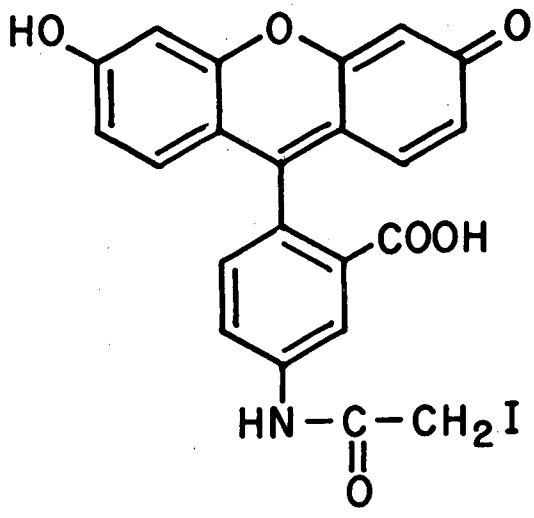

5-IODOACETAMIDOFLUORESCEIN (5IAF)

XBL7411-7885

Fig. 4.1

TABLE I

5-IAF Labeling of CF

The labeling reaction occurs at pH 7.5 in 40 mM Tricine-NaOH, 2mM EDTA. The mixture is incubated at room temperature in the dark.

Reaction Duration	Molar Ratio 5-IAF/CF During Reaction	Molar Ratio 5-IAF Attached per CF
0.5 hr	100	0.06
1	400	0.26
1	1100	0.82
2	1200	0.80
4	1200	1.04

Fig. 4.2. SDS gel electrophoresis of 5-IAF-CF. From let to right, the gels contain 27 ug, 13 ug, and 110, ug respectively of 5-IAF-CF. The photograph of the two gels on the left show the Coomassie blue staining pattern of the subunits. The two major staining bands in the middle of the gels are the α and β subunits. The γ, δ and ε subunits are visible towards the bottom of the gels in order of decreasing molecular weight (Nelson et al., 1973; McEvoy and Lynn, 1973). In the middle gel, under light loading conditions, the δ and ε subunits appear to coalesce into a single band. The photograph of the unstained gel on the right was taken utilizing the green emission from the 5-IAF label as excited by an ultraviolet light source.

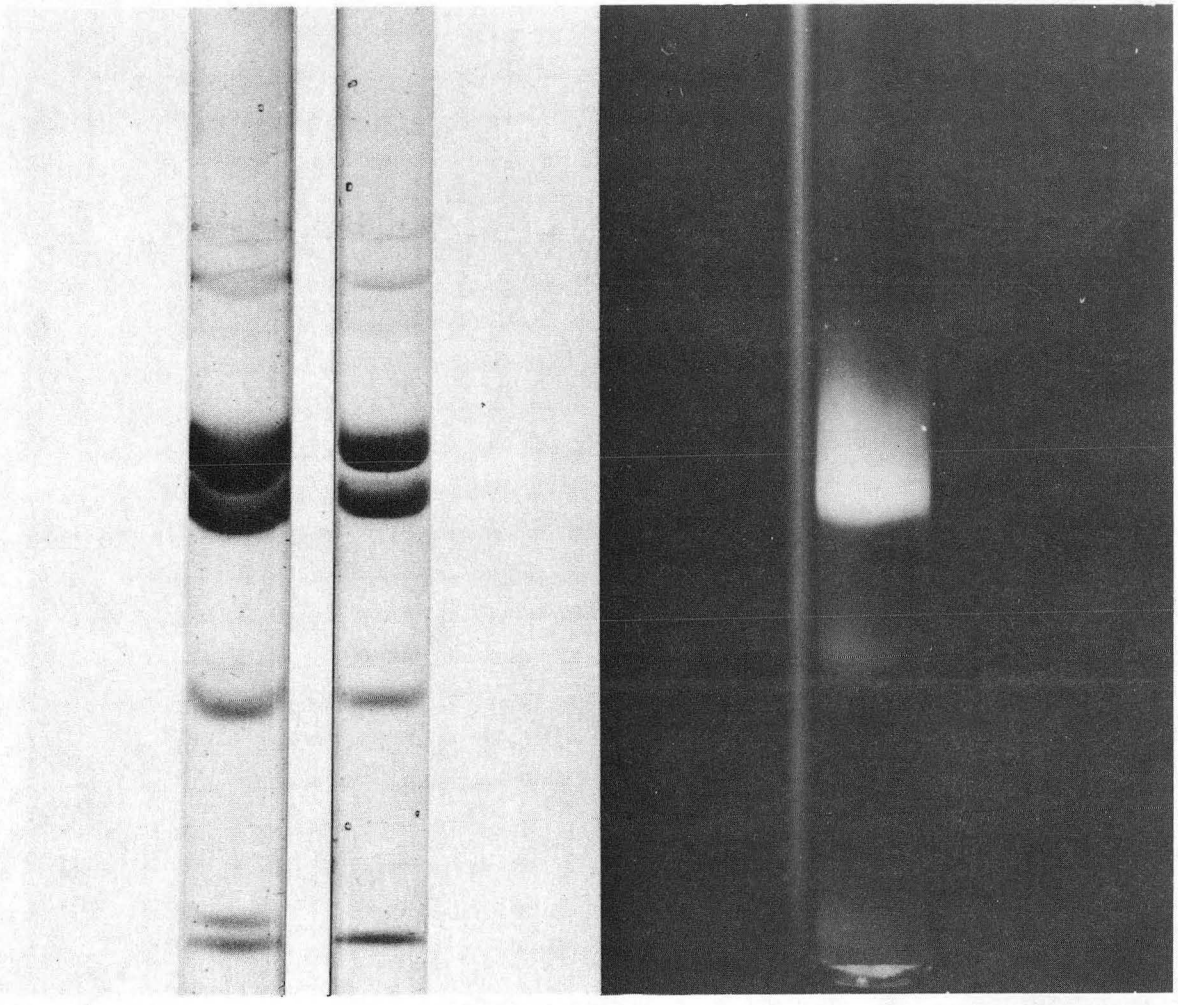

XBB 757-5773

Fig. 4.2

utilizing the green emission from the 5-IAF label as excited by an ultraviolet light source. The majority of the 5-IAF emission clearly originates in the β subunit, with a small portion distributed among the other subunits and some tailing from the β subunit.

The thin layer chromatography scanning accessory of the Perkin-Elmer MPF 2A can be adapted to provide spatial scans of the 5-IAF emission from SDS gels (Hartig and Sauer, 1976). Assuming that the emission quantum yield of 5-IAF is the same on each subunit, we can estimate the distribution of the label from the area of the emission peak associated with each subunit. From such scans, we observe that approximately 75% of the label is localized in the α and β subunits. Trailing of the β subunit emission peak in the vicinity of the α subunit makes estimation of the relative labeling efficiencies between these two subunits more difficult. From the ratio of peak heights, it appears that the ratio of label on the β subunit to label on the α subunit is at least four to one. Taken together with the data of Table I, this suggests that the majority of the label is localized on the β subunit of the enzyme at a single saturable site. Since the iodoacetamide moiety of 5-IAF reacts preferentially with SH residues at pH 7.5 (Means and Feeney, 1971) the site of reaction on the β subunit is presumably a cysteine residue.

A calcium dependent ATPase activity appears in CF following a brief trypsin digestion (Vambutas and Racker, 1965). In Table II the ATPase rates of CF and 5-IAF labeled CF are compared. Approximately 85% of the native activity of CF is retained following the labeling reaction. The effective retention of native activity in the labeled enzyme provides an indication that the labeled protein will provide an accurate description of processes and properties of native CF.

The natural biological activity of CF is photophosphorylation. In Table III

TABLE II

Trypsin Activated Ca^{++}ATPase Activity

Each rate is an average of three experiments.

	ATPase Rate (μmoles P_i/min/mg protein)	% of Control
CF	17.9	100
51AF-CF	15.3	85

TABLE III

Photophosphorylation Rates

Cyclic photophosphorylation with PMS as the cofactor. The photophosphorylation rate is given as μmole ATP produced per hr per mg chlorophyll. The 5-IAF-CF efficiency relative to CF is normalized per mg protein.

Sample	μg CF added	Photophosphorylation Rate	% of Control Rate	Relative Efficiency 5-IAF-CF / CF
Chloroplast		705	100	
EDT Chloroplasts		11.8	1.7	
CF + EDTA				
Chloroplasts	92	172	24	
(36 μg Chl.)	46	142	20	
5-IAF-CF + EDTA				
Chloroplasts	100	116	16	72%
(36 μg Chl.)	50	85	12	62%

we observe that labeled CF has the ability to restore photophosphorylation in EDTA treated chloroplasts. At both the 100 μg and 50 μg levels we find that the photophosphorylation activity in the reconstitution system using 5-IAF labeled CF is more than 60% of that obtained using unmodified CF. An ambiguity does, however, remain in this and all photophosphorylation experiments. It has been shown that the protein crosslinking reagent, DCCD, can cause a significant restoration of photophosphorylation in EDTA treated chloroplasts (McCarty and Racker, 1967). The DCCD effect presumably arises from the ability of DCCD to decrease the proton permeability of the membrane and activate ATP production by residual CF left on the membrane following EDTA treatment (McCarty and Racker, 1967; Uribe, 1972). Thus, stimulation of photophosphorylation on addition of CF does not prove that the added enzyme is active. It may bind to the membrane, decrease proton permeability and activate ATP production in residual CF without itself catalyzing ATP production. The ATPase and photophosphorylation data are, however, strongly suggestive of a minimal perturbation of CF by the presence of the 5-IAF label.

Investigation of spectroscopic properties of the 5-IAF label provides detailed information on the microenvironment surrounding the single labeling site on the β subunit. Figure 3 shows the visible absorption region of soluble 5-IAF and of 5-IAF attached to CF. A 7 nm red shift in the absorption maximum occurs during the labeling reaction. The optical density increase in the short wavelength region is primarily due to increased light scattering in the protein-containing sample. In addition, the absorption peak is broadened following attachment of the label. This broadening may account for a portion of the decrease of the peak molar absorptivity observed following attachment. A red shift of 4 nm is observed for the corrected emmision maximum during labeling. The corrected emission maximum of 5IAF-CF is 522 nm. The red shift

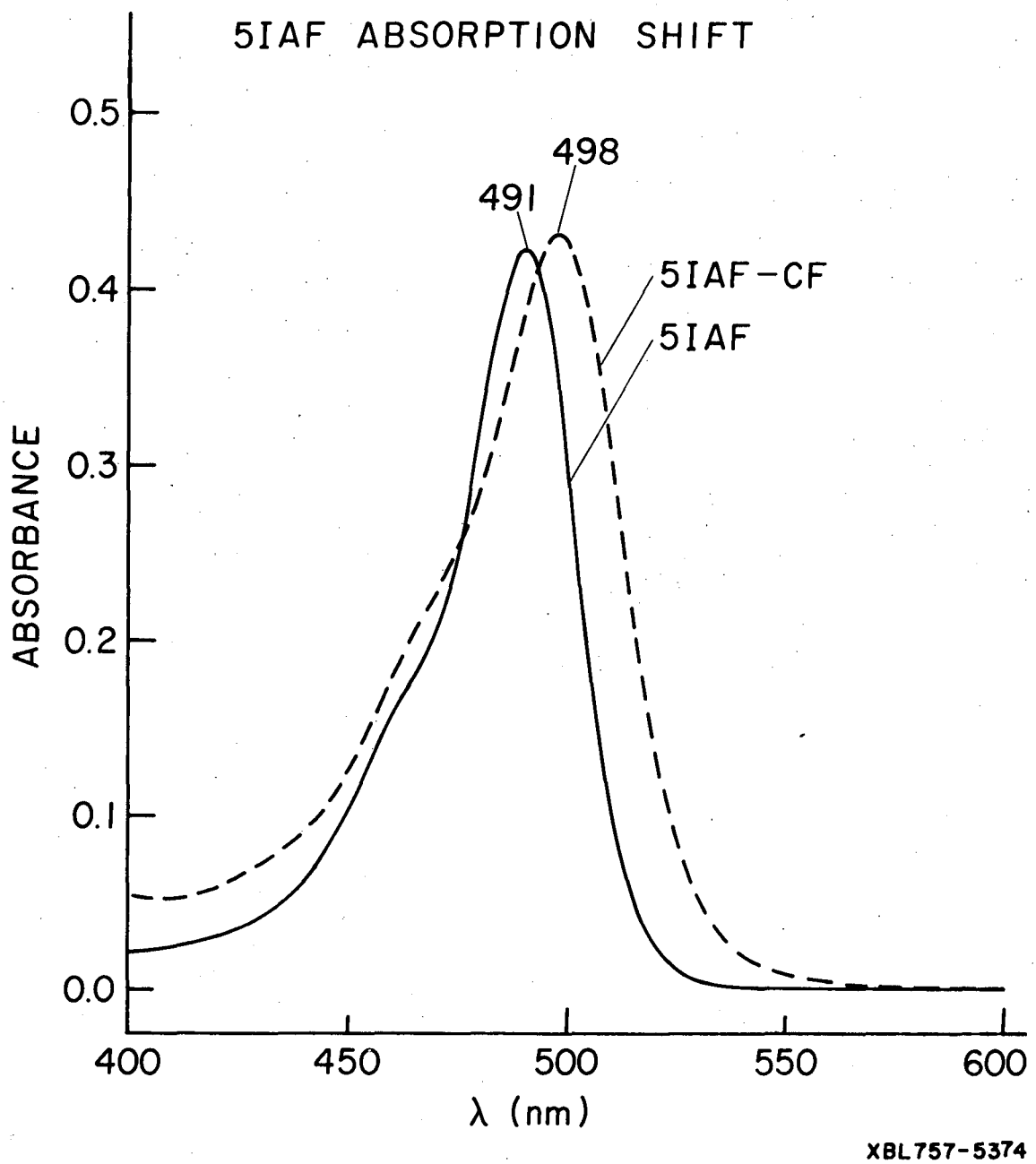

Fig. 4.3. Both 5-IAF and 5-IAF-CF were suspended in 40 mM Tricine-NaOH, 2 mM EDTA, pH 8.0 for the absorption measurements.

in the absorption and emission maxima in 5-IAF-CF is consistent with the transfer of the label into a more hydrophobic microenvironment, as noted from solvent effects on 5-IAF absorption and emission.

The quenching of fluorescence emission by heavy ions serves as a probe for the accessibility of the fluorophore to the ionic solution phase (Lehrer 1971; McGowan et al., 1974). If the fluorescence quenching is dependent upon a collisional encounter between the fluorophore and the quenching ion, then the Stern-Volmer equation will be obeyed (Stern and Volmer, 1919). Figure 4 shows a Stern-Volmer plot of the quenching of 5-IAF emission by potassium iodide for the free dye in solution and for the label attached to CF. The free dye deviates slightly from the linear behavior characteristic of pure collisional quenching. The attached label has a significantly shallower slope (decreased Stern-Volmer constant) than the free label. In a control experiment potassium chloride, a non-quenching salt, had no effect on either 5-IAF or 5-IAF-CF emission. Thus, the decreased slope for 5-IAF-CF indicates that the accessibility of the label to quenching by potassium iodide is dramatically decreased on the protein. We conclude that the label is only partially accessible to the solvent phase in 5-IAF-CF.

The steady state fluorescence polarization of fluorescence labels reflects their rotational motion (Weber, 1953). Measurements of the polarization of emission and P_o for fluorescein, 5-IAF, and 5-IAF-CF are presented in Table IV along with literature values. As expected, the polarizations of fluorescein and 5-IAF emission in solution are identical, within experimental error.

A polarization of 0.252, which is intermediate between the values for the free and completely immobilized dye, was determined for 5-IAF attached to CF. The CF protein is known from electron microscopy to be approximately spherical in shape with a radius of 45 Å (Lien and Racker, 1971a; Racker et al., 1971; Howell and Moudrianakis, 1967). This value agrees well with the spherical radius

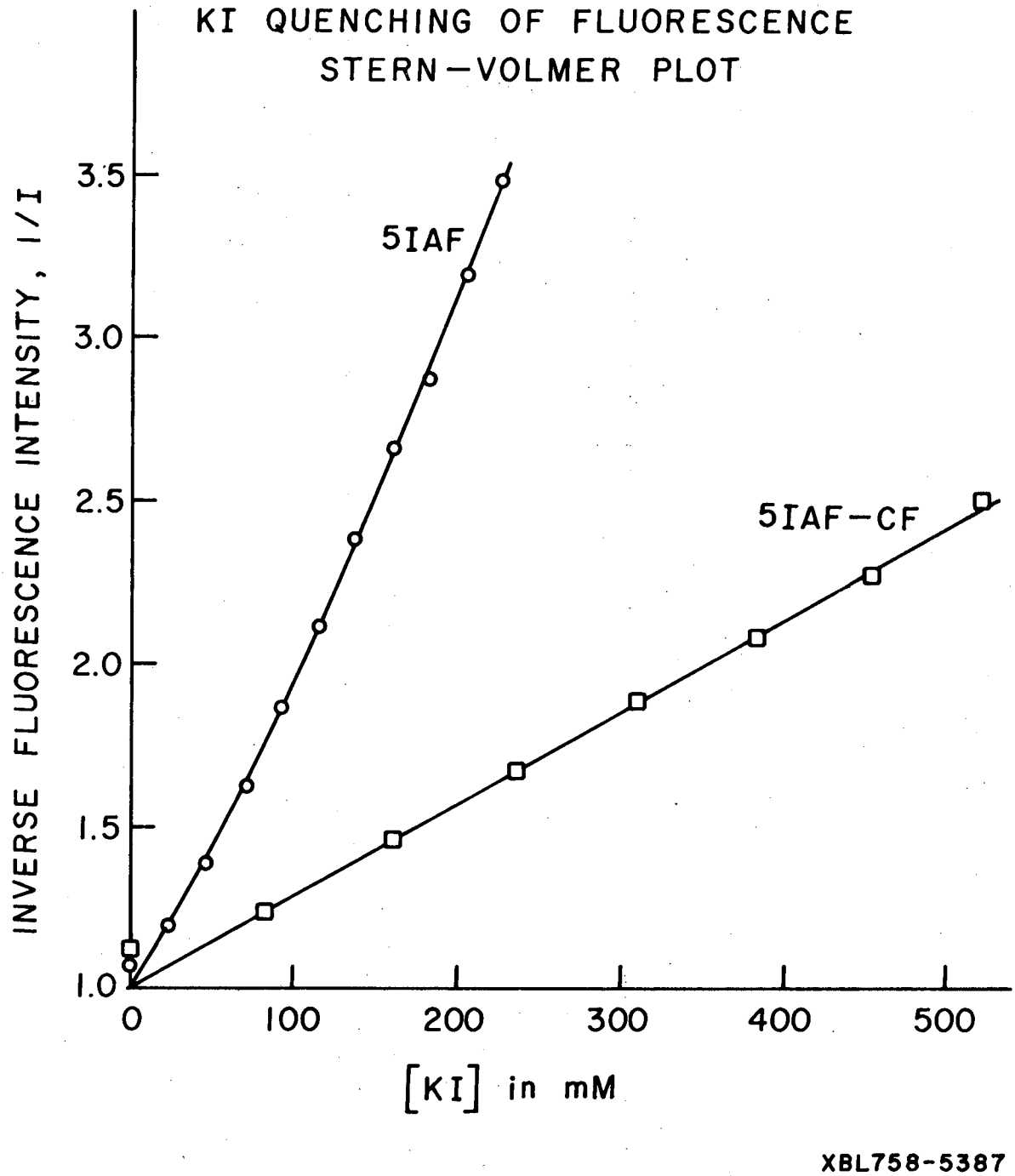

Fig. 4.4. The fluorescence intensity was measured at 520 nm using 490 nm exciting light.

TABLE IV

Fluorescence Polarization of Fluorescein, 5-IAF and 5-IAF-CF

Measurement conditions are described in the Experimental section. Rotational correlation times for 5-IAF and 5-IAF-CF were calculated from a rigid sphere model using observed P and P_o values in the Perrin equation. The rotational correlation time for CF was calculated from the known spherical radius of 45 Å. A measured fluorescence lifetime of 3.8 nsec for 5-IAF has been used in correlation time calculations.

	Polarization P	Limiting Polarization P_o	Rotational Correlation time, nsec
fluorescein	0.017[a]	0.44[b]	
5-IAF	0.018	0.43	0.5
5-IAF-CF	0.252	(0.43)[c]	14.
CF			260.

A. Weber, 1953

b. Perrin, 1926

c. Observed polarization in 95% glycerol at 23° C.

calculated from the known density and molecular weight (Farron, 1970). The hard sphere rotational correlation time (Weber, 1953) for a 45 Å sphere is 260 ns in water solution at 23° C. If the 5-IAF label were rigidly attached to a 45 Å sphere, a fluorescence polarization of 0.42 would be predicted from the Perrin equation (Perrin, 1976). Since the observed polarization for 5-IAF-CF is distinctly lower, we can conclude that considerable independent motion of the label occurs at the labeling site. As an additional point of comparison, the equivalent hard sphere rotational correlation times calculated from the observed polarization for 5-IAF attached to CF and calculated for 5-IAF from the Perrin equation are tabulated in Table IV. We see that the label displays considerable independent motion from the rotation of the spherical protein but is appreciably less mobile than the free dye in solution. In these calculations we have ignored the effect of hydration. The effect of hydration will be to increase the spherical radius of CF and increase the value of its rotational correlation time. If significant hydration occurs, then the label on 5-IAF-CF exhibits somewhat greater freedom of motion than is indicated in Table IV.

Coupling factor displays no catalytic activities when isolated from chloroplast membranes by EDTA treatment. A short trypsin digestion activates a calcium dependent ATPase activity (Vambutas and Racker, 1965). When trypsin is added to 5-IAF-CF samples in the same concentration as is required for activation of the ATPase activity, an 18% increase in the 5-IAF fluorescence intensity is observed following one minute of incubation. The 5-IAF fluorescence intensity continues to rise, reaching a final increase of approximately 30% after 8 minutes of incubation. No changes in the position of the excitation or emission peaks is observed during trypsin treatment. It is interesting to note that a fluorescence intensity increase of approximately the same magnitude is observed when the 5-IAF-CF is denatured by heating at 60° C in the presence of urea and DTT. We

can conclude that trypsin activation of the ATPase activity of CF involves dramatic changes in the vicinity of the labeling site on the β subunit.

We investigated the affect of substrate addition on the fluorescence properties of 5-IAF labeled CF. Addition of 2 mM ADP or ATP to the labeled enzyme causes no changes in the 5-IAF emission intensity or peak position within a 3% experimental error. In view of the fact that 5-IAF labeling does not greatly alter the catalytic activities of CF, we can conclude that the labeling site is not at the active. The fluorescence data further indicates that the microenvironment of the label is not altered by substrate binding. The labeling site is apparently located in a region of the enzyme which does not experience significant conformational changes which occur on substrate binding (Hartig and Sauer, 1976).

DISCUSSION

In this work, we have introduced the use of 5-iodoacetamidofluorescein as a fluorescent reporter group for proteins. A number of properties make this molecule particularly promising. The unusually high absorptivity and fluorescence efficiency of the fluorescein function makes 5-IAF a sensitive fluorescent probe molecule, useful at low concentrations. The long wavelength emission and excitation bands provide freedom from interfering light scattering and protein emission artifacts. These same properties also make 5-IAF desirable as a donor or acceptor for long range excitation transfer studies. Finally, the iodoacetamide moiety provides a means for covalent attachment to proteins with a high degree of selectivity for SH groups under certain conditions (Means and Feeney, 1971).

Attachment of 5-IAF to CF results in a red shift in both the emission and excitation maxima of the dye. This red shift is consistent with transfer of the dye to a more hydrophobic environment. Potassium iodide quenching studies on 5-IAF and 5-IAF-CF indicate that the label on the protein is partially accessible to solvent, but much less accessible than the free dye in solution. The steady state polarization measurements show that the label demonstrates motion that is independent of the tumbling of the whole protein, but with a much slower correlation time than the free dye. Taken together, these three independent bits of information suggest that the point of attachment of the label, on the β subunit of CF, is in a cleft region of the protein. This region is partially hydrophobic and partially accessible to bulk solvent and it tends to restrict the rotational motion of the label. We can further conclude that the attachment site is remote from the enzyme active site since the catalytic activities are only slightly affected by the presence of the label and the binding of substrate has only a minimal effect on the probe's fluorescence properties. In another investigation (Deters et al., 1975) attachment of two equivalents of NBD

chloride to the β subunit led to a loss of 80% of the ATPase activity of CF. We conclude that these two fluorescent probes bind to different regions of the β subunit, because their effects on the catalytic activities are so different. These different sites should provide useful references for dissection of β subunit structure and function.

Alternative interpretations of some of the data cannot yet be ruled out. The polarization data could also be interpreted in terms of a model in which the label is rigidly immobilized on the protein backbone, but the local protein chain exhibits considerable independence motion from the protein as a whole on the short time scale. The greater than tenfold difference in rotational correlation times for a rigid sphere CF and the attached 5-IAF label seems large for local chain motion alone, but little information exists to quantitate such motions. In addition, the spectral shift in the label may arise partially from changes in solvent shell motion or other factors in addition to solvent dielectric constant (Radda and Vanderkooi, 1972). Again, such factors are difficult to quantitate.

In this study, one 5-IAF label binds per CF molecule predominantly at a single site on the β subunit. Cantley and Hammes (1975a, b) find a single active site in the vicinity of the β subunit. Cantley, Baird and Hammes propose that there are at least two copies of the β subunit per CF molecule (Cantley and Hammes, 1975b; Baird and Hammes, 1976). The labeling evidence indicates that the two β subunits are non-identical. Whether the difference occurs between two identical subunits because of a non-symetric quaternary structure for CF or because of the presence of two non-identical forms of the β subunit cannot yet be determined.

It appears that the bulky fluorescent probe, 5-IAF is more selective in its binding to SH sites than is iodoacetamide. The fluorescent probe binds

to a single site per CF, while iodoacetamide labels two sites in the native protein (Farron and Racker, 1970). In this case the bulky fluorescent moiety provides additional site selectivity over the simple SH label.

We have looked for 5-IAF-CF fluorescence on the chloroplast membrane after reconstitution. These attempts have so far not succeeded, apparently due to background light scattering problems and low reconstitution efficiencies.

The single β subunit labeling site identified in this investigation has been characterized biophysically and identified as remote from the active site, probably in a cleft region. We have shown that changes in the vicinity of the labeling site are involved in trypsin activation of the ATPase activity of CF. In conjunction with the growing list of other well characterized labeling sites on CF, it should provide a reference point for investigations of structure and function in this important energy transducing complex.

ACKNOWLEDGEMENTS

We thank Dr. Richard Haugland for his generous gift of 5-iodoacetamido-fluorescein for this study. We wish to acknowledge excellent technical assistance provided by Ms. Nancy Bertrand in the isolation of CF and a number of the biochemical assays. We thank Dr. Richard Chain for helpful suggestions for the photophosphorylation experiments.

PH AND SUBSTRATE INDUCED CONFORMATIONAL CHANGES IN CHLOROPLAST COUPLING FACTOR: BASIS FOR A MODEL OF PHOSPHORYLATION COUPLING

INTRODUCTION

It has been approximately ten years since the discovery of a water soluble, membrane surface protein named coupling factor (CF) in spinach chloroplasts that is capable of restoring photophosphorylation in EDTA inhibited membranes (Vambutas and Racker, 1965; McCarty and Racker, 1966). This photophosphorylation enzyme presumably links oxidation-reduction reactions occurring within the photosynthetic membrane to the production of ATP in a dehydration reaction occurring near the membrane surface. It has become increasingly accepted that this coupling occurs through a proton electrochemical gradient across the membrane (Mitchell, 1972a; Skulachev, 1971; Jagendorf and Uribe, 1966). The molecular details of this process, however, remain obscure. A conformational theory of energy coupling has been proposed in which energy linked protein conformational changes are directly involved in ATP production (Boyer, 1974; Boyer et al., 1975; Jagendorf, 1975). Evidence that phosphorylating conditions induce conformational changes in CF has been obtained in several laboratories (Ryrie and Jagendorf, 1971, 1972; McCarty et al., 1972; Kraayenhof and Slater, 1974).

We have used the covalent fluorescent label 5-iodoacetamidofluorescein (5-IAF) to label CF. Under certain conditions, a single labeling site on the β subunit is saturated without extensive loss of the ATPase and photophosphorylation capabilities of the labeled enzyme (Hartig et al., 1976). That study demonstrates that 5-IAF can be used to label

CF with only minimal perturbation of the enzyme's native activities. In the present study, the fluorescent labeling reaction itself is used as a probe for structural changes occurring in CF. The presence or absence of substrate and small changes in the pH of the labeling mixture cause changes in the extent and subunit localization of the labeling. These labeling changes reflect conformational rearrangements in CF induced by pH changes and by the addition of substrate. The implications of these findings for the conformational theory of energy coupling will be discussed.

EXPERIMENTAL

5-IAF was synthesized by Dr. Richard Haugland (Hamline University, St. Paul, Minn.) and obtained from him as a gift. 5-IAF has recently become available through Molecular Probes, 1775 Maple Lane, Roseville, Minn. 55113. Its properties are described elsewhere together with the purification method for CF used in this study (Hartig et al., 1976).

5-IAF Labeling of CF The basic labeling procedure and the method for determining the ratio of attached labels is described elsewhere Hartig et al., 1976). The labeling procedure is modified for these experiments by adjustment of the pH and addition or deletion of ATP before the incubation period. Aliquots of 40% K_3PO_4 or 40% KH_2PO_4 are added to a solution of approximately 1.5 mM 5-IAF in 0.2 ml of 40 mM tricine-NaOH, 2 mM EDTA, pH 8.0 with or without 3.5 mM ATP to bring the pH to approximately the desired value. A solution containing 0.5 to 5 mg of CF in 1 ml of the same buffer is added, and the pH is adjusted to the incubation value by addition of aliquots of the phosphate solutions. The incubation and determination of the labeling ratio proceeds are described (Hartig et al., 1976). A molar absorbtivity of 42,000 ($l\text{-mole}^{-1}\text{-cm}^{-1}$) at the 498 nm adsorption peak is used for 5-IAF attached to CF.

SDS Gel Electrophoresis The procedure of Laemmli (1970) for 9% polyacrylamide gels with 0.1% SDS at pH 8.8 is used without a stacking gel. The gels are stained with Coomasie blue using the procedure of Fairbanks et al., (1971) unless a fluorescence emission scan is to be taken. No staining or fixation is used on gels that are scanned for fluorescence. Samples containing approximately 0.5 mg of 5-IAF-CF in 1 ml are given 10 mg of Pierce SDS and 20 µl of 2-mercaptoethanol.

The samples are capped and incubated at 37°C in the dark for 2 hours. A few crystals of sucrose are added to each sample before application to the gels. The gels are run for approximately 5 hours at 1 mA/gel.

Fluorescence Emission Scans of SDS Gels Gels are removed from the running buffer immediately after the run with the glass tube gel casing left intact. The glass tubes are secured to the TLC plate holder of a model 018-0057 Thin Layer Chromatography Accessory for a Perkin-Elmer MPF 2A spectrofluorometer. Excitation wavelength is 480 nm and emission wavelength is 520 nm. A non-reflective background is placed behind the gels to minimize light scattering. The emission and excitation slits and the TLC accessory slit are adjusted for optimal resolution with a good signal to noise ratio. The gels are mechanically scanned and the positions of major fluorescence features are correlated with physical locations on the gels.

RESULTS

We have shown that labeling of the chloroplast photophosphorylation coupling factor (CF) at pH 7.5 in the presence of ATP leads to saturation of a single labeling site on the β subunit of the enzyme (Hartig et al., 1976). Slight variations in the pH of the reaction mixture and the presence or absence of ATP have a profound effect on the extent of the labeling, as shown in Fig 1. The number of attached labels varies between 0.7 and 3.2 for pH values between 6.4 and 8.5 in the presence or absence of 3.5 mM ATP. The extent of labeling reaches a minimum of approximately 1 label per CF at pH 7.8 in the presence of 3.5 mM ATP and increases dramatically as the pH is either raised or lowered. The effect of ATP addition is to cause a decreased labeling of 1/2 to 1-1/2 labels per CF over the entire pH range.

We have examined the subunit specificity of the labeling reaction as a function of reaction pH and the presence or absence of ATP. Samples of 5-IAF labeled CF produced under different reaction conditions were subjected to SDS polyacrylamide gel electrophoresis under dissociating conditions. We observed the 5-IAF emission arising from each subunit of CF using a thin layer chromatography scanning accessory on a standard spectrofluorometer as described in the Experimental section. This technique avoids the laborious slicing and elution that is frequently employed to remove peptides from the gel. Fig 2 shows the fluorescence emission scan for CF labeled with 5-IAF at pH 6.6 in the presence or absence of ATP. The positions of the α, β and γ subunits of CF (Nelson et al., 1973, McEvoy and Lynn, 1973) on the gels were determined by Coomassie blue staining of other gels in the same batch run under

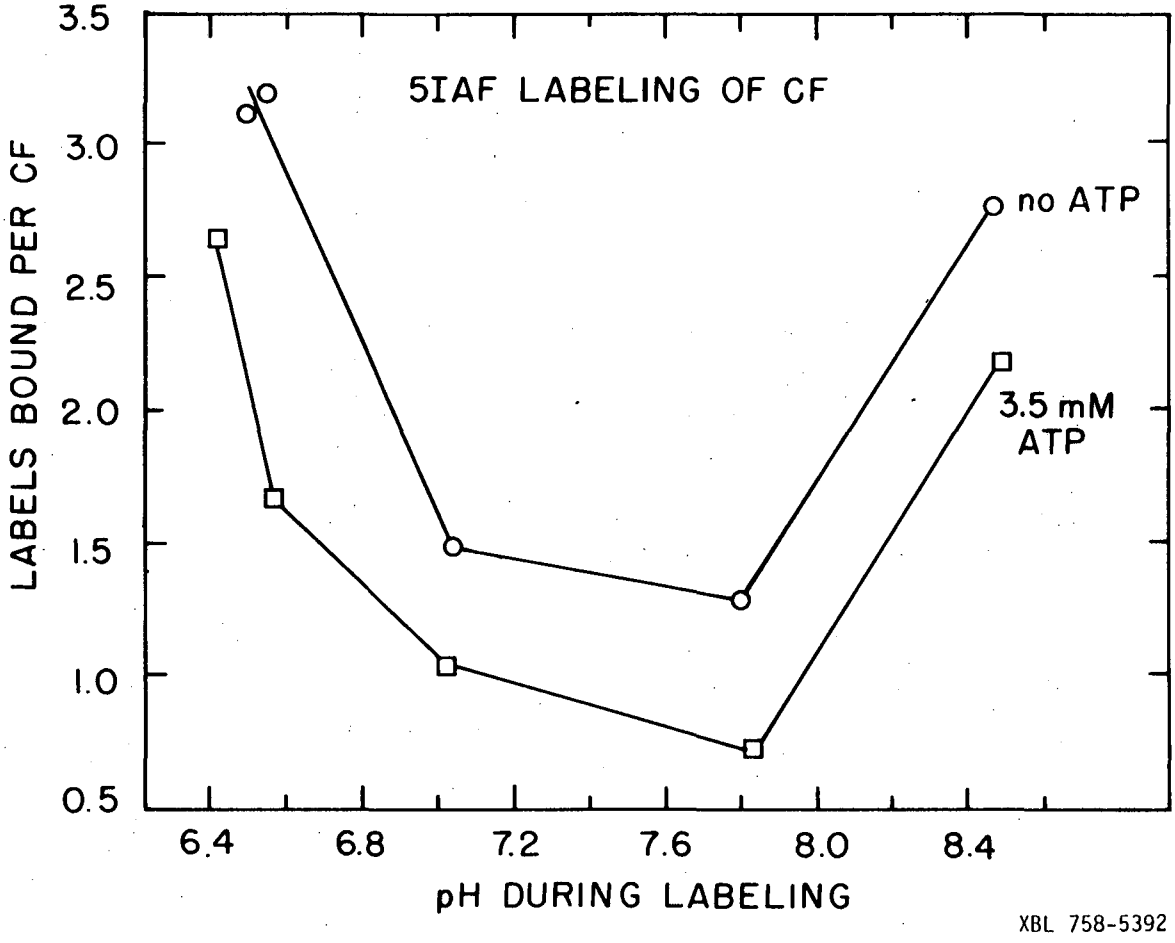

Fig. 5.1. PH dependence of the 5-IAF labeling of CF. The conditions for the labeling reaction are described in the text. O—O, labeling reactions with no addition; □—□, labeling reactions with 3.5 mM ATP added during the reaction.

Fig. 5.2. Fluorescence emission scans of SDS gels of 5-IAF-CF labeled at pH 6.6. Aliquots of CF labeled with 5-IAF at pH 6.57 in the presence of 3.5 mM ATP and labeled at pH 6.55 without ATP were run on SDS polyacrylamide gels. The 5-IAF fluorescence was excited at 490 nm and observed at 520 nm as the gels were scanned. The positions of the major CF subunits are marked along the horizontal axis. The sharp spike at the gel origin is a light scattering artifact.

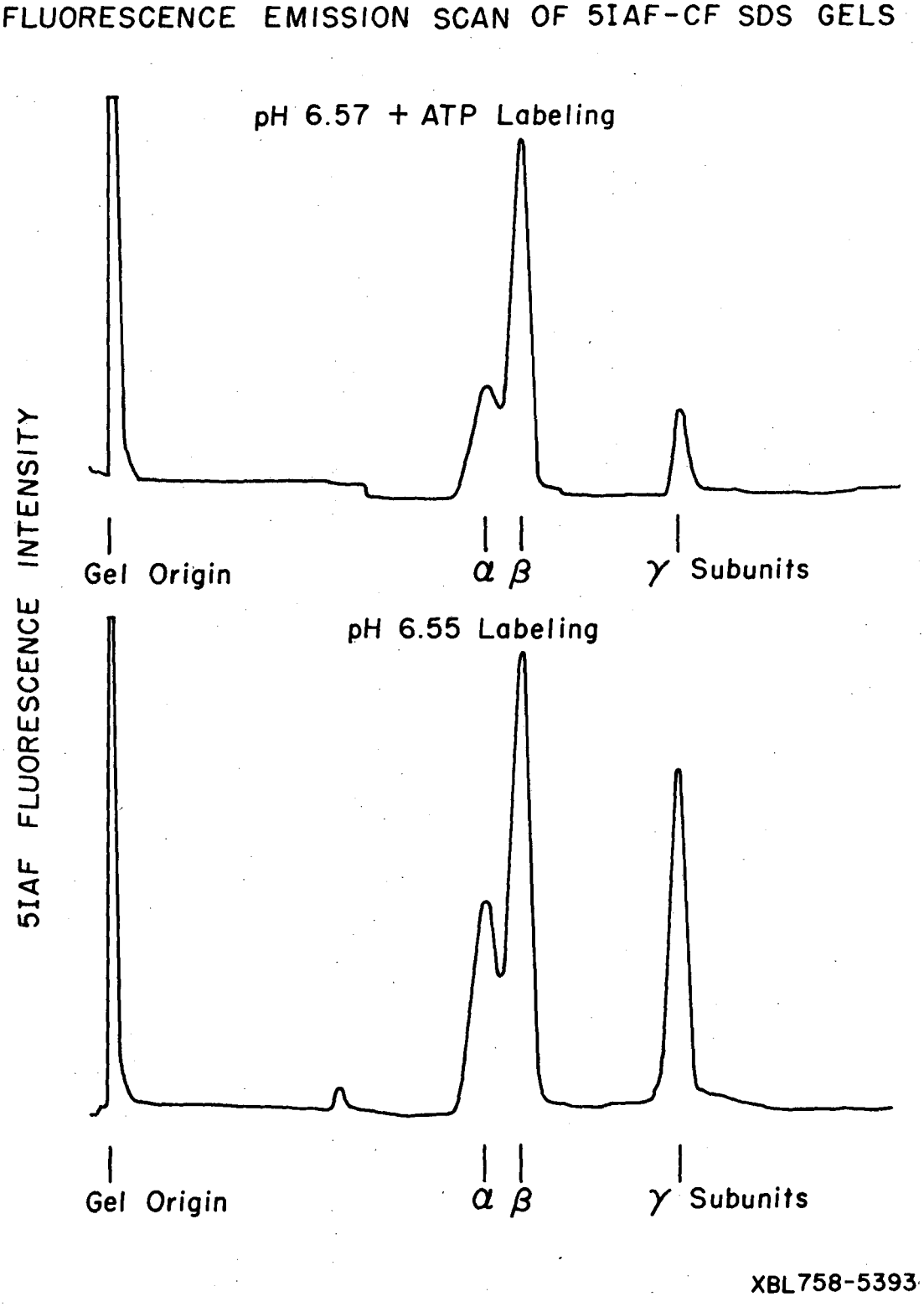
FLUORESCENCE EMISSION SCAN OF 5IAF-CF SDS GELS
pH 6.57 + ATP Labeling
5IAF FLUORESCENCE INTENSITY
Gel Origin
α β
γ Subunits
pH 6.55 Labeling
Gel Origin
α β
γ Subunits
XBL758-5393

Fig. 5.2

identical conditions. The subunit positions are marked in the figure. We did not investigate the low level of labeling which occurs on the δ and the ε subunits due to problems with light scattering and a small amount of free 5-IAF near the running front at the bottom of the gels. The sharp spike recorded at the gel origins arises from light scattering at the top surface of the gels. The data indicate that at pH 6.6 a significant decrease in the extent of labeling of the γ subunit occurs when ATP is added to the reaction mixture. A smaller but reproducible decrease in the labeling of the α subunit is also seen when ATP is added at this pH. We have estimated the total number of labels attached to each subunit from the integrated emission peak areas. The decreased labeling of the γ subunit accounts for the majority of the labeling decrease which occurs when ATP is added at pH 6.6 as seen in Fig 1.

The labeling pattern which occurs at pH 8.5 in the presence or absence of ATP is shown in Fig.3. At this pH, binding of ATP to CF does not induce strong shielding of a specific subunit during the labeling reaction. Since no change is observed in the labeling ratios of specific subunits, we conclude that the decreased labeling seen in Fig 1 at pH 8.5 when ATP is added arises from a generalized decrease in the labeling rate over all three subunits, or from changes in labeling of the δ and ε subunits, which were not examined. The specific increase in labeling of the γ subunit observed in the absence of ATP at pH 6.6 does not occur at pH 8.5. Comparison of the labeling distributions at pH 6.6 and pH 8.5 in Figs 2 and 3 shows that the higher pH induces a much stronger relative labeling of the γ subunit

Fig. 5.3. Fluorescence emission scans of SDS gels of 5-IAF-CF labeled at pH 8.5. Samples of 5-IAF-CF labeled at pH 8.49 with 3.5 mM ATP and at pH 8.47 without ATP were run on SDS gels, and the fluorescence emission was analyzed as described in the Fig. 5.2 caption.

FLUORESCENCE EMISSION SCAN OF 5IAF-CF SDS GELS

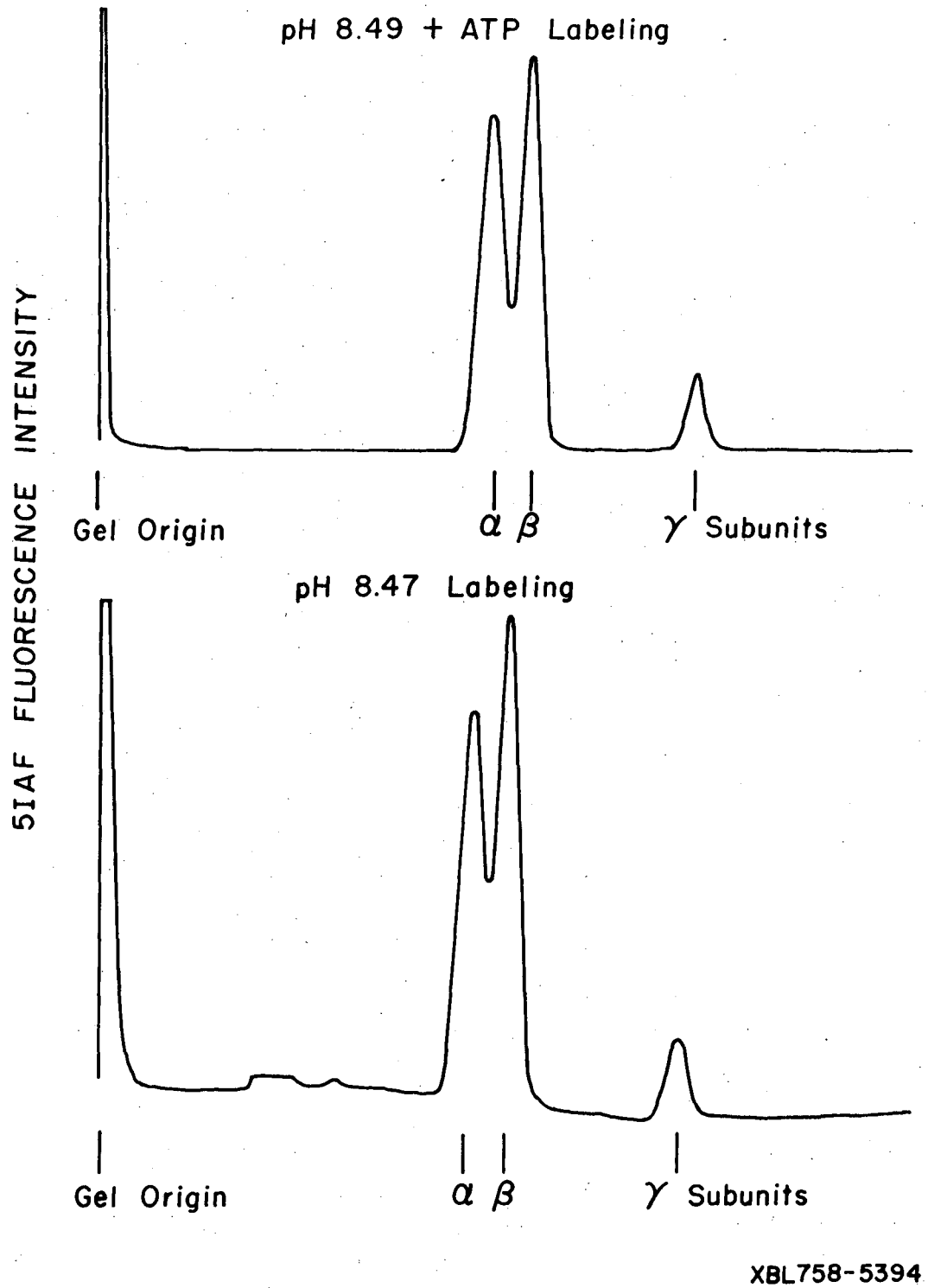

Fig. 5.3

in both the presence and absence of ATP. Thus, the affect of high pH is expressed primarily as an increase in the extent of labeling of the γ subunit.

At pH values between 6.6 and 8.5 the labeling pattern can be generally described as intermediate between the two extremes present in Figs 2 and 3. For example, labeling at pH 7.0 produces a fluroescence emission peak height ratio for the γ subunit (γ/β) of 0.80 in the absence of ATP and only 0.40 in the presence of ATP. Thus at pH 7.0 as well as at pH 6.6, addition of ATP induces a selective decrease in labeling on the γ subunit. Labeling reactions which occur near the bottom of the curve in Fig 1 produce a highly localized labeling. At pH 7.5 in the presence of ATP, we observe a low level of labeling of all subunits except at the β subunit where a single site is saturated (Hartig et al., 1976). Labeling reactions at pH values above 7.5 produce increased labeling of the α subunit. At pH 7.8 for example, the fluorescence emission peak height for the α subunit is approximately 50% of the value for the β subunit in both the presence and absence of ATP.

DISCUSSION

Substrate Induced Conformational Changes in CF

Addition of ATP over the pH range from 6.4 to 8.5 causes a decrease in the extent of labeling by the fluorescent probe 5-IAF. We interpret these changes in accessibility of labeling sites upon addition of ATP as indicative of substrate induced conformational changes in the coupling factor. The alternative explanation of direct shielding can be ruled out as discussed below. The substrate induced conformational changes in CF invariably decrease the exposure of reactive sites for the labeling reaction and may result from a generalized conformational 'tightening' of the enzyme structure caused by ATP binding.

Deters et al., (1975) have demonstrated that an α and β subunit complex of CF is active as an ATPase. Thus, the active site ATP binding locus must be on either the α or β subunits. Several laboratories have reported two tight binding sites for substrate in CF (Livne and Racker, 1969; Roy and Moudrianakis, 1971; Cantley and Hammes, 1975a). Cantley and Hammes (1975b) have tentatively assigned the tight binding sites to the α subunits. They have located on the β subunit a third site, which is exposed by heat activation of the ATPase activity. This third site was identified as the active site for the ATPase reaction. Recent excitation transfer measurements indicate that the two tight ATP binding sites are located more than 47 Å from labeled cysteine sites on the γ subunit (Cantley and Hammes, 1976a, 1976b). In summary, the data indicate that ATP binds only to the α and β subunits and that these sites are distant from the γ subunit. We have demonstrated that addition of ATP to CF at pH 6.6 causes a significant decrease in the accessibility of the γ subunit to labeling by 5-IAF. A direct shielding of

the γ subunit labeling sites by local ATP binding is ruled out because ATP binds only to the α and β subunits. We conclude that a conformational change occurs in the α or β subunit upon ATP binding and that this change is transmitted via inter-subunit forces to induce a conformational change in the γ subunit, decreasing the extent of labeling by 5-IAF. An alternative explanation is that the α and β subunits shield the γ subunit and that the binding of ATP changes the degree of shielding. However, it is likely that the γ subunit is directly accessible to 5-IAF because antibody binding studies (Nelson, et al., 1973) have shown that the γ subunit is directly accessible from the solvent phase.

ATP protects CF against heat inactivation. This effect displays positive cooperativity with a Hill coefficient approaching 4 (Livne and Racker, 1969). The discovery of positive cooperativity in substrate binding to CF and our observation of intersubunit conformational changes provides another demonstration of the generality of conformationally mediated cooperativity in oligomeric proteins as proposed in the models of Monod et al., (1965) and Koshland et al., (1966).

pH Induced Conformational Changes in CF

CF labeling at pH 7.5 in the presence of ATP occurs predominantly at a single site on the β subunit and without loss of catalytic activities (Hartig et al., 1976). Strong labeling of the β subunit is retained at all values of pH in the presence and absence of substrate. The fact that the catalytic activity is retained on labeling of the β subunit site indicates that the labeling site is not an active site residue. The reactive iodoacetyl moiety of 5-IAF should show the same general reactivity as iodoacetamide. Over the range of physiological pH,

only the cysteine sulfhydryl group and certain highly reactive active site residues show a rapid rate of reaction with iodoacetamide (Means and Feeney, 1971). Thus, the β subunit labeling site is most likely a cysteine sulfhydryl group. The other labeling sites accessible between pH 6.4 and 8.5 are also probably sulfhydryl sites since the other potentially reactive nucleophilic amino acids are significantly less reactive than cysteine over this pH range (Means and Feeney, 1971).

The cysteine sites should exhibit a pK_a of approximately 10.5 for the reactive sulfhydryl group (Edsall, 1943). The large difference between the pK_a of cysteine and the reaction pH used in this study make it unlikely that the increased labeling between pH 8.0 and 8.5 is due to the small increase in unprotonated sulfhydryl groups that appears in this range. Similarly, the pK_a of approximately 10.8 expected for the lysine ε-amino group and the fact that even the unprotonated form is 1/100 as reactive as cysteine makes lysine an unlikely candidate for the labeling increase at pH values above 8.0 (Dawson et al., 1969; Means and Feeney, 1971). In any case the decreased reactivity of CF observed as the pH is raised from 6.4 to 8.0 cannot be assigned to any direct effect of pH on the side chain reactivity.

The effect of pH on the reactivity of CF to 5-IAF is also not an artifact of denaturation. The Ca^{++}-ATPase activity of soluble CF is stable at room temperature at pH 8.0 and at pH 6.5 (McCarty and Racker, 1966). Between pH 6.7 and 8.7 there is no pH dependence to the Mg^{++}-ATPase rate of light activated chloroplasts in Tricine buffer (McCarty and Racker, 1968). These data indicate that CF is stable over the physiological pH range used in this study. We conclude that the variations observed in the extent and distribution of the labeling

as a function of pH can be assigned to a pH induced conformational change of possible physiological significance in photophosphorylation. We believe that this is the first direct demonstration of pH induced conformational changes in coupling factor.

A Model for Photophosphorylation

The pH and substrate induced conformational changes revealed in these experiments are interdependent. For example, at pH 6.6 we observe that ATP addition induces conformational changes specific for the γ subunit. At pH 8.5, addition or deletion of ATP does not induce the same effect. A similar interdependence has been observed in conformational changes induced by substrate binding and illumination of chloroplasts. McCarty and Fagan (1973) discovered that ADP plus inorganic phosphate largely prevented the γ subunit incorporation of NEM by CF that occurs during illumination of chloroplasts. Ryrie and Jagendorf (1972) found that ADP plus inorganic phosphate limits the extent of light induced conformational changes in CF as detected by tritium incorporation.

The existence of these interdependent ATP induced and pH or illumination induced conformational changes suggests that pH changes in vitro or illumination of chloroplasts can affect the active site conformation of CF. This concept can be incorporated into a model for phosphorylation. The Chemisomotic theory of phosphorylation coupling proposes that the energy for phosphorylation is provided by a transmembrane proton electrochemical gradient (Mitchell, 1970). The Conformational Coupling theory proposes that energy driven conformational changes occur in CF which can drive net ATP synthesis. This conformational coupling occurs by direct contact of CF with electron transport components

which undergo oxidation-reduction associated conformational changes (Slater, 1972; Boyer, 1974) or by some unspecified coupling of CF conformation to the transmembrane electrochemical gradient (Jagendorf, 1975). The evidence presented in this work is consistent with both models and leads to the proposal that the mode of coupling of the transmembrane electrochemical potential to conformational changes in the CF is through a direct effect of the pH inside and outside the thylakoid vesicle on the conformation of CF. Thus, the illumination induced transmembrane proton gradient may directly induce conformational changes at the active site of CF leading to a net ATP synthesis. The essential features of this proposed model are:

1) Electron transport induced by illumination is coupled to the production of a proton electrochemical gradient across the chloroplast thylakoid membrane.

2) Coupling Factor is situated on a transmembrane proton channel where regions of the enzyme are accessible to the internal and external pH.

3) Direct contact of CF with protons under the influence of the transmembrane electrochemical potential induces conformational changes at the active site which provide the energy for net ATP synthesis.

The evidence which supports this model is extensive. A number of investigators have observed conformational changes in CF associated with photophosphorylation and pH gradients. Ryrie and Jagendorf (1971, 1972) discovered that illumination of chloroplasts in the presence of tritiated water led to the entrapment of tritium in buried regions of CF. It is especially significant that an acid-base induced transmembrane Δ pH was capable of causing tritium incorporation in a manner similar to the

illumination induced conformational change. Thus, both illumination and pH changes induce similar conformational changes in CF. These conformational changes were directly associated with ATP production. McCarty et al., (1972) observed that treatment of chloroplasts with NEM in the light but not in the dark leads to a partial inhibition of photophosphorylation. They interpret these results as evidence for a conformational change induced by illumination that leads to exposure of new labeling sites. Kraayenhof and Slater (1974) observed that fluorescamine labeled CF shows an emission peak shift on illumination that indicates a conformational change which places the fluorescent label in a more hydrophobic environment. Indirect evidence for pH induced conformational changes in CF has also been obtained. From examination of the ratio of internal pH to the rate of electron flow as a function of the external pH, Portis et al., (1975) concluded that the conformation of CF is altered at high external pH values, leading to increased proton efflux. The association of conformational changes with ATP production during photophosphorylation is thus well established. In addition, the evidence suggests that pH gradients alone induce similar conformational changes.

Our direct observation of CF conformational changes induced by ATP binding and pH changes provides evidence that the pH differential across illuminated membranes may directly induce conformational changes in CF leading to net ATP production. The magnitude of the steady state transmembrane Δ pH has been estimated at 2.5 to 3.5 pH units by a variety of techniques (Uribe and Jagendorf, 1967; Rumberg and Siggel, 1969; Heldt et al., 1973; Portis and McCarty, 1973; Pick et al., 1973). The conformational changes observed in this study occur over the pH range

of 6.4 to 8.5. We see that CF conformational changes occur over the Δ pH range believed to exist across illuminated membranes. These pH driven conformational changes may play a direct role in ATP synthesis by CF on the membrane.

Evidence exists that CF is situated on a transmembrane proton pore which allows it to experience the pH both inside and outside the thylakoid vesicles. Removal of CF from the membrane leads to a decrease in the net transmembrane Δ pH during illumination (Neumann and Jagendorf, 1964; McCarty and Racker, 1966). In addition, the rate of dark decay of the transmembrane proton gradient is accelerated by removal of CF (McCarty and Racker, 1967). Both the electrical conductance of the thylakoid membrane and the dark relaxation rate of the light induced transmembrane Δ pH increase 100 fold following CF removal (Schmid and Junge, 1974). Experiments with the protein cross-linker DCCD indicate that a proton pore becomes accessible to chemical modification when CF is removed from the membrane (McCarty and Racker, 1967; Uribe, 1972). These data indicate that CF removal increases the proton leakiness of the membrane and suggest that CF is situated on a proton conductance channel through the membrane. Thus, both the internal and external pH should be accessible to regions of the CF enzyme.

The role of the transmembrane electrical potential in this model is not yet clearly delineated. The potential may raise the net electrochemical activity of protons (Mitchell, 1974; Mitchell and Moyle, 1974) leading to conformational changes in CF. Another possibility is that protonation and deprotonation of CF provides charged groups which can

be influenced by either the transmembrane Δ pH or the electrical potential. Evidence that the transmembrane potential is capable of driving a protein conformational change in CF was obtained in the work of Ryrie and Jangendorf (1972).

Role of the γ Subunit as an Allosteric Mediator

The findings of this study, in conjunction with previous research, suggest a special role for the γ subunit as an allosteric mediator which may serve to transmit conformational forces generated by pH differentials to the active site for use in net ATP synthesis. In this work, we discovered that at pH 6.6 the binding of ATP to remote subunits is sensed by the γ subunit via conformational changes. This conformational sensing is dependent on pH since the same effects are not observed at pH 8.5. This evidence suggests that the γ subunit conformation is sensitive both to pH and to substrate binding and may be capable of transmitting to the active site conformational forces induced by the transmembrane pH differential. The γ subunit appears to be essential for photophosphorylation coupling. Deters et al., (1975) showed that an α and β subunit complex of CF is active as an ATPase but not as a coupling factor and that only the ε subunit of CF may be removed without affecting the coupling activity. McCarty and Fagan (1973) discovered that light induced conformational changes occur on CF that are expressed by exposure of a sulfhydryl site or sites on the γ subunit for labeling by NEM. No other subunit showed increased NEM labeling upon illumination. Since the reaction of NEM with the γ subunit inhibits phosphorylation, it has been proposed that the γ subunit sulfhydryl site may be functionally important in phosphorylation (McCarty and Fagan, 1973; Nelson

et al., 1973). Anti-γ strongly inhibits phosphorylation (Nelson et al., 1973). In addition, the light dependent tritium uptake of CF resulting from conformational changes is inhibited by anti-γ (Gregory and Racker, 1973; Deters et al., 1975). These findings suggest that binding of anti-γ may inhibit conformational changes in CF required for phosphorylation (Deters et al., 1975). Also, anti-γ does not cause agglutination of chloroplasts, suggesting that the antigenic site is accessible from the external solvent but is oriented toward the membrane face (Nelson et al., 1973). Thus, it is in a position where it may have access to the transmembrane proton channel and be capable of sensing the pH both inside and outside the thylakoid vesicle.

In summary, the γ subunit is essential for photophosphorylation, it exhibits conformational changes during illumination, pH changes and substrate binding, and it is in a position to experience the transmembrane pH differential. Because it does not bind substrate directly, the γ subunit may serve as an essential allosteric mediator which transmits conformational forces derived from the transmembrane proton electrochemical potential to the active site for use in ATP synthesis.

The evidence presented in this paper demonstrates the existence of complex pH and substrate induced conformational changes in CF. Certain interdependences were observed in this work and in other laboratories between conformational changes induced by substrate and conformational changes induced by illumination or pH changes. These interdependences suggest that pH induced conformational changes may be transmitted to the active site for net ATP synthesis. We have suggested a model of phosphorylation in which CF on the membrane is directly accessible to

the transmembrane proton electrochemical potential. This transmembrane potential induces conformational changes in CF providing the energy for net ATP synthesis. In this study we have shown that the conformation of CF changes as the bathing pH changes. It remains to be shown whether simultaneous exposure of CF on the membrane to the internal and external pH induces similar conformational changes at the active site which drive ATP synthesis.

REFERENCES

Adolfsen, R., McClung, J. and Moudrianakis, E. (1975), Biochem. 14, 1727.

Alfano, R. and Shapiro, S., (1972), Opt. Commun. 6, 98.

Alfano, R. and Shapiro, S., (1973), Sci. Amer. 228, 43.

Allen, J. and Hall, D., (1973), Biochem. Biophys. Res. Commun. 52, 856.

Arnon, D., (1949), Plant Physiol. 24, 1.

Arnon, D., (1956), Ann. Rev. Plant Physiol. 7, 325.

Arnon, D., (1968), in Biological Oxidations (T. Singer ed.) J. Wiley and Sons, New York, pp. 123-170.

Asada, K., Kiso, K. and Yoshikawa, K., (1974), J. Biol. Chem. 249, 2175.

Avron, M., (1960), Biochim. Biophys. Acta 40, 257.

Avron, M., (1962), J. Biol. Chem. 237, 2011.

Avron, M., (1971), in Structure and Function of Chloroplasts (M. Gibbs ed.) Springer-Verlag, New York, p. 165.

Avron, M. and Neumann, J., (1968), Ann. Rev. Plant Physiol. 19, 137.

Baird, B. and Hammes, G., (1976), J. Biol. Chem., in press.

Bakker-Grunwald, T. and Van Dam, K., (1973) Biochim. Biophys. Acta 292, 808.

Bakker-Grunwald, T. and Van Dam, K., (1974) Biochim. Biophys. Acta 347, 290.

Balny, C., and Douzou, P., (1974), Biochem. Biophys. Res. Commun. 56, 386.

Bamberger, E., Rottenberg, H. and Avron, M., (1973) Eur. J. Biochem. 34, 557.

Bennun, A., and Racker,E. (1969), J. Biol. Chem. 244, 1325.

Berlman, I. (1971), Handbook of Fluorescence Spectra of Aromatic Compounds, Academic Press, N.Y., 2nd ed., p. 356.

Birks, J. and Munro, I. (1967) in Progress in Reaction Kinetics ed. G. Porter, Pergamon Press, New York, vol. 4 p. 239.

Blankenship, R. and Sauer, K. (1974) Biochim. Biophys. Acta 357, 252.

Boyer, P. (1974), in Dynamics of Energy Transducing Membranes, Ernster, L., Estabrook, R., and Slater, E., Ed., New York, Elsevier Publishing, p. 289.

Boyer, P. (1975), FEBS Let. 58, 1.

Boyer, P., Cross, R., and Momsen, W. (1973) Proc. Nat. Acad. Sci., USA 70, 2837.

Boyer, P., Stokes, B., Wolcott, R., and Degani, C. (1975), Fed. Proc. 34, 1711.

Brody, S., Rev. (1957), Rev. Sci. Instrum. 28, 1021.

Cantley, L., and Hammes, G. (1975a), Biochemistry 14, 2968.

Cantley, L., and Hammes, G. (1975b), Biochem. 14, 2976.

Cantley, L., and Hammes, G. (1976a), Biochem. 15, 1.

Cantley, L., and Hammes, G. (1976b), Biochem. 15, 9.

Carmeli, C.,(1970) FEBS Let. 7, 297.

Chang, I. C., and Kahn, J. S. (1966), Arch. Biochem. Biophys. 117, 282.

Clayton, R. (1965), Molecular Physics in Photosynthesis, Blaisdell Publishing, New York.

Coates, P. (1968) J. Sci. Instrum. (J. of Phys. E.) [2], 1, 878.

Davies, M. and Jones, R. (1954) J. Chem. Soc. 120.

Davis, C. and King, T. (1970) J. Phys. A., 3, 101.

Dawson, R., Elliott, D., Elliott, W. and Jones, K., (1969), Data for Biochemical Research, Oxford University Press, New York.

Deamer, D., Crofts, A. and Packer, L. (1967) Biochim. Biophys. Acta 131, 81.

Deters, D., Racker, E., Nelson, N. and Nelson, H. (1975), J. Biol. Chem. 250, 1041.

Donohue, D. and Stern, R. (1972), Rev. Sci. Instrum. 43, 791.

Edsall, T. (1943), in Proteins, Amino Acids and Peptides as Ions and Dipolar Ions, E. Cohn and J. Edsall, eds., Reinhold, New York, p. 75.

Eisenthal, K. (1975) Accts. Chem. Res. 8, 118.

Elstner, E. and Kramer, R. (1973), Biochim. Biophys. Acta 314, 340.

Epel, B. and Neumann, J. (1973), Biochim. Biophys. Acta 325, 520.

Fairbanks, G., Steck, T., and Wallach, D. (1971), Biochem. 10, 2606.

Farron, F., (1970), Biochemistry 9, 3823.

Farron, F. and Racker, E. (1970), Biochemistry 9, 3829.

Forster, Th. (1965), in Modern Quantum Chemistry, Part III O. Sinanoglu, ed., Academic Press, New York, pp. 93-137.

Forti, G., Rosa, L. and Garlaschi, F. (1972), FEBS Let. 27, 23.

Gafni, A., Modlin, R., and L. Brand (1975), Biophys. J. 15, 263.

Garber, M. and Steponkus, P. (1974), J. Cell Biol. 63, 24.

Girault, G., Galmiche, J., and Vermeglio, A. (1974), Proc. Third Int. Cong. on Photosynthesis, 839.

Girault, G., Kleo, J., and Galmiche, J. (1971), Second Int. Cong. on Photosynthesis, 1145.

Gornall, A., Bardawill, C., and David, M. (1949), J. Biol. Chem. 177, 751.

Gould, J. and Ort, D. (1973), Biochim. Biophys. Acta 325, 157.

Green, D., Ji, S and Brucker, R. (1973), Bioenergetics 4, 253.

Greenberg, A., Furst, M. and Kallmann, H. (1966) International Symposium on Luminescence. The Physics and Chemistry of Scintillators, Verlag Karl Thiemig, Munich, p. 71.

Gregory, P., and Racker, E. (1973), abstracts of the Ninth International Congress of Biochemistry, (Abstract), Stockholm, 1-7 July 1973, p. 238.

Harris, D., and Slater, E. (1975), Biochim. Biophys. Acta 387, 335.

Hartig, P. (1976), PhD. thesis, University of California, Berkeley.

Hartig, P., Bertrand, N., and Sauer, K. (1976), in preparation for Biochemistry, see Ch. 4 this thesis.

Hartig, P., and Sauer, K. (1976), in preparation for Biochemistry, see Ch. 5 this thesis.

Hartig, P., Sauer, K., Lo, C., and Leskovar, B. (1976), Rev. Sci. Instrum., in press.

Hazan, G., Grinvald, A., Maytal, M. and Steinberg, I., (1974), Rev. Sci. Instrum. 45, 1602.

Heber, U. (1973), Biochim. Biophys. Acta 305, 140.

Heldt, H., Werdan, K., Milovancev, M. and Geller, G. (1973), Biochim. Biophys. Acta 314, 224.

Hind, G. and Jagendorf, A. (1963), Proc. Natl. Acad. Sci. U.S. 49, 715.

Howell, S. and Moudrianakis, E. (1967), Proc. Nat. Acad. Sci. U.S. 58, 1261.

Isenberg, I. (1973), J. Chem. Phys. 59, 5696.

Isenberg, I. (1975), in Biochemical Fluorescence: Concepts , vol. 1, eds. Chen, R., and Edelhoch, H., Marcel Dekker Inc., New York, p. 43.

Isenberg, I. and Dyson, R. (1969), Biophys. J. 9, 1338.

Isenberg, I., Dyson, R. and Hanson, R. (1973), Biophys. J. 13, 1090.

Jagendorf, A., (1975), Fed. Proc. 34, 1718.

Jagendorf, A. and Uribe, E. (1966), Brookhaven Symp. Biol. 19, 215.

Junge, W. and Witt, H. (1968), Zeitschrift Naturforschung 23b, 244.

Karlish, S. and Avron, M. (1968), in Comparative Biochemistry and Biophysics of Photosynthesis eds. Shibata, K., Takamiya, A., Jagendorf, A., and Fuller, R., University Park Press, State College, Penn., p. 214.

Knight, A. and Selinger, B. (1973), Austral. J. Chem. 26, 1.

Konev, S. (1967), Fluorescence and Phosphorescence of Proteins and Nucleic Acids, Plenum Press, New York.

Koshland, D., Nemethy, G. and Filmer, D. (1966), Biochem. 5, 365.

Kraayenhof, R. and Slater, E. (1974), Proc. Third Int. Cong. Photosyn, 985.

Laemmli, U. (1970), Nature 227, 680.

Lehninger, A. (1965), Bioenergetics: The Molecular Basis of Biological Energy Transformations, W. A. Benjamin Inc., New York.

Lehrer, S. (1971), Biochem. 10, 3254.

Leskovar, B. (1975), Nucl. Instrum. Methods 128, 115-119.

Leskovar, B. Lo, C., (1972), IEEE Trans. Nucl. Sci. U.S. 19, 50.

Leskovar, B. and Lo, C. (1975), Nucl. Instrum. Methods 123, 145.

Leskovar, B., Lo, C., Hartig, P. and Sauer, K. (1976), Rev. Sci. Instrum., in press.

Lewis, C., Ware, W., Doemeny, L. and Nemzek, T. (1973), Rev. Sci. Instrum. 44, 107.

Lien, S., Berzborn, R. and Racker, E. (1972), J. Biol. Chem. 247, 3520.

Lien, S. and Racker, E. (1971a), J. Biol. Chem. 246, 4298.

Lien, S. and Racker, E. (1971b), Methods in Enzymology 23, 547.

Lindberg, O. and Ernster, L. (1956), Meth. Biochem. Anal. 3, 1.

Livne, A. and Racker, E., (1969), J. Biol. Chem. 244, 1332.

Lo, C. and Leskovar, B. (1974), IEEE Trans. Nucl. Sci., NS-21, 1, 93.

Lowry, O., Rosenbrough, N., Farr, A. and Randall, R. (1951), J. Biol. Chem. 193, 265.

Lynn, W. and Straub, K. (1969), Biochem. 8, 4789.

Mahler, H. and Cordes, E. (1971), Biological Chemistry, 2nd Ed., Harper and Row, New York, p. 201.

Martin, R. and Ames, B., (1961), J. Biol. Chem. 236, 1372.

Martin, J. and Doty, D., (1949), Anal. Chem. 21, 965.

Martin, M. and Lindqvist, L. (1973), Chem. Phys. Let. 22, 309.

Maurer, ., (1971), Disc Electrophoresis and Related Techniques of Polyacrylamide Gel Electrophoresis, Walter de Gruyter Co., New York.

McCarty, R. (1969), J. Biol. Chem. 244, 4292.

McCarty, R. (1971), Methods in Enzymology 23, 251.

McCarty, R. and Fagan, J., (1973), Biochem. 12, 1503.

McCarty, R., Pittman, P. and Tsuchiya, Y., (1972), J. Biol. Chem. 247, 3048.

McCarty, R. and Racker, E., (1966), Brookhaven Symp. Biol. 19, 202.

McCarty, R. and Racker, E., (1967), J. Biol. Chem. 242, 3435.

McCarty, R. and Racker, E., (1968), J. Biol. Chem. 243, 129.

McEvoy, F. and Lynn, W., (1973), Arch. Biochem. Biophys. 156, 335.

McGowan, E., Silhavy, T. and Boos, W., (1974), Biochem. 13, 993.

Means, G. and Feeney, R., (1971), Chemical Modification of Proteins, Holden-Day Inc., San Francisco.

Miller, K. and Staehelin, A., (1976), J. Cell Biol. 68, 30.

Mitchell, P., (1970), Symp. Soc. Gen. Microbiol. 20, 121.

Mitchell, P., (1972), Bioenergetics 3, 5.

Mitchell, P., (1974a), Biochem. Soc. Trans. 2, 31.

Mitchell, P., (1974b), FEBS Let. 43, 189.

Mitchell, P., and Moyle, J., (1974), Biochem. Soc. Spec. Publ. 4, 91.

Monod, J., Wyman, J. and Changeux, J., (1965), J. Mol. Biol. 12, 88.

Mourou, G. and Malley, M., (1974), Opt. Commun. 11, 282.

Muhlenthaler, K., (1971), in Structure and Function of Chloroplasts (M. Gibbs ed.) Springer-Verlag, New York, p. 7.

Munro, I. and Ramsay, I., (1968), J. Sci. Instrum. 1, 147.

Nelson, N., Deters, D., Nelson, H. and Racker, E., (1973), J. Biol. Chem. 248, 2049.

Nelson, N., Nelson, H. and Racker, E., (1972a), J. Biol. Chem. 247, 6506.

Nelson, N., Nelson, H. and Racker, E., (1972b), J. Biol. Chem. 247, 7657.

Netzel, T., Struve, W. and Rentzepis, P., (1973), Ann. Rev. Phys. Chem. 24, 473.

Neumann, J. and Jagendorf, A., (1964), Arch. Biochem. Biophys. 107, 109.

Niizuma, S., Sato, Y., Konishi, S. and Kokubun, H., (1974), Bull. Chem. Soc. Japan 47, 2121.

Ortec, Incorporated, (1972), Model 9352 Nanosecond Light Pulser, Operating and Service Manual.

Park, R. and Sane, P., (1971), Ann. Rev. Plant. Physiol. 22, 395.

Perrin, F., (1926), J. Phys. Radium 7, 390.

Perrin, F., (1929), Ann. Physique X, 12, 169.

Petrack, B., Craston, A., Sheppy, F. and Farron, F., (1965), J. Biol. Chem. 240, 906.

Petrack, B. and Lipmann, F., (1961), in Light and Life (McElvoy, W., and Glass, H. eds.) p. 621, The John Hopkins Press, Baltimore.

Peusner, L., (1974), Concepts in Bioenergetics Prentice-Hall Inc., Englewood Cliffs, New Jersey.

Pick, U., Rottenberg, H. and Avron, M., (1973), FEBS Let. 32, 91.

Porter, G., Reid, E. and Tredwell, C., (1974), Chem. Phys. Lett. 29, 469.

Portis, A., Magnusson, R. and McCarty, R., (1975), Biochem. Biophys. Res. Commun. 64, 877.

Portis, A. and McCarty, R., (1973), Arch. Biochem. Biophys. 156, 621.

Portis, A. and McCarty, R., (1974), J. Biol. Chem. 249, 6250.

Racker, E., Hauska, G., Lien, S., Berzborn, R. and Nelson, N., (1971), Second Int. Cong. on Photosynthesis 1097.

Racker, E. and Stoeckenius, W., (1974), J. Biol. Chem. 249, 662.

Radda, G. and Vanderkooi, J., (1972), Biochim. Biophys. Acta 265, 509.

Rentzepis, P., (1973), Adv. Chem. Phys. 23, 189.

Rinderknecht, H., (1960), Experientia 16, 430.

Rinderknecht, H., (1962), Nature 193, 167.

Roy, H. and Moudrianakis, E., (1971a), Proc. Nat. Acad. Sci. U.S. 68, 464.

Roy, H. and Moudrianakis, E., (1971b), Proc. Nat. Acad. Sci. U.S. 68, 2720.

Rumberg, B. and Siggel, U., (1969), Naturwissenschaften 56, 130.

Ryrie, I. and Jagendorf, A., (1971), J. Biol. Chem. 246, 3771.

Ryrie, I. and Jagendorf, A., (1972), J. Biol. Chem. 247, 4453.

Saha, S., Ouitrakul, R., Izawa, S. and Good, N., (1971), J. Biol. Chem. 246, 3204.

Schmid, R. and Junge, W., (1974), Proc. Third Int. Cong. Photosyn. 821.

Schroeder, H., Muhle, H. and Rumberg, B., (1971), Second Int. Cong. Photosyn. 920.

Schuldiner, S. Rottenberg, H. and Avron, M., (1973), Eur. J. Biochem. 39, 455.

Schuyler, R. and Isenberg, I., (1971), Rev. Sci. Instrum. 42, 813.

Schuyler, R., Isenberg, I. and Dyson, R., (1972), Photochem. Photobiol. 15, 395.

Senior, A., (1973), Biochim. Biophys. Acta. 301, 249.

Seybold, P., Gouterman, M. and Callis, J., (1969), Photochem. Photobiol. 9, 229.

Shen, Y. and Shen, G., (1962), Scientia Sinica 11, 1097.

Shoshan, V. and Shavit, N., (1973), Eur. J. Biochem. 37, 355.

Singer, S. and Nicholson, G., (1972), Science 175, 720.

Skulachev, V., (1971), Current Topics in Bioenergetics 4, 127.

Skulachev, V., (1972), Bioenergetics 3, 25.

Slater, E., (1971), Quart. Rev. Biophys. 4, 35.

Slater, E., (1972), Mitochondria/Biomembranes, Amsterdam, North Holland Publishers, p. 133.

Spencer, R. and Weber, G., (1969), Anal. New York Acad. Sci. 158, 361.

Steinberg, I., (1971), Ann. Rev. Biochem. Vol. 40 (E. Snell et al., eds.), Ann. Reviews Inc., Palo Alto, pp. 83-114.

Steiner, R. and Edelhoch, H., (1962), Chem. Rev. 62, 457.

Stern, O. and Volmer, M., (1919), Phys. Z. 20, 183.

Stevens, S. and Longworth, J, (1972), IEEE Trans. Nucl. Sci. U.S. 19, 356.

Strotmann, H., Bickel, S. and Huchzermeyer, B., (1976), FEBS Let. 61, 194.

Strotmann, H., Hesse, H. and Edelmann, K., (1973), Biochim. Biophys. Acta 314, 202.

Stryer, L., (1968), Science 162, 526.

Taussky, H. and Shorr, E., (1953), J. Biol. Chem. 202, 675.

Telfer, A. and Evans, M., (1972), Biochim. Biophys. Acta 256, 625.

Timmermans, (1932), in Physico Chemical Constants of Binary Systems, vol. 4, ed. Sheely, .

Trebst, A., (1974), Ann. Rev. Plant Physiol. 25, 423.

Uribe, E. (1972), Biochemistry 11, 4228.

Uribe, E. and Jagendorf, A., (1967), Plant Physiol. 42, 706.

Uribe, E. and Li, B., (1973), Bioenergetics 4, 435.

Vambutas, V. and Racker, E., (1965), J. Biol. Chem. 240, 2660.

Vogel, A., (1961), in Quantitative Inorganic Analysis, (third ed.), Longman Group Ltd., London, p. 374.

Wahl, Ph., Auchet, J. and Donzel, B., (1974), Rev. Sci. Instrum. 45 28.

Walker, D. A., (1971), in Methods in Enzymology Vol. 23 (A. San Pietro ed.) Academic Press, New York, p. 216.

Walker, D. and Crofts, A., (1970), Ann. Rev. Biochem. 39, 389.

Warburg, O. and Christian, W., (1941), Biochem. Z. 310, 384.

Ware, W., (1971), in Creation and Detection of the Excited State ed. Lamola, Marcel Dekker, New York, Vol. 1, Part A, p. 213.

Ware, W., Doemeny, L. and Nemzek, T., (1973), J. Phys. Chem. 77, 2038.

Weber, G., (1953), Adv. Protein Chem. 8, 415.

Wessels, J. and Baltsheffsky, H., (1960), Acta Chem. Scand. 14, 233.

Yguerabide, J., (1965), Rev. Sci. Instrum. 36, 1734.

Yguerabide, J., (1972), in Methods in Enzymology, C.H.W. Hirs and S. N. Timasheff, eds. Academic Press, New York, Vol. 26, pp. 498-578.

This report was done with support from the United States Energy Research and Development Administration. Any conclusions or opinions expressed in this report represent solely those of the author(s) and not necessarily those of The Regents of the University of California, the Lawrence Berkeley Laboratory or the United States Energy Research and Development Administration.

TECHNICAL INFORMATION DIVISION
LAWRENCE BERKELEY LABORATORY
UNIVERSITY OF CALIFORNIA
BERKELEY, CALIFORNIA 94720